

9650

NATIONAL LIBRARY
OTTAWA



BIBLIOTHÈQUE NATIONALE
OTTAWA

NAME OF AUTHOR... *R. H. SUMNER*.....

TITLE OF THESIS... *CRYSTAL STRUCTURE*.....
... STUDIES OF SOME.....
... TRANSITION METAL COMPLEXES.....

UNIVERSITY... ~~OF~~ *ALBERTA*.....

DEGREE FOR WHICH THESIS WAS PRESENTED... *PH.D*.....

YEAR THIS DEGREE GRANTED... *1971*.....

Permission is hereby granted to THE NATIONAL LIBRARY
 OF CANADA to microfilm this thesis and to lend or sell copies
 of the film.

The author reserves other publication rights, and
 neither the thesis nor extensive extracts from it may be
 printed or otherwise reproduced without the author's
 written permission.

(Signed)... *[Signature]*.....

PERMANENT ADDRESS:

P.O. Box 1192.....
T. H. M. PSON.....
MANITOBA.....

DATED... *Sept 7*..... 19*71*

NL-91 (10-68)

THE UNIVERSITY OF ALBERTA
CRYSTAL STRUCTURE STUDIES OF SOME TRANSITION METAL
COMPLEXES

by

© RODNEY HOWARD SUMNER

A THESIS
SUBMITTED TO THE FACULTY OF GRADUATE STUDIES AND RESEARCH
IN PARTIAL FULFILMENT OF THE REQUIREMENTS FOR THE DEGREE
OF
DOCTOR OF PHILOSOPHY

DEPARTMENT OF CHEMISTRY
EDMONTON, ALBERTA
FALL, 1971

THE UNIVERSITY OF ALBERTA
FACULTY OF GRADUATE STUDIES AND RESEARCH

The undersigned certify that they have read, and recommend to the Faculty of Graduate Studies and Research for acceptance, a thesis entitled
CRYSTAL STRUCTURE STUDIES OF SOME TRANSITION METAL COMPLEXES.

submitted by RODNEY HOWARD SUMNER in partial fulfilment of the requirements for the degree of Doctor of Philosophy.

..... *M.J. Bennett*
M.J. Bennett, Supervisor

..... *H.B. Dunford*
H.B. Dunford

..... *G. Horlick*
G. Horlick

..... *M.J. Bennett for R.B. Jordan*
R.B. Jordan

..... *R.D. Morton*
R.D. Morton

..... *D.L. Weaver*
External Examiner
D.L. Weaver

Date *September 3rd 1971*

ABSTRACT

The crystal and molecular structure of *hexakis*(dimethylformamide)iron(III) perchlorate, $\text{Fe}(\text{DMF})_6(\text{ClO}_4)_3$, has been determined from 1164 independent, non-zero reflections collected using Mo K α radiation. The crystal data are: space group C2/c, $a = 20.504 \pm 0.009 \text{ \AA}$, $b = 13.642 \pm 0.003 \text{ \AA}$, $c = 13.12 \pm 0.01 \text{ \AA}$, $\beta = 99.50 \pm 0.05^\circ$, density 1.43 g./cm.^3 (by flotation), 1.453 g./cm.^3 ($Z=4$), $V = 3622.8 \text{ \AA}^3$. The structure has been refined by full-matrix least squares refinement to a conventional R-factor of 8.7%. The molecule is ionic with the octahedrally coordinated iron atom of the cation sitting on an inversion centre. The coordinations of the three non-equivalent nitrogen are planar. One anion is required to sit on a twofold axis, the other two in general positions. All three exhibit considerable thermal motion

The crystal and molecular structure of *tris*(dimethyldithiophosphinato)chromium(III), $\text{Cr}(\text{S}_2\text{PMe}_2)_3$, has been determined, using Cu K α radiation. The crystal data are: space group $P2_12_12_1$, $a = 9.123 \pm 0.001 \text{ \AA}$, $b = 21.550 \pm 0.002 \text{ \AA}$, $c = 9.637 \pm 0.001 \text{ \AA}$, $V = 1894.6 \text{ \AA}^3$, density $1.51 \pm 0.02 \text{ g./cm.}^3$ (by flotation), 1.499 g./cm.^3 ($Z=4$). A total of 1387 independent, non-zero reflections were used and refined by full-matrix least squares to final unweighted and weighted residuals of 0.037 and 0.061 respectively. The approximate D_3 symmetry of the molecule is destroyed by the bending of each ligand along a line joining the two sulphur atoms of each ligand.

The crystal and molecular structure of *bis*(dimethyl-dithiophosphinato)cobalt(II), $\text{Co}(\text{S}_2\text{PMe}_2)_2$, has been determined, using Mo K α radiation. The crystal data are: space group Pccn, $a = 15.446 \pm 0.001 \text{ \AA}$, $b = 8.093 \pm 0.001 \text{ \AA}$, $c = 9.430 \pm 0.001 \text{ \AA}$, $V = 1178.8 \text{ \AA}^3$, density $1.720 \pm 0.006 \text{ g./cm.}^3$ (by flotation), 1.714 g./cm.^3 ($Z=4$). Refinement of 815 non-zero intensities by full-matrix least squares gave a conventional R-factor of 3.8%. The structure is polymeric with infinite chains in the {001} direction and is the first example of such a structure in which the bridging ligand contains two sulphur atoms. The cobalt atoms lie on twofold axes, as required by symmetry, and the expected tetrahedral coordination is maintained.

The crystal and molecular structure of *bis*(dimethyl-dithiophosphinato)oxovanadium(IV), $\text{VO}(\text{S}_2\text{PMe}_2)_2$, has been determined, using Cu K α radiation. The crystal data are: space group $\text{P}2_1/\text{c}$, $a = 10.889 \pm 0.002 \text{ \AA}$, $b = 12.072 \pm 0.002 \text{ \AA}$, $c = 10.208 \pm 0.001 \text{ \AA}$, $\beta = 91.96 \pm 0.01^\circ$, $V = 1341.1 \text{ \AA}^3$, density $1.57 \pm 0.01 \text{ g./cm.}^3$ (by flotation), 1.571 g./cm.^3 ($Z=4$). The structure was solved by direct methods and has refined to $R = 0.059$. The coordination of the vanadium atom is square pyramidal and the apical oxygen-vanadium bond length is $1.583(5) \text{ \AA}$. There is no coordination to the vacant sixth position of the vanadium atom. Ligand geometry is strongly influenced by intramolecular forces.

ACKNOWLEDGEMENTS

The author wishes to express his gratitude and appreciation to:

Dr. T. N. Waters and Dr. D. Hall for introducing me to X-ray crystallography.

Dr. M. J. Bennett for his guidance during the course of this research.

The University of Alberta crystallographic group for their help and friendship.

The University of Alberta for financial assistance.

My wife, Sharon, whose encouragement and help were so necessary during the work for this thesis.

TABLE OF CONTENTS

	Page
ABSTRACT.....	i
ACKNOWLEDGEMENTS.....	iii
LIST OF TABLES	vi
LIST OF FIGURES.....	x
CHAPTER I: THE CRYSTAL STRUCTURE OF HEXAKIS (DIMETHYLFORMAMIDE) IRON (III) PERCHLORATE	
Introduction.....	1
Experimental.....	2
Solution and Refinement.....	7
Results.....	16
Discussion.....	31
CHAPTER II: THE DITHIO LIGANDS.....	36
CHAPTER III: THE CRYSTAL STRUCTURE OF TRIS (DIMETHYL- DITHIOPHOSPHINATO) CHROMIUM (III)	
Experimental.....	41
Solution and Refinement.....	48
Results.....	62
Discussion.....	75

Table of Contents
(Continued)

	Page
CHAPTER IV: THE CRYSTAL STRUCTURE OF BIS(DIMETHYLDITHIOPHOSPHINATO) COBALT(II)	
Experimental.....	83
Solution and Refinement.....	87
Results.....	92
Discussion.....	100
CHAPTER V: THE CRYSTAL STRUCTURE OF BIS(DIMETHYL- DITHIOPHOSPHINATO)OXOVANADIUM(IV)	
Experimental.....	105
Solution and Refinement.....	110
Results.....	124
Discussion.....	136
CHAPTER VI: THE (S₂PR₂) LIGAND.....	142
REFERENCES:	150
APPENDIX A: Conventional Crystallographic Symbols.....	161
APPENDIX B: Programs used in Crystal Structure Solution, Refinement, and Analysis.....	163

LIST OF TABLES

	Page
CHAPTER I:	THE CRYSTAL STRUCTURE OF HEXAKIS (DIMETHYLFORMAMIDE) IRON (III) PERCHLORATE
Table 1	Derivation of the Harker vectors for space group Cc..... 12
Table 2	Derivation of the Harker vectors for special position b (Ξa) of space group C2/c..... 13
Table 3	Derivation of the Harker vectors for special position c (Ξd) of space group C2/c..... 14
Table 4	Derivation of the Harker vectors for special position e of space group C2/c..... 15
Table 5	Atomic Coordinates and Equivalent Isotropic Thermal Parameters..... 21
Table 6	Anisotropic Thermal Parameters..... 22
Table 7	Intramolecular distances for the Fe(DMF) ₆ cation. 23
Table 8	Intramolecular distances for the (ClO ₄) ⁻ anions..... 24
Table 9	Intramolecular angles for the Fe(DMF) ₆ cation..... 25
Table 10	Intramolecular angles for the (ClO ₄) ⁻ anions..... 26
Table 11	Interion contacts..... 27
Table 12	Weighted mean molecular planes..... 29
Table 13	Observed and calculated structure amplitudes..... 30
Table 14	Comparison of DMF containing compounds 31

List of Tables
(continued)

		Page
CHAPTER III: THE CRYSTAL STRUCTURE OF TRIS(DIMETHYLDITHIOPHOSPHINATO) CHROMIUM(III)		
Table 15	General Harker vectors for the space group $P2_12_12_1$	57
Table 16	Derivation of the Cr-S image vectors for the Harker plane $x=\frac{1}{2}$	58
Table 17	Derivation of the Cr-S image vectors for the Harker plane $y=\frac{1}{2}$	59
Table 18	Derivation of the Cr-S image vectors for the Harker plane $z=\frac{1}{2}$	60
Table 19	Possible sign combinations for the three minimum functions $M_2(x)$, $M_2(y)$, and $M_2(z)$	61
Table 20	Minimum function sign sharing.....	50
Table 21	Magnitude and signs of Δx_1 , Δy_1 , Δz_1 , etc.....	52
Table 22	Atomic coordinates and equivalent isotropic thermal parameters.....	66
Table 23	Anisotropic thermal parameters.....	67
Table 24	Intramolecular distances.....	68
Table 25	Intramolecular angles.....	69
Table 26	Intermolecular non-bonded contacts....	71
Table 27	Weighted mean molecular planes.....	72
Table 28	Observed and calculated structure amplitudes.....	74
Table 29	Structural data for tris-substituted dithio complexes.....	77

List of Tables
(continued)

		Page
CHAPTER IV:	THE CRYSTAL STRUCTURE OF BIS(DIMETHYLDITHIOPHOSPHINATO) COBALT(II)	
Table 30	Atomic coordinates and equivalent isotropic temperature parameters....	95
Table 31	Anisotropic temperature parameters..	96
Table 32	Intramolecular distances.....	97
Table 33	Intramolecular angles.....	98
Table 34	Observed and calculated structure amplitudes.....	99
Table 35	Comparison of bond angles of polymeric compounds.....	102
 CHAPTER V:	 THE CRYSTAL STRUCTURE OF BIS(DIMETHYL-DITHIOPHOSPHINATO)OXOVANADIUM(IV)	
Table 36	Atomic coordinates and equivalent isotropic thermal parameters.....	128
Table 37	Anisotropic thermal parameters.....	129
Table 38	Intramolecular distances.....	130
Table 39	Intramolecular angles.....	131
Table 40	Intermolecular non-bonded contacts .	132
Table 41	Weighted mean molecular planes.....	133
Table 42	Observed and calculated structure amplitudes.....	135
Table 43	Comparison of oxovanadium(IV) complexes.....	139

List of Tables
(continued)

	Page
CHAPTER VI: THE (S ₂ PR ₂) LIGAND	
Table 44 Comparison of (S ₂ PR ₂) ligand parameters.....	143

LIST OF FIGURES

		Page
CHAPTER I:	THE CRYSTAL STRUCTURE OF HEXAKIS(DIMETHYLFORMAMIDE)IRON(III) PERCHLORATE	
Figure 1	The $\{\text{Fe}(\text{DMF})_6\}(\text{ClO}_4)_3$ formula unit with the atoms scaled in the ratio of their Van der Waals radii, showing the spatial arrangement of the ions.....	17
Figure 2	A perspective view of the $\text{Fe}(\text{DMF})_6$ cation with 50% probability ellipsoids.....	18
Figure 3	A perspective view of the 'general' perchlorate group with 40% probability ellipsoids.....	19
Figure 4	A perspective view of the 'special' perchlorate group with 40% probability ellipsoids.....	20
CHAPTER III:	THE CRYSTAL STRUCTURE OF TRIS- (DIMETHYLDITHIOPHOSPHINATO) CHROMIUM(III)	
Figure 5	A perspective view of the $\text{Cr}(\text{S}_2\text{PMe}_2)_3$ molecule with 50% probability ellipsoids.....	63
Figure 6	The molecular packing of $\text{Cr}(\text{S}_2\text{PMe}_2)_3$ projected onto the ab plane.....	64
Figure 7	The molecular packing of $\text{Cr}(\text{S}_2\text{PMe}_2)_3$ projected onto the bc plane.....	65
CHAPTER IV:	THE CRYSTAL STRUCTURE OF BIS(DIMETHYLDITHIOPHOSPHINATO) COBALT(II)	
Figure 8	A perspective view of the $\text{Co}(\text{S}_2\text{PMe}_2)_2$ entity with 60% probability ellipsoids.....	93

List of Figures
(continued)

		Page
Figure 9	The molecular packing of $\text{Co}(\text{S}_2\text{PMe}_2)_2$ viewed approximately down the b axis.....	94
Figure 10	A schematic view of the 'singly and triply' bridging mode of the phosphinate polymers.....	101
Figure 11	A schematic view of the eight membered ring 'dimer' of phosphinates	101
CHAPTER V:	THE CRYSTAL STRUCTURE OF <i>BIS</i> (DIMETHYLDITHIOPHOSPHINATO) OXOVANADIUM(IV)	
Figure 12	A perspective view of the $\text{VO}(\text{S}_2\text{PMe}_2)_2$ molecule with 50% probability ellipsoids.....	125
Figure 13	A side on view of the $\text{VO}(\text{S}_2\text{PMe}_2)_2$ molecule where M1 and M2 are the mid-points between the atoms S1-S2 and S3-S4 respectively.....	126
Figure 14	The molecular packing of $\text{VO}(\text{S}_2\text{PMe}_2)_2$ onto the ac plane.....	127

The work done for this thesis involves X-ray diffraction. Undefined symbols have their standard crystallographic meaning and are defined in Appendix A. The standard theoretical and experimental procedures may be found in detail elsewhere.^{1,2,3}

CHAPTER I

**THE CRYSTAL STRUCTURE OF
(HEXAKIS (DIMETHYLFORMAMIDE) IRON (III) PERCHLORATE**

INTRODUCTION

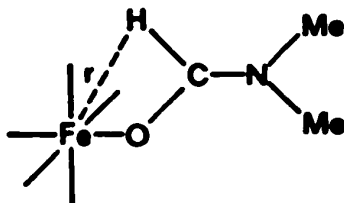
Interest in the line broadening effects in n.m.r. spectroscopy lead to the investigation of the series $M(\text{DMF})_x(\text{ClO}_4)_y$ where

$M = \text{Fe, V, Cr}$

DMF = dimethylformamide

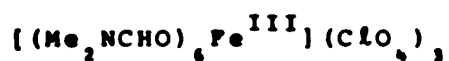
$x, y = \text{stoichiometric ratios}$

This effect is partially dependent on the distance between the metal atom and the hydrogen atom attached to the chain carbon of the dimethylformamide group. The factor involved is $\frac{1}{r^6}$ where r is defined by



Matwiyoff⁴ estimated this distance using published values for bond angles and bond lengths⁵ of the DMF molecule and the metal ion under consideration. Acceptable agreement between experimental and theoretical values of n.m.r. data, using the calculated distance, was not realised however.

Consequently the crystal structure of *hexakis*(dimethylformamide)iron(III) perchlorate,



was undertaken to try and establish the distance r .

The bright yellow prisms of $\text{Fe}(\text{DMF})_6(\text{ClO}_4)_3$, kindly supplied by Dr. N. S. Angerman,⁶ were prepared by the reaction of FeCl_3 , AgClO_4 , and DMF in the presence of molecular sieves and under vacuum. After filtering off the precipitated silver chloride and distilling off the excess DMF, crystals very sensitive to moisture were formed. The analysis figures as supplied by Dr. Angerman are as follows:

	<u>H</u>	<u>N</u>	<u>C</u>
Calculated:	5.34%	10.62%	27.30%
Found:	5.23%	10.66%	27.29%

EXPERIMENTAL

Collection and Reduction of Data

Preliminary Weissenberg ($h0l$, $h1l$, $hk0$, hkl) and precession ($hk0$, $0kl$) photographs taken with Cu K α ($\lambda = 1.5418\text{\AA}$) and Mo K α ($\lambda = 0.7107\text{\AA}$) radiation respectively exhibited the following systematic absences:

$$hkl: \quad h+k = 2n+1; \quad h0l: \quad l = 2n+1$$

These absences correspond to the space groups $Cc(C_2^h, \text{No.9})$ or $C2/c(C_{2h}^2, \text{No.15})$. The unit cell dimensions were obtained at 20°C using Zr filtered Mo K α radiation ($\lambda = 0.71069\text{\AA}$) and are:

$$\begin{array}{ll} a = 20.504 \pm 0.009\text{\AA} & \alpha = 90.0^\circ \\ b = 13.642 \pm 0.003\text{\AA} & \beta = 99.50^\circ \pm 0.05^\circ \\ c = 13.12 \pm 0.01\text{\AA} & \gamma = 90.0^\circ \end{array}$$

The errors in the cell parameters were obtained from the errors in reciprocal lattice spacings, which were calculated by least squares analysis.⁷ The camera was calibrated by comparison of results from an axial determination using the Picker diffractometer. The experimental density, measured by flotation in a chlorobenzene and bromobenzene mixture, was 1.43 g./cm.³ The value calculated for a formula weight of 792.67 a.m.u., a unit cell volume of 3622.8 Å³, and Z=4 was 1.453 g./cm.³

An initial set of data was collected using the Weissenberg equi-inclination film technique with Ni filtered Cu K α radiation. Two crystals, of major dimensions (0.16 mm. \times 0.10 mm. \times 0.21 mm.) and (0.31 mm. \times 0.24 mm. \times 0.20 mm.), were mounted on glass fibres and dipped in shellac to prevent decomposition and had their b and c axes respectively, aligned coincident with the rotation axis of the camera. Reciprocal lattice levels (h0 ℓ - h1 $\ell\ell$) and (hk0 - hk2) were collected and 1530 above background intensities were estimated by visual comparison with an intensity strip. Data reduction was done using the method of Hamilton, Rollett and Sparks⁸ and the usual Lorentz and polarization corrections were applied. The dimensions of the two crystals were carefully measured and absorption corrections ($\mu_{\text{Cu}} = 62.63 \text{ cm.}^{-1}$) were made⁹; transmission factors were in the range 0.249 - 0.402. Unit weight was

applied to all reflections during refinement.

Intensity data were collected also on a Philips PAILRED fully automated diffractometer with Mo K α radiation ($\lambda = 0.7107\text{\AA}$) monochromatised by the (002) reflection of a graphite crystal and using a tube take-off angle of 6.0° . The prism used for data collection, which had major dimensions $0.36\text{ mm.} \times 0.42\text{ mm.} \times 0.12\text{ mm.}$, was mounted on a glass fibre and then dipped in shellac solution to prevent decomposition. The crystal was mounted with its b-axis coincident with the ω -axis of the diffractometer. The crystal was 13.0 cm. from the source while the distance from the source to the circular aperture of the detector was 10.0 cm. The source collimator was 0.039 inches in diameter. Intensities were measured using a scintillation counter with the pulse height analyser set to accept approximately 90% of the transmitted peak when the window was centered on the K α peak. The equi-inclination technique and a moving crystal-stationary counter (ω -scan) scanning procedure were employed. A scan speed $1.0^\circ/\text{minute}$ was used at all times. Reciprocal lattice levels $h0l - h11l$ were scanned, but as the PAILRED diffractometer uses Weissenberg geometry due allowances had to be made for the expansion of the reflection as μ , the equi-inclination angle, was increased. This necessitated increasing the circular aperture from 2.5° for the $h0l - h5l$ layers inclusive to 3.0° for the

remaining six layers. Corresponding changes in half scan widths were also needed:

Level:	h(0-2)l	h(3-5)l	h(6-8)l	h(9,10)l	h11l
1/2 scan in:	1.4°	1.4°	1.4°	1.8°	2.3°
1/2 scan out:	0.8°	1.0°	1.0°	1.4°	1.8°

Stationary background counts were measured for twenty seconds immediately before and after each scan. A total of 3413 independent reflections were scanned with $2\theta \leq 62.0^\circ$. Nine zero layer reflections were monitored after each layer to check for crystal and electronic instability. No systematic trend was evident and the maximum intensity variation was approximately 10%. These data were then used to put all data onto a common scale. Thirteen very intense reflections whose count ratios exceeded the linear response range of the counting system were remeasured at a lower power, obtained by lowering the milliamperage and voltage on the X-ray tube. To scale these reflections to a level common with the rest of the data, five intense reflections at full power, were also measured at the same reduced power and the resulting intensity ratios were then used as a scaling factor.

Experimental data were corrected for background assuming a linear variation over the scan range. The integrated intensities obtained were then corrected for Lorentz and polarization effects, Weissenberg geometry,

and a relatively scaled set of $|F_o|$ and $|F_o|^2$ calculated.¹⁰
 A total of 1164 independent intensities were found to be statistically significant using the dual criteria:

$$I > 0 \text{ and } \frac{\Delta(I)}{I} \leq 0.35$$

where $I = T - \tau B$

$$\Delta(I) = (T + \tau^2 B)^{\frac{1}{2}}$$

and

T = peak count

B = total background count

τ = ratio of peak counting time to the total background counting time i.e. $\tau_T / (\tau_1 + \tau_2)$.

Only these statistically significant reflections were used during the subsequent refinement. Standard deviations in $|F_o|$ were derived from the standard deviations of the experimental intensities, according to Doedens and Ibers,¹¹ using an uncertainty factor, p , of 0.06. The weighting scheme used throughout the refinement was $w = \frac{1}{\sigma^2} \cdot (|F_o|)$. In the final stages of refinement absorption corrections were applied to these data.⁹ The crystal was accurately measured and absorption corrections ($\mu_{Mo} = 7.164 \text{ cm}^{-1}$) applied to I and $\sigma(F)$. The calculated transmission factors were in the range 0.824 - 0.924.

SOLUTION AND REFINEMENT OF THE STRUCTURE

The space group C2/c was initially preferred as a result of the observation that well formed crystals had symmetry 2/m. The choice of space group received additional support from the distribution of the vector peaks (q.v.) in the three dimensional Patterson map calculated from the film data.

Density measurements had indicated that there were four formula units per unit cell. The space group C2/c has eight general positions, thus restricting the iron atom to a special position; the choices here, because of the expected octahedral coordination of the iron atoms were inversion centres or twofold axes. The unit cell contains twelve perchlorate ions and assuming that they are tetrahedral and not disordered, the only special positions compatible with the Td symmetry of the ions are twofold axes. The twelve ions may be distributed as follows:

(a) Three ions lying on each of the four twofold axes, where, for example, the chlorine atoms would have coordinates $(0, y_1, \frac{1}{2})$, $(0, y_2, \frac{1}{2})$, and $(0, y_3, \frac{1}{2})$. This arrangement, while possible, is extremely unlikely because of the destabilising influence of the repulsive forces that would be expected from the close approach of ions of the same charge.

(b) Eight perchlorate ions in general positions and four ions on twofold axes. This arrangement allows three

ions to be grouped around each iron atom at approximately equal distances and hence was preferred.

The position of the iron atom and the space group were found by analysis of the Patterson map with reference to the Harker vectors for C2/c and Cc that are listed in Tables 1-4. The two largest peaks, of equal height, were found at $(0, \frac{1}{2}, \frac{1}{2})$ and $(\frac{1}{2}, 0, \frac{1}{2})$ and these are consistent with an iron atom sitting on an inversion centre at special positions, of Wyckoff notation, c or d [c was used, $(\frac{1}{4}, \frac{1}{4}, \frac{1}{2})$] of space group C2/c. Space group Cc would only have been possible if the y coordinate had been 0.25 exactly, and this was unlikely. Special positions a and b of C2/c would have also required the y coordinate to have been 0.25.

The 'general' chlorine was located by deducing the expected Fe-Cl_G vectors as follows:

	$\bar{x}, \bar{y}, \bar{z};$	$x, \bar{y}, \frac{1}{2}-z;$	$\bar{x}, y, \frac{1}{2}-z$
$\frac{1}{2}, \frac{1}{2}, 0$	$\frac{1}{2}+x, \frac{1}{2}+y, +z$	$\frac{1}{2}-x, \frac{1}{2}+y, \frac{1}{2}-z$	$\frac{1}{2}+x, \frac{1}{2}-y, \frac{1}{2}-z$

The next three largest peaks were consistent with these vectors and produced coordinates (-0.154, 0.111, 0.127) for Cl_G. The 'special' chlorine, Cl_S, was easily found using the Harker vectors listed in Table 3 and had coordinates (0.50, 0.098, 0.25). The successful identification of the iron-iron, iron-chlorine and chlorine-chlorine vectors strongly supported the space group C2/c.

These heavy atom coordinates were inserted into a structure factor calculation¹² and an F_{obs} Fourier was computed.¹³ Twelve out of the remaining nineteen light atoms were located and then these atoms were subjected to two cycles of isotropic least squares refinement¹² giving $R = 0.325$, ($R = \frac{\sum ||F_o| - |F_c||}{\sum |F_o|}$). A difference Fourier was computed and all remaining atoms except the oxygen atoms attached to the 'general' chlorine were found. Four more cycles of refinement reduced R to 0.259 and the remaining light atoms were found from a difference Fourier. Three cycles of refinement with all atoms isotropic gave an R index of 0.217. Analysis of the observed and calculated structure factors showed the film data to be unreliable on comparing the calculated and observed structure factors and a new set of data was collected on the PAILRED diffractometer.

Refinement using the atomic parameters from film data analysis and the PAILRED structure factors gave a discrepancy index of 0.253 after three cycles. A difference Fourier computed at this stage showed atoms 04 - 09, C31 and C32 had been assigned incorrect atomic positions. The atoms were inserted with their correct coordinates and seven cycles of isotropic refinement reduced R to 0.158.

Absorption and decomposition corrections were performed next and the iron and perchlorate groups were allowed to refine anisotropically as indicated by residual electron density around their positions. Refinement proceeded using the program SFLS5,¹⁴ after three cycles, to $R_1 = 0.107$ and $R_2 = 0.137$ where

$$R_1 = \frac{\sum ||F_o| - |F_c||}{\sum |F_o|} \text{ and } R_2 = \left[\frac{\sum w(|F_o| - |F_c|)^2}{\sum w|F_o|^2} \right]^{1/2}$$

where $\sum w(|F_o| - |F_c|)^2$ was minimised and $w = 1/\sigma^2(F)$.

Three cycles with all atoms except O_n , C_n , N_n ($n=1-3$) anisotropic (165 variables) converged with $R_1 = 0.098$ and $R_2 = 0.125$.

The layer (h1l) showed particularly bad agreement between observed and calculated structure factor values and was therefore recollected using the same crystal, scan speeds, etc. as before. Scaling with the old data was effected by also remeasuring the h0l layer and using the ratio obtained with the initial h0l layer as a scaling factor. Four more cycles of refinement (165 variables) saw convergence at $R_1 = 0.087$ and $R_2 = 0.119$.

A final difference Fourier was computed and the highest residual peak was $0.42e^-/\text{\AA}^3$. From this Fourier an attempt was made to locate the three hydrogen atoms attached to C1, C2, and C3 but it was unsuccessful.

Analysis of the weighting scheme exhibited lack of dependence of $w\Delta^2$ ($\Delta = |F_o| - |F_c|$) when divided into ranges according to $|F_o|$ and $(\sin\theta)/\lambda$ values in accordance with Cruickshank's criterion.¹⁵ Scattering factors used were those due to Cromer and Waber¹⁶ and the anomalous dispersion corrections for iron ($\Delta f' = 0.40e^-$, $\Delta f'' = 1.0e^-$) and chlorine ($\Delta f' = 0.1e^-$, $\Delta f'' = 0.20e^-$) applied to F_{calc} were taken from International Tables of X-ray Crystallography.¹⁷

x, y, z $x, -y, z$ $x+x, y+y, z$ $x+x, y-y, z+z$

x, y, z	$0, 0, 0$	$0, 2y, z$	$x, z, 0$	$x, z+2y, z$
$x, -y, z+z$	$0, -2y, z$	$0, 0, 0$	$x, z-2y, z$	$x, z, 0$
$x+x, y+y, z$	$x, z, 0$	$x, z+2y, z$	$0, 0, 0$	$0, +2y, z$
$x+x, y-y, z+z$	$x, z+2y, z$	$x, z, 0$	$0, -2y, z$	$0, 0, 0$

Table 1. Derivation of the Harker Vectors for Space Group Cc.

$0, \frac{1}{2}, 0$	$0, \frac{1}{2}, 0$	$0, \frac{1}{2}, \frac{1}{2}$	$\frac{1}{2}, 0, 0$	$\frac{1}{2}, 0, \frac{1}{2}$
$0, \frac{1}{2}, \frac{1}{2}$	$0, 0, 0$	$0, 0, \frac{1}{2}$	$\frac{1}{2}, 0, 0$	$\frac{1}{2}, \frac{1}{2}, \frac{1}{2}$
$\frac{1}{2}, 0, 0$	$0, 0, \frac{1}{2}$	$0, 0, 0$	$\frac{1}{2}, \frac{1}{2}, \frac{1}{2}$	$\frac{1}{2}, \frac{1}{2}, 0$
$\frac{1}{2}, 0, \frac{1}{2}$	$\frac{1}{2}, 0, 0$	$\frac{1}{2}, \frac{1}{2}, \frac{1}{2}$	$0, 0, 0$	$0, 0, \frac{1}{2}$

Table 2. Derivation of the Harker Vectors for Special Position b ($\bar{3}m$) of Space Group C2/c.

$\frac{1}{2}, \frac{1}{2}, 0$	$\frac{1}{2}, \frac{1}{2}, \frac{1}{2}$	$\frac{3}{4}, \frac{3}{4}, 0$	$\frac{1}{2}, \frac{1}{2}, \frac{1}{2}$
$\frac{1}{2}, \frac{1}{2}, 0$	$0, 0, 0$	$\frac{1}{2}, \frac{1}{2}, 0$	$0, \frac{1}{2}, \frac{1}{2}$
$\frac{3}{4}, \frac{1}{4}, \frac{1}{2}$	$\frac{1}{2}, 0, \frac{1}{2}$	$0, \frac{1}{2}, \frac{1}{2}$	$\frac{1}{2}, \frac{1}{2}, 0$
$\frac{3}{4}, \frac{3}{4}, 0$	$\frac{1}{2}, \frac{1}{2}, 0$	$0, \frac{1}{2}, \frac{1}{2}$	$\frac{1}{2}, 0, \frac{1}{2}$
$\frac{1}{2}, \frac{3}{4}, \frac{1}{2}$	$0, \frac{1}{2}, \frac{1}{2}$	$\frac{1}{2}, 0, \frac{1}{2}$	$0, 0, 0$

Table 3. Derivation of the Harker Vectors for Special Position c ($\bar{3}d$) of Space Group C2/c.

$0, y, k$	$0, -y, k$	$0, 2y, k$	$0, 0, 0$	$0, -y, k$	$k, k+y, k$	$k, k-y, k$
$0, y, k$	$0, 0, 0$	$0, 2y, k$	$0, 0, 0$	$k, k, 0$	$k, k+2y, k$	$k, k, 0$
$0, -y, k$	$0, -2y, k$	$0, 0, 0$	$0, 0, 0$	$k, k-2y, k$	$0, 0, 0$	$0, 2y, k$
$k, k+y, k$	$k, k, 0$	$k, k+2y, k$	$k, k, 0$	$k, k, 0$	$0, -2y, k$	$0, 0, 0$
$k, k-y, k$	$k, k-2y, k$	$k, k, 0$	$k, k-2y, k$	$k, k, 0$		

Table 4. Derivation of the Harker Vectors for Special Position e of Space Group

C2/c.

RESULTS

Figure 1 shows the spatial arrangement of the ions of $\text{Fe}(\text{DMF})_6(\text{ClO}_4)_3$, and the atom numbering scheme. Figure 2 is a view of the cation showing the thermal ellipsoids of vibration.¹⁸ The two anions are illustrated in Figures 3 and 4. Table 13 lists the final calculated and observed structure amplitudes. Table 5 reports the fractional coordinates and isotropic temperature factors (where applicable) for the atoms of the asymmetric unit. Anisotropic thermal parameters are listed in Table 6. Tables 7-12 contain data on molecular bond lengths, angles, inter-ion approach distances, and least squares planes.

Figure 1

A view of the $\text{Fe}(\text{DMF})_6(\text{ClO}_4)_2$ formula unit with the atoms scaled in the ratios of their Van Der Waals radii showing the spatial arrangement of the ions.

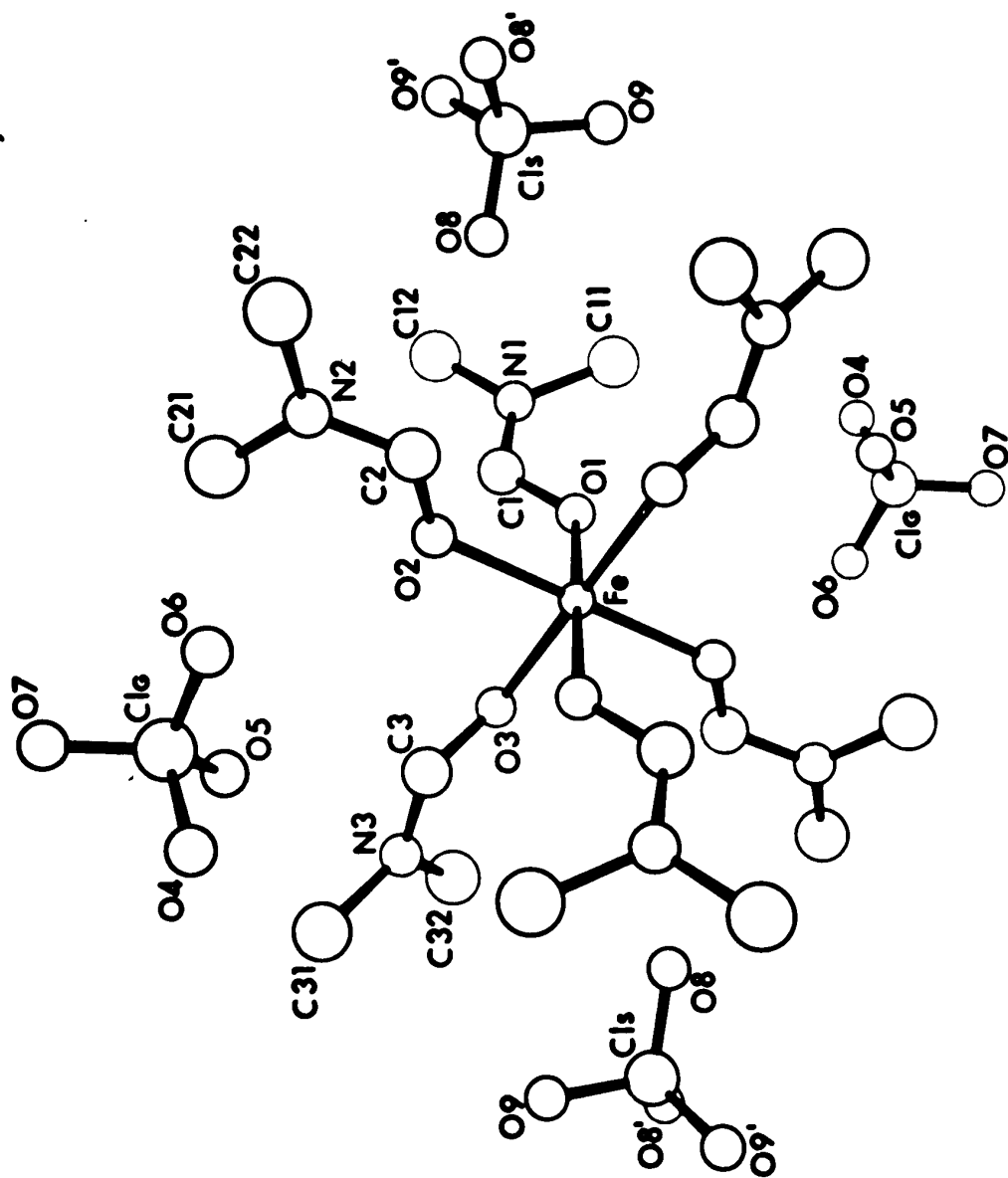


Figure 2

A perspective view of the $\text{Fe}(\text{DMF})_6^{3+}$ cation
with 50% probability ellipsoids.

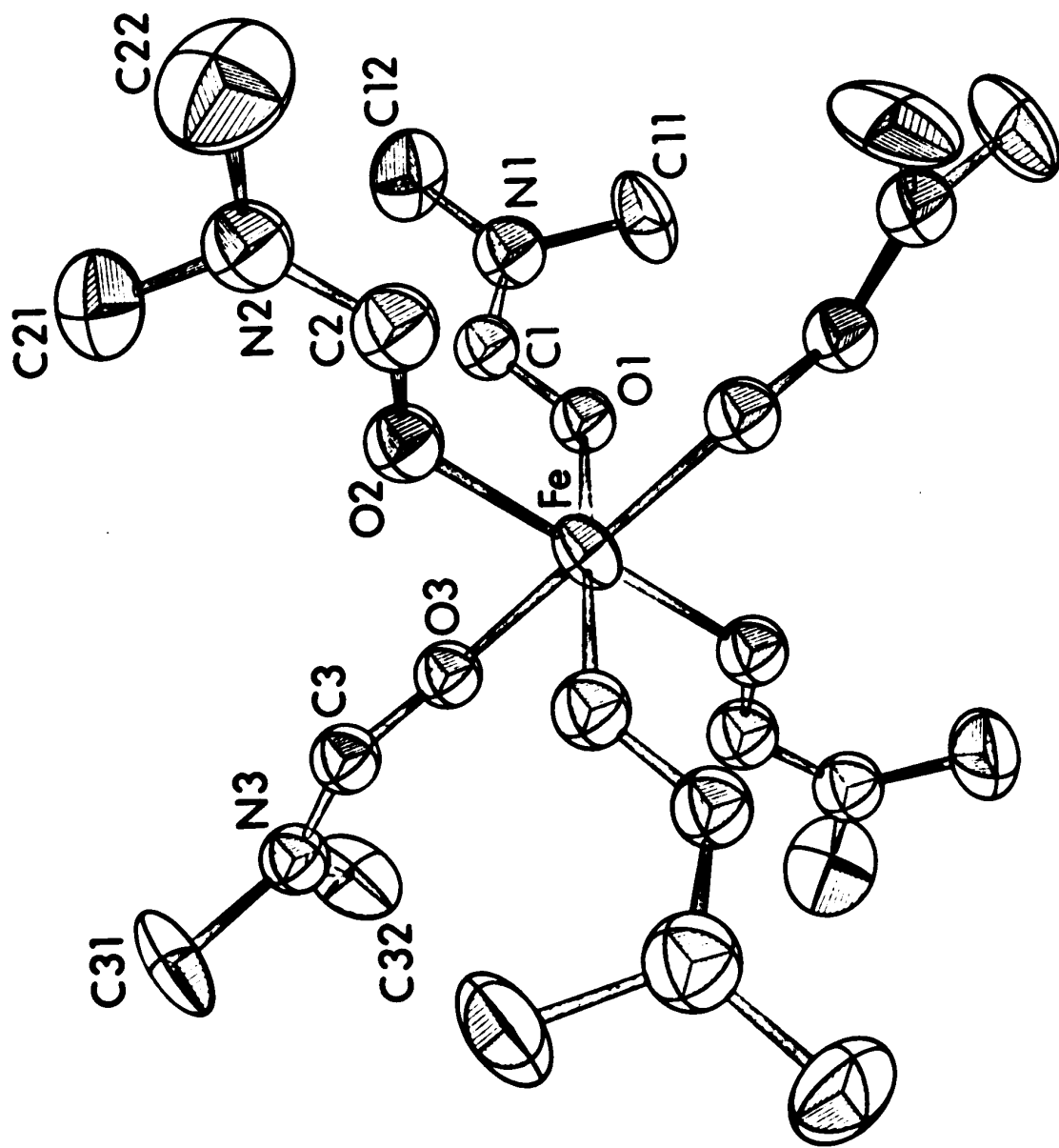


Figure 3

A perspective view of the 'general' perchlorate group with 40% probability ellipsoids.

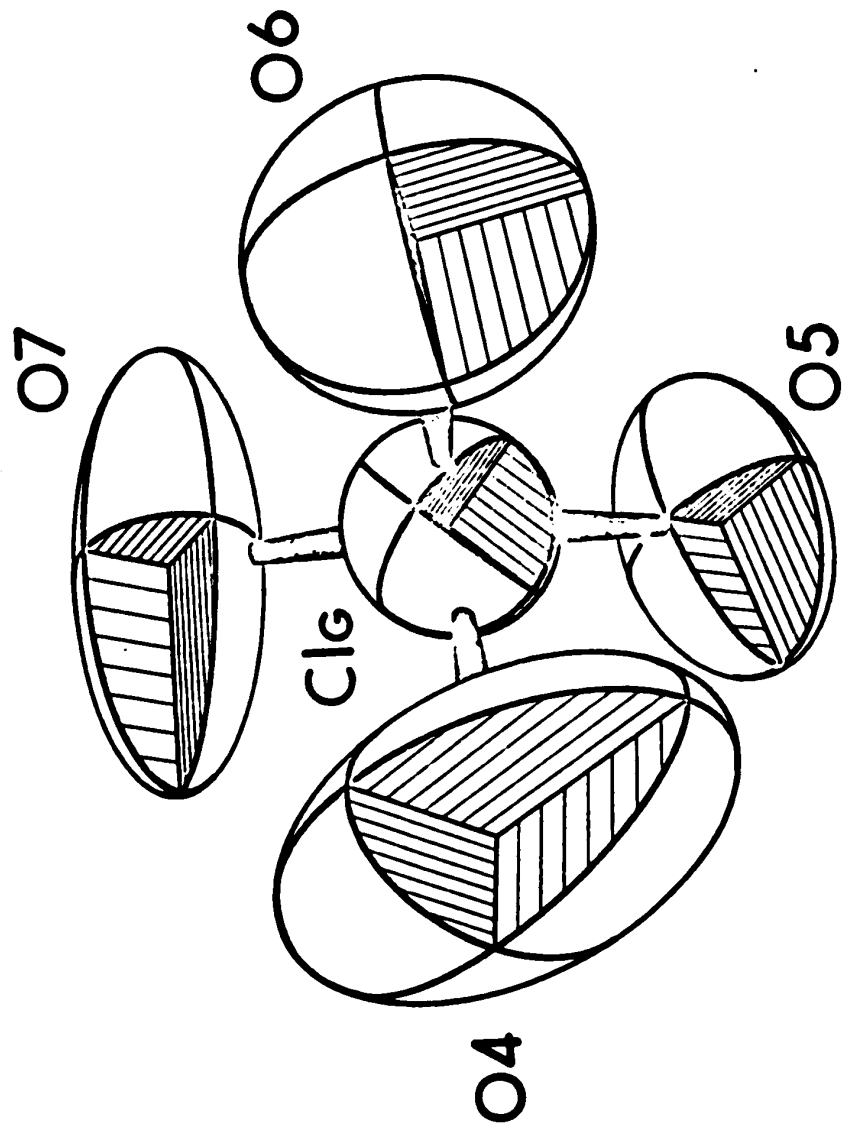


Figure 4

A perspective view of the 'special' perchlorate group with 40% probability ellipsoids.

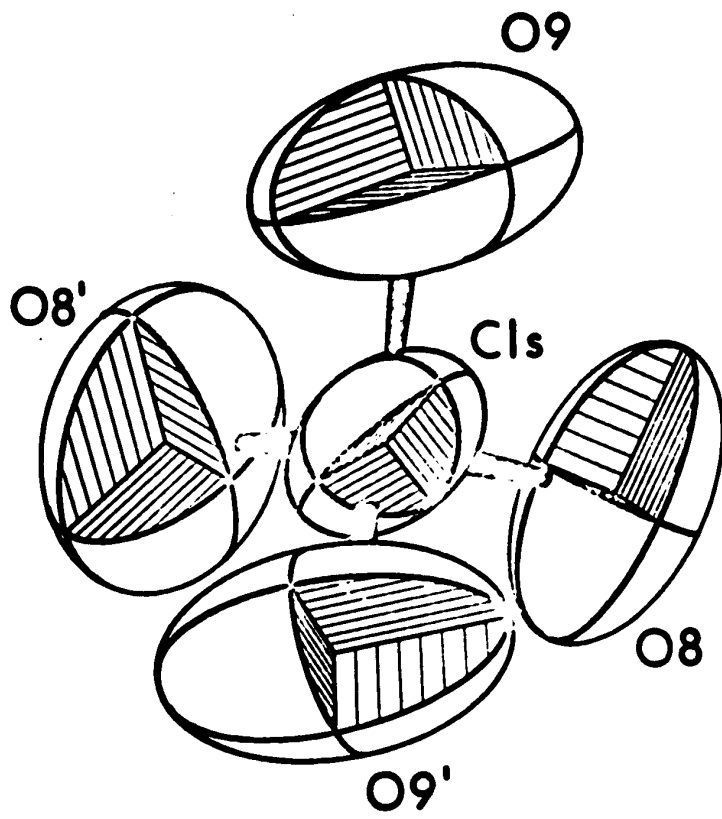


Table 5

**Final Atomic Coordinates and Equivalent Isotropic
Temperature Factors for $\text{Fe}(\text{DMF})_6 \cdot (\text{ClO}_4)_3$.**

	\underline{x}	\underline{y}	\underline{z}	$B, \text{\AA}^2$
Fe	0.75 [#]	0.25 [#]	0.5 [#]	4.07 [*]
O1	0.7839(3) ^a	0.2244(5)	0.6487(5)	4.4(2)
O2	0.8364(4)	0.2133(5)	0.4629(5)	4.8(2)
O3	0.7239(3)	0.1108(5)	0.4801(5)	4.4(1)
C1	0.8366(5)	0.1744(7)	0.6859(8)	4.5(2)
C2	0.8826(6)	0.2690(8)	0.4478(8)	5.2(2)
C3	0.7320(5)	0.0600(8)	0.3981(7)	4.4(2)
N1	0.8622(5)	0.1847(7)	0.7836(7)	6.1(2)
N2	0.9390(5)	0.2358(7)	0.4266(6)	5.3(2)
N3	0.6887(4)	-0.0192(6)	0.3777(6)	4.6(2)
C11	0.8403(7)	0.2641(9)	0.8491(9)	7.63 [*]
C12	0.9194(7)	0.1291(11)	0.8263(10)	8.38 [*]
C21	0.9486(7)	0.1344(10)	0.4152(12)	8.71 [*]
C22	0.9914(8)	0.3017(12)	0.4058(13)	9.76 [*]
C31	0.6882(8)	-0.0712(9)	0.2797(10)	8.07 [*]
C32	0.6460(7)	-0.0544(10)	0.4463(10)	7.74 [*]
Cl _G	0.8464(2)	0.1075(3)	0.1290(3)	6.39 [*]
Cl _S	0.5 [#]	0.1006(5)	0.25 [#]	9.24 [*]
O4	0.8007(10)	0.1260(25)	0.0447(13)	26.16 [*]
O5	0.8119(6)	0.0666(7)	0.2003(8)	10.75 [*]
O6	0.8737(8)	0.1960(10)	0.1501(13)	15.74 [*]
O7	0.8892(9)	0.0460(9)	0.1017(14)	18.04 [*]
O8	0.5436(8)	0.1546(12)	0.3160(10)	15.21 [*]
O9	0.5354(9)	0.0428(14)	0.1976(15)	21.30 [*]

^aNumbers in parentheses are estimated standard deviations occurring in the last digits listed.

^{*}The anisotropic temperature factors for these atoms are listed in Table 6.

[#]These parameters were not refined because of restraints due to site symmetry.

Table 6. Anisotropic Temperature Parameters ($\times 10^5$) for Fe(DMF)₆·(ClO₄)₃.^b

Atom	β_{11}	β_{22}	β_{33}	β_{12}	β_{13}	β_{23}
Fe	356(8) ^a	397(14)	525(14)	-50(9)	102(7)	-20(12)
C11	744(60)	735(96)	720(85)	161(60)	9(56)	-284(70)
C12	545(55)	1242(131)	899(102)	365(67)	-145(61)	110(85)
C21	450(51)	897(124)	1821(158)	116(59)	185(74)	-362(102)
C22	497(57)	1246(139)	1920(178)	-117(70)	449(84)	404(121)
C31	731(62)	697(94)	1140(116)	-118(60)	320(69)	-564(83)
C32	477(50)	1018(101)	1293(123)	-503(60)	364(65)	-218(89)
Cl ^G	475(13)	693(25)	959(27)	-94(15)	166(16)	117(20)
Cl ^S	642(26)	740(41)	1676(65)	0 [*]	39(37)	0 [*]
O4	944(75)	6478(515)	1885(180)	-710(166)	-379(102)	1534(240)
O5	869(50)	1116(80)	1760(110)	-195(51)	795(66)	143(71)
O6	1051(67)	1323(124)	3176(201)	-568(78)	628(98)	-423(123)
O7	1354(92)	1000(102)	4496(274)	-181(75)	2002(151)	-216(117)
O8	1256(79)	1656(131)	1698(129)	-648(87)	-143(84)	-94(95)
O9	1270(103)	1847(207)	4321(319)	364(94)	286(137)	-1281(188)

^a These parameters were not refined because of restraints due to site symmetry.

^b Numbers in parentheses are estimated standard deviations in the last digits listed.

^c Anisotropic thermal parameters defined by

$$\exp[-(\beta_{11}h^2 + \beta_{22}k^2 + \beta_{33}l^2 + 2\beta_{12}hk + 2\beta_{13}hl + 2\beta_{23}kl)]$$

Table 7Intramolecular Distances (Å) for the $\text{Fe}(\text{DMF})_3^{3+}$ Cation

<u>Atoms</u>	<u>Distance</u>
Fe - O1	1.991(6) ^a
Fe - O2	1.978(7)
Fe - O3	1.979(7)
O1 - C1	1.256(11)
O2 - C2	1.256(11)
O3 - C3	1.277(11)
C1 - N1	1.327(12)
C2 - N2	1.313(12)
C3 - N3	1.293(12)
N1 - C11	1.497(14)
N1 - C12	1.432(14)
N2 - C21	1.409(15)
N2 - C22	1.461(15)
N3 - C31	1.467(13)
N3 - C32	1.439(13)

^aNumbers in parentheses are estimated standard deviations occurring in the last digits listed.

Table 8Intramolecular Distances (Å) for the $(\text{ClO}_4)^-$ Anions.

<u>Atoms</u>	<u>Distance</u>
$\text{Cl}_G - 04$	1.349(16) ^a
$\text{Cl}_G - 05$	1.380(9)
$\text{Cl}_G - 06$	1.341(13)
$\text{Cl}_G - 07$	1.306(13)
$\text{Cl}_S - 08$	1.355(12)
$\text{Cl}_S - 09$	1.336(15)

^aNumbers in parentheses are estimated standard deviations occurring in the last digits listed.

Table 9Intramolecular Angles (Degree) for the $\text{Fe}(\text{DMF})_6^{3+}$ Cation

<u>Atoms</u>	<u>Angle</u>
O1 - $\hat{\text{Fe}}$ - O2	90.9(3) ^a
O1 - $\hat{\text{Fe}}$ - O3	90.3(3)
O2 - $\hat{\text{Fe}}$ - O3	87.6(3)
Fe - $\hat{\text{O}}1$ - C1	127.3(6)
Fe - $\hat{\text{O}}2$ - C2	128.0(7)
Fe - $\hat{\text{O}}3$ - C3	126.7(7)
O1 - $\hat{\text{C}}1$ - N1	121.3(10)
O2 - $\hat{\text{C}}2$ - N2	122.6(10)
O3 - $\hat{\text{C}}3$ - N3	124.0(9)
C1 - $\hat{\text{N}}1$ - C11	120.3(9)
C1 - $\hat{\text{N}}1$ - C12	121.7(10)
C2 - $\hat{\text{N}}2$ - C21	120.3(11)
C2 - $\hat{\text{N}}2$ - C22	121.9(11)
C3 - $\hat{\text{N}}3$ - C31	120.7(9)
C3 - $\hat{\text{N}}3$ - C32	121.1(9)
C11 - $\hat{\text{N}}1$ - C12	117.6(10)
C21 - $\hat{\text{N}}2$ - C22	117.6(11)
C31 - $\hat{\text{N}}3$ - C32	118.0(9)

^aNumbers in parentheses are estimated standard deviations occurring in the last digit listed.

Table 10Intramolecular Angles (degree) for the $(\text{ClO}_4)^-$ Anions.

<u>Atoms</u>	<u>Angle</u>
04 - $\hat{\text{Cl}}_G$ - 05	105.5(10) ^a
04 - $\hat{\text{Cl}}_G$ - 06	102.2(15)
04 - $\hat{\text{Cl}}_G$ - 07	107.6(15)
05 - $\hat{\text{Cl}}_G$ - 06	117.9(8)
05 - $\hat{\text{Cl}}_G$ - 07	111.6(8)
06 - $\hat{\text{Cl}}_G$ - 07	111.0(9)
08 - $\hat{\text{Cl}}_S$ - 09	106.9(11)
08 - $\hat{\text{Cl}}_S$ - 08'	114.1(15)
08 - $\hat{\text{Cl}}_S$ - 09'	110.5(10)
09 - $\hat{\text{Cl}}_S$ - 08'	110.5(10)
09 - $\hat{\text{Cl}}_S$ - 09'	107.6(19)
08' - $\hat{\text{Cl}}_S$ - 09'	106.9(11)

^a Numbers in parentheses are estimated standard deviations occurring in the last digits listed.

Table 11Inter Ion Contacts ($\leq 4.0\text{\AA}$) for $\text{Fe}(\text{DMF})_6(\text{C}_2\text{O}_4)_3$

<u>Atoms</u>	<u>Distance, \AA</u>	<u>Symmetry Position of Second Atom</u>		
O4 - N3	3.25	x,	y,	$-\frac{1}{2} + z$
O4 - C32	3.37	x,	y,	$-\frac{1}{2} + z$
O4 - C11	3.39	x,	y,	$-1 + z$
O4 - C3	3.42	x,	$-y,$	$-\frac{1}{2} + z$
O4 - O3	3.63	x,	$-y,$	$-\frac{1}{2} + z$
O4 - C11	3.73	$\frac{3}{2} - x,$	$\frac{1}{2} - y,$	$1 + z$
O4 - C31	3.92	x,	$-y,$	$-\frac{1}{2} + z$
O4 - N1	3.92	x,	y,	$-1 + z$
O5 - C1	3.33	x,	$-y,$	$-\frac{1}{2} + z$
O5 - C3	3.41	x,	y,	z
O5 - C31	3.45	x,	y,	z
O5 - C12	3.68	x,	$-y,$	$-\frac{1}{2} + z$
O5 - N1	3.69	x,	$-y,$	$-\frac{1}{2} + z$
O5 - C21	3.75	x,	y,	z
O5 - C11	3.85	$\frac{3}{2} - x,$	$\frac{1}{2} - y,$	$1 + z$
O5 - N3	3.89	x,	y,	z
O5 - O2	3.95	x,	y,	z
O5 - O3	3.97	x,	$-y,$	$-\frac{1}{2} + z$
O6 - C22	3.31	$2 - x,$	y,	$\frac{1}{2} - z$
O6 - C31	3.63	$\frac{3}{2} - x,$	$\frac{1}{2} + y,$	$\frac{1}{2} - z$
O6 - C32	3.60	$\frac{3}{2} - x,$	$\frac{1}{2} + y,$	$\frac{1}{2} - z$
O6 - C21	3.66	x,	y,	z
O6 - N2	3.70	x,	y,	z

Table 11 (continued)Inter Ion Contacts ($\leq 4.0\text{\AA}$) for $\text{Fe}(\text{DMF})_6(\text{C}_2\text{O}_4)_3$

<u>Atoms</u>	<u>Distance, \AA</u>	<u>Symmetry Position of Second Atom</u>		
O6 - C21	3.97	2 - x,	y,	$\frac{1}{2} - z$
O7 - C1	3.46	x,	- y,	$-\frac{1}{2} + z$
O7 - C21	3.58	2 - x,	y,	$\frac{1}{2} - z$
O7 - C12	3.77	x,	- y,	$-\frac{1}{2} + z$
O7 - C21	3.81	x,	- y,	$-\frac{1}{2} + z$
O7 - C12	3.93	x,	y,	$-1 + z$
O8 - N1	3.33	$\frac{3}{2} - x,$	$\frac{1}{2} - y,$	$1 + z$
O8 - C2	3.38	$\frac{3}{2} - x,$	$\frac{1}{2} - y,$	$1 + z$
O8 - C1	3.44	$\frac{3}{2} - x,$	$\frac{1}{2} - y,$	$1 + z$
O8 - C12	3.64	$\frac{3}{2} - x,$	$\frac{1}{2} - y,$	$1 + z$
O8 - C11	3.65	$\frac{3}{2} - x,$	$\frac{1}{2} - y,$	$1 + z$
O8 - N2	3.66	$\frac{3}{2} - x,$	$\frac{1}{2} - y,$	$1 + z$
O8 - C32	3.78	x,	y,	z
O8 - N3	3.79	x,	y,	z
O8 - O1	3.86	$\frac{3}{2} - x,$	$\frac{1}{2} - y,$	$1 + z$
O8 - C3	3.88	x,	y,	z
O8 - C22	3.88	$\frac{3}{2} - x,$	$\frac{1}{2} - y,$	$1 + z$
O8 - C12	3.92	$-\frac{1}{2} + x,$	$\frac{1}{2} - y,$	$-\frac{1}{2} + z$
O8 - O2	3.92	$\frac{3}{2} - x,$	$\frac{1}{2} - y,$	$1 + z$
O9 - C31	3.50	x,	y,	z
O9 - C22	3.57	$\frac{3}{2} - x,$	$-\frac{1}{2} + y,$	$\frac{1}{2} - z$
O9 - N3	3.71	x,	y,	z
O9 - C11	3.78	$\frac{3}{2} - x,$	$\frac{1}{2} - y,$	$1 + z$
O9 - C32	3.89	x,	y,	z
C1 _G - C1	3.94	x,	- y,	$-\frac{1}{2} + z$

Table 12. Weighted Mean Molecular Planes for Fe(DMF)₆(ClO₄)₃^a.

<u>Atoms Contained in the Plane</u>	<u>No.</u>	<u>Equation</u>
O1, C1, N1, C11, C12	1	-0.6732X - 0.6671Y + 0.3190Z = 9.3607
O2, C2, N2, C21, C22	2	0.2267X - 0.0428Y + 0.9730Z = -9.3733
O3, C3, N3, C31, C32	3	0.6920X - 0.5559Y + 0.4605Z = -11.5943

Distances of Atoms from Planes (Å)^b

- Plane 1: O1, 0.004; C1, -0.020; N1, 0.036; C11, -0.017; C12, -0.010; Fe, -0.591
 Plane 2: O2, 0.001; C2, 0.000; N2, 0.025; C21, -0.009; C22, -0.021; Fe, 0.025
 Plane 3: O3, -0.002; C3, 0.004; N3, 0.026; C31, -0.024; C32, -0.008; Fe, -0.598

^aThe orthogonal coordinate system (X,Y,Z) corresponds to the crystal a,b,c axes.

^bAverage estimated standard deviations in atom positions derived from uncertainties in fractional coordinates are as follows:

(Å): Fe, 0.006; O, 0.007; Cn(n = 1-3), 0.010; N, 0.009; Cmn(m = 1-3, n = 1,2), 0.011

Table 13

Observed and calculated structure amplitudes ($\times 10$)
in electrons for $\text{Fe}(\text{DMF})_6 \cdot (\text{ClO}_4)_3$.

DISCUSSION

The cation has the expected octahedral coordination with the mean $\text{O}-\hat{\text{Fe}}-\text{O}$ angle being 89.6° . Table 14 compares bond length and bond angles for other formamide compounds. The iron-oxygen distances show good agreement and compare well with those in other compounds.

<u>Compound</u>	<u>$\text{Fe}-\overset{\circ}{\text{O}}$(Å)</u>	<u>Reference</u>
$\text{Fe}(\text{DMF})_6(\text{ClO}_4)_3$	1.983(6)	—
$\text{Fe}(\text{acac})_3$	1.992	19
$\text{FeCl}_3(\text{DMSO})_2$	2.006(6)	20

The geometry of the coordinated dimethylformamide ligand in this structure can be compared with that observed in other complexes and with the geometry of the free ligand.

Table 14

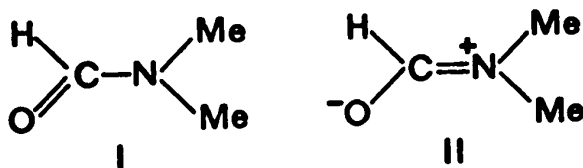
<u>Compound</u>	<u>$\text{O}-\overset{\circ}{\text{C}}$(Å)</u>	<u>$\text{C}-\overset{\circ}{\text{N}}$(Å)</u>	<u>$\text{O}-\hat{\text{C}}-\text{N}$(Deg)</u>	<u>Ref.</u>
$\text{Fe}(\text{DMF})_6(\text{ClO}_4)_3$	1.263(9)	1.311(12)	122.6(10)	—
$\text{SbCl}_5 \cdot \text{DMF}$	1.300(10)	1.287(12)	120.15(89)	21
$[\text{Co}(\text{sal})]_2 \cdot \text{O}_2 \cdot (\text{DMF})_2$	1.222(11)	1.310(11)	126.7(10)	22
$\text{NaI} \cdot (\text{DMF})_3$	1.23(4)	1.34(4)	123.6(20)	23
DMF*	1.20	1.36	123.0	24
HCONH_2	1.25(13)	1.30(13)	121.5	25

* electron diffraction

(Numbers in parentheses are estimated standard deviations occurring in the last digits listed.)

The carbonyl oxygen of the DMF ligand acts as the donor atom and this has been shown to be a frequent occurrence for amides.²⁶⁻²⁸ The length of the oxygen-carbon bond seems to be significantly longer than in the free ligand. A consequence of this donor interaction is that there is an electron density withdrawal from the oxygen atom thus causing a reduction in the bond order and hence an increase in bond length.²⁹ The coordination of the nitrogen atom is planar (see Table 12), within experimental error, for all three non-equivalent DMF groups, compared to the nearly planar framework of free DMF.²⁴

DMF may be represented as two resonance forms:



The electron density increase which the carbonyl carbon atom experiences when the complex is formed increases the σ -bond order of the carbon-nitrogen bond in the OCN group. The effect of this would be to increase the π -bond order of the nitrogen-carbon bond because of the electron density withdrawal from the amide increases the delocalisation of the lone pair of electrons of the nitrogen atom, i.e. the contribution of resonance form II is increased. These changes in σ and π -bond orders may be expected to cause a decrease in the length of the carbon-nitrogen bond when

compared to the free donor, however, the value of $1.34(4)\text{\AA}$ found by Vilkov *et al*²⁴ for free DMF is not of sufficient accuracy to be able to show any significant deviation from the observed mean value of $1.311(13)\text{\AA}$. Lide's³⁰ proposed value of $1.36(2)\text{\AA}$ for sp^2 hybridized carbon in free amides does lend support to this argument. Archambault and Rivest³¹ have reported spectroscopic evidence for the shortening of the carbon-nitrogen bond in adducts of with titanium(IV) halides when compared to free DMF. Brun *et al*²¹ reported a nitrogen-methyl carbon length of $1.504(36)\text{\AA}$ for $\text{SbCl}_5 \cdot \text{DMF}$, as compared to $1.45(2)\text{\AA}$ for free DMF,²³ and suggested that this was due to the increasing contribution from the number II resonance form of DMF. The value of $1.451(28)\text{\AA}$ for the bond length in this structure would seem not to support this argument, but the estimated corrections in bond length for thermal vibrations³² can alter the nitrogen-carbon distance by as much as 0.05\AA . This could bring the bond length for each compound into good agreement. Gobellon *et al*²³ suggested that form I is the major contributor to the electronic structure of the DMF ligand and although this structural analysis does lend some credence to the donor properties of DMF within the $\text{Fe}(\text{DMF})_6^{3+}$ cation the contribution of form II does not seem to be as great as in $\text{SbCl}_5 \cdot \text{DMF}$ molecule.

The two perchlorate anions, shown in Figures 3 and 4 show large thermal ellipsoids for the oxygen atoms which are indicative of high dynamic disorder.³³⁻³⁵ The high thermal amplitudes are consistent with the rapid fall off of significant intensities with $\sin\theta/\lambda$ and limits the precision of the structural analysis.

One of the purposes of this analysis was to find the distance between the carbonyl hydrogen atoms and the iron atom for use in n.m.r. studies. As the attempt to find the atoms from the final difference Fourier, calculated at $R = 8.7\%$, was unsuccessful, the atomic positions were calculated using vector methods.³⁶ Assuming (i) an sp^2 hybridisation for the carbon atom, and (ii) a carbon-hydrogen distance of 1.07\AA , the three independent iron-hydrogen contacts can be calculated as

Fe - H1 (attached to C1)	3.04
Fe - H2 (attached to C2)	3.02
Fe - H3 (attached to C3)	3.08
Mean	<u>3.05</u>

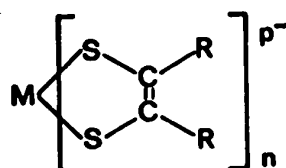
This distance is 0.35\AA longer than that estimated by Matwiyoff⁴ and has been used in calculations giving satisfactory agreement between experimental and theoretical results.³⁷ Also this metal-hydrogen distance is considerably greater than 2.59\AA for $\text{RuCl}_2[\text{P}(\text{C}_6\text{H}_5)_3]_2$,³⁸ 2.8\AA for $\text{trans}\text{-}\{\text{PdI}_2[\text{P}(\text{C}_6\text{H}_5)_3]_2\}$ ³⁹ and 2.51\AA (minimum) for $\text{trans}\text{-}[\text{Co}(\text{mesityl})_2(\text{PEt}_2\text{Ph})_2]$.⁴⁰ While for the first two

of these three complexes the hydrogen was effectively the sixth atom of a distorted octahedra around the central metal atom and for the third probably the cause of the 'stepping' of the mesityl groups, no such chemical significance can be attached to the iron-hydrogen distance in the $\text{Fe}(\text{DMF})_6$ cation.

CHAPTER II

THE DITHIO LIGANDS

In recent years great interest has been aroused in ligands that have sulphur as the donor atoms(s), especially those systems which show a series of complexes differing only in the number of valence electrons.⁴¹⁻⁵⁷ These ligands have the form



R = CN⁻, CF₃, C₆H₅, CH₃, H.

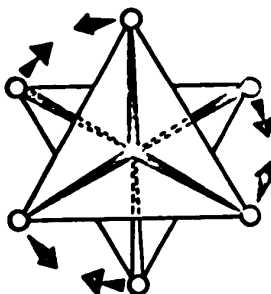
n = 2; p = 0, 1, 2; M = Co, Ni, Cu, Pd, Pt, Au, Rh

n = 3; p = 0, 1, 2, 3; M = V, Cr, Mo, W, Re, Co.

The *bis* ligand systems, discovered first with Ni²⁺ and Co²⁺, received initial attention because of the stabilisation of the square planar geometry for a variety of central metals and electron configurations. Also these complexes showed, with no change in coordination geometry, an apparent ease of oxidation and reduction,⁴³⁻⁴⁶ thus enabling the study of similar transition metal complexes in a series of formal oxidation states.

The chemistry of these ligands was extended to the preparation and characterisation of *tris* systems that also readily underwent electron-transfer reactions without change in coordination.⁵⁸⁻⁶³ Initial interpretations of the physical properties assumed D₃ symmetry with a distorted octahedral coordination about the central metal atom.^{59,62}

This symmetry is the most likely because it is common to the two extremes, namely O_h (octahedron MS_6) and D_{3h} (trigonal prism). Distortion of an octahedron may occur via (a) compression (or expansion) of the octahedron along a threefold axis, (b) rotation of one-half of the octahedron relative to the other when viewed down a threefold axis as shown below:



or (c) a combination of (a) and (b). Since the symmetry classification, D_3 , covers the expected range of geometries, it is not useful as an identifying label and the discussions emphasise the limiting cases, i.e. octahedral or trigonal prismatic coordination.

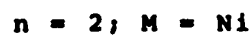
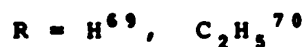
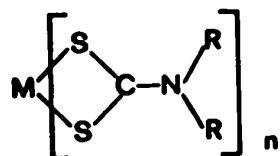
As the spectra of the *tris* systems were not typical of the spectra of octahedral $(Co(III))$, Langford *et al*⁶⁰ suggested the possibility of a trigonal prismatic or at least, a strongly trigonally distorted six coordinate structure. Three complexes, all with the formula $M[S_2C_2(C_6H_5)_2]_3$, where $M = Mo$,⁶⁴ Re ,⁶⁵ and V ⁶⁶ have been reported to have a trigonal prism of sulphur atoms surrounding the central metal atom. Steifel and coworkers⁶⁷

have reported that $[\text{Me}_4\text{N}] \cdot \{\text{V}[\text{S}_6\text{C}_6(\text{CN})_2]_3\}$ has a coordination between the two extremes of octahedral and trigonal coordination.

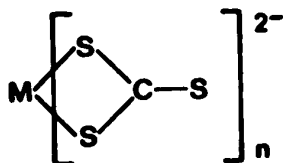
The stability of the trigonal prismatic coordination has been attributed,⁶⁸ in part, to interligand bonding forces between the two sulphur atoms, which are considerably stronger than in the classical octahedral, tetrahedral, or planar complexes. Shortening of metal-sulphur bonds might also be expected because of this interaction.

Other complexes of sulphur containing ligands have been studied to investigate the similarities and differences from the 1,2-dithiolene ligands. These systems include:

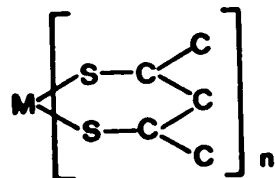
(a)

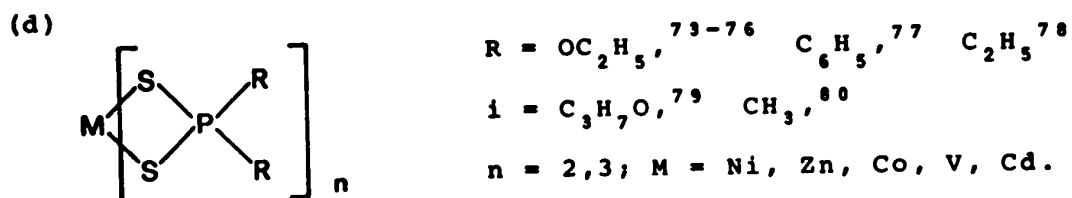


(b)



(c)





The latter group (d) have received attention for a variety of reasons, e.g. (i) as important lubricating oil additives and (ii) because the presence of the phosphorus atom allows e.s.r. spectroscopy to be used to greater effect in the structural studies of these complexes. Day *et al*⁸¹ have synthesised a series of complexes using the $(=\text{S}_2\text{PR}_2)$ ligand (e.g. $R = \text{Me}, \text{CF}_3$) and various transition metals (e.g. $R = \text{Co}, \text{Cr}, \text{V}, \text{Fe}, \text{Mo}$). Three complexes were chosen, $\text{Cr}(\text{S}_2\text{PMe}_2)_3$, $\text{VO}(\text{S}_2\text{PMe}_2)_2$ and $\text{Co}(\text{S}_2\text{PMe}_2)_2$, such that comparisons could be made between representative complexes having a range of coordination geometries and to provide structural models as a basis for detailed spectroscopic studies. Other workers have also been investigating the structural trends in complexes of this ligand and comparisons with the work of this thesis is discussed later. All three structures were unknown and each had several possible structures.

The chromium complex was assigned, on the basis of its spectra⁸¹ (i.r., vis., u.v.), a distorted octahedral structure. Ideally the complex would have D_3 symmetry, but the exact nature of the distortion was unknown.

The $\text{Co}(\text{S}_2\text{PMe}_2)_2$ complex, on comparing its spectra (i.r., u.v., vis.) with those of $\text{Co}[\text{S}_2\text{P}(\text{OEt}_2)]_2$,⁸² was tentatively assigned tetrahedral coordination. Apart from marked insolubility in many solvents there was no indication that the structure would not be monomeric.

The structure of $\text{VO}(\text{S}_2\text{PMe}_2)_2$ was of special interest as the e.s.r. spectrum exhibited super hyperfine splitting due to the interaction of the unpaired electron with the nuclear spin ($\frac{1}{2}$) of the ^{31}P nuclei indicating some delocalisation onto the ligands. Also it was hoped to be able to provide data for the investigation of the anomalous solvent dependence of spectral properties (u.v., vis., i.r., Raman) that have been reported for some VO^{2+} systems;^{83,84} these anomalies (shifts of spectral bands) that have been attributed to axial ligation i.e. the formation of a six coordinate complex or a change in electronic structure.⁸⁵

For the reasons stated above the structural analyses of the $\text{Cr}(\text{S}_2\text{PMe}_2)_3$, $\text{Co}(\text{S}_2\text{PMe}_2)_2$, and $\text{VO}(\text{S}_2\text{PMe}_2)_2$ complexes were undertaken.

CHAPTER III

THE CRYSTAL STRUCTURE OF

TRIS(DIMETHYLDITHIOPHOSPHINATO)CHROMIUM(III)

EXPERIMENTALPart 1. Space Group and Unit Cell Data.

Deep purple crystals of $\text{Cr}^{\text{III}}(\text{S}_2\text{PMe}_2)_3$, were initially supplied by D. Day. However, as supplied the crystals were unsuitable for X-ray analysis so recrystallisation was effected, with difficulty, from a solution of 75% absolute ethanol and 25% benzene. (Often no crystals would form; if some did they were usually multiple crystals.) Analysis figures before and after recrystallisation were:

	C	H	S
Calculated	16.86%	4.24%	45.00%
Found (D.Day)	16.76%	4.54%	—
Found after recrystallisation	16.21%	4.16%	41.54%*

Preliminary Weissenberg ($0kl - 2kl$) and precession ($h0l, hk0$) photographs, taken with Cu K α radiation ($\lambda = 1.5418\text{\AA}$) and Mo K α radiation ($\lambda = 0.7107\text{\AA}$) respectively, exhibited the following systematic absences:

$$h00: h = 2n+1; 0k0: k = 2n+1; 00l: l = 2n+1$$

These absences are consistent with the orthorhombic space group $P2_12_12_1(D_2^h, \text{no. } 19)$. Unit cell dimensions were obtained, at 22°C , on a manual Picker 4 circle

* Sulphur determinations are usually 2-3% too small.

diffractometer using Cu K α radiation ($\lambda = 1.5405\text{\AA}$),
 by accurately centering 15 high 2θ reflections
 ($2\theta \geq 99.0^\circ$). The 2θ values obtained were refined by
 least squares⁶ and the axial lengths calculated were:

$$\begin{array}{ll} a = 9.123 \pm 0.001\text{\AA} & \alpha = 90.0^\circ \\ b = 21.550 \pm 0.002\text{\AA} & \beta = 90.0^\circ \\ c = 9.637 \pm 0.001\text{\AA} & \lambda = 90.0^\circ \end{array}$$

The experimental density, measured by flotation in a
 zinc bromide solution, was $1.51 \pm 0.02 \text{ g./cm.}^3$. The
 value calculated for a formula weight of 427.48 a.m.u.,
 a unit cell volume of 1894.6\AA^3 and $Z=4$ was 1.499 g./cm.^3

Part II. Picker Data Collection

Intensity data were collected on a manual Picker
 4 circle diffractometer, using Cu K α radiation
 ($\lambda = 1.5418\text{\AA}$) monochromatised by the (002) reflection of
 a graphite crystal, using a tube take-off angle of 2.0° .
 The needle-like crystal, which had approximate dimensions
 0.1 mm. \times 0.1 mm. \times 0.2 mm., was mounted on a glass fibre,
 such that the a/a^* axis was coincident with the ϕ axis of
 the diffractometer. The crystal was 20.0 cm. from both
 the source and counter windows and the source and counter
 collimators were 1.0 mm. in diameter. Intensities were
 measured using a scintillation counter with the pulse
 height analyser set to accept 96% of the transmitted peak

when the window was centered on the $K\alpha$ peak. A coupled ω - 2θ moving crystal, moving counter technique with a scan rate of $2.0^\circ/\text{minute}$, was used to scan a range of 2.0° in 2θ , centered on the calculated position of the $K\alpha$ peak.⁸⁷ Stationary background counts were measured for thirty seconds immediately before and after each scan. A total of 1644 reflections were scanned with $2\theta \leq 120.0^\circ$. A periodic check (approximately every twelve hours) of seven well distributed reflections showed some instability, in the order of 10%, but with no 2θ dependence. This information was used to set all data onto a common scale. Seven very intense reflections, whose count ratios exceeded the linear response range of the counting system were remeasured at a lower power, obtained by lowering the milliamperage and voltage on the X-ray tube. To scale these reflections to a level common with the rest of the data, four intense reflections, at full power, were also measured at the same reduced power and the resulting intensity ratios were then used as a scaling factor.

Experimental data were corrected for background, assuming a linear variation over the scan range. The integrated intensities obtained were then corrected for Lorentz and polarization effects, and a relatively scaled set of $|F_o|$ and $|F_o|^2$ was calculated.⁸⁸ It was found that 1387 independent intensities were statistically

significant using the dual criteria:

$$I > 0, \quad I / \left[P + (\tau_P / \tau_B)^2 (B_1 + B_2) \right]^{1/2} \geq 3.$$

where τ_P = total counting time for peak

τ_B = total counting time for background

P, B_1, B_2 = counts of the peak and the two backgrounds
respectively.

Only these statistically significant reflections were used during the subsequent refinement. Standard deviations in $|F_o|$ were derived from the standard deviation of the experimental intensities according to Doedens and Ibers,¹¹ using an uncertainty factor p^2 , of 0.002. The weighting scheme used throughout the refinement was $\omega = \frac{1}{\sigma^2} \cdot (|F_o|)$. In the final stages of the refinement absorption corrections were applied to these data.⁸⁹ The crystal faces were identified as {021}, $\bar{1}00$, $00\bar{1}$, 110, $\bar{1}10$, 130, and the dimensions were very carefully measured. Equations for the plane faces were calculated assuming one end face to be ($\bar{1}00$). Slight variations (up to 10%) in the parameters for these equations were permitted to give optimum agreement between the calculated and observed absorption curves for the h00 reflections, obtained by rotation of the crystal about the ϕ axis at $\chi = 90.0^\circ$.

Absorption corrections ($\mu_{Cu} = 132.82 \text{ cm}^{-1}$) to I and $\sigma(F)$ gave a relatively scaled set of $|F_o|$ and $\sigma(F)$.⁸⁹

The calculated transmission factors were in the range 0.236 - 0.355 and the variation in I_{h00} of 40% before absorption correction was reduced to approximately 10% after correction for absorption.

Part III. PAILRED Data Collection

Intensity data were collected on a Philips PAILRED fully automated diffractometer with Cu K α radiation ($\lambda = 1.5418\text{\AA}$) monochromatised by the (002) reflection of a graphite crystal and using a tube take-off angle of 6.0°. The needle crystal used for data collection, which had dimensions 0.090 mm. \times 0.080 mm. \times 0.400 mm., was mounted on a glass fibre with its a axis coincident with the ω axis of the diffractometer. The crystal was 13.0 cm. from the source and 10.0 cm. from the circular aperture of the counter. The source collimator was 0.039 inches in diameter. Intensities were measured using a scintillation counter with the pulse height analyser set to accept approximately 90% of the transmitted peak when the window was centered on the K α peak. The equ-inclination technique and a moving crystal-stationary counter (ω -scan) scanning procedure were employed. A scan speed of 1.0°/minute was used at all times.

Reciprocal lattice levels $0kl - 8kl$ were scanned, but as the PAILRED diffractometer uses Weissenberg geometry, allowances had to be made for the expansion of

the reflection as μ , the equi-inclination, was increased. The necessary adjustments in aperture size and 1/2 scan widths were as follows:

<u>Layer</u>	<u>1/2 scan in</u>	<u>1/2 scan out</u>	<u>Aperture</u>
0kl-2kl	0.8°	0.6°	2.0°
3kl	1.0°	0.7°	2.0°
4kl	1.0°	0.7°	3.0°
5kl	1.3°	0.8°	3.0°
6kl	1.4°	0.9°	3.5°
7kl	1.5°	1.0°	4.0°
8kl	1.6°	1.2°	4.0°

Stationary background counts were measured for ten seconds immediately before and after each scan. A total of 3506 independent reflections were scanned with $(\sin\theta)/\lambda \leq 0.93$. Eleven zero layer reflections were checked, after each layer, but no reflection deviated by greater than 3.5σ from its mean value, thereby indicating no crystal or electronic instability. Five very intense reflections, whose count ratios exceeded the linear response range of the counting system were remeasured at a lower power, obtained by lowering the milliamperage and voltage on the X-ray tube. To scale these reflections to a level common with the rest of the data, five intense reflections at full power were also measured at the same reduced power and the resulting intensity ratios were then used as a scaling factor.

Experimental data were corrected for background assuming a linear variation over the scan range. The resulting integrated intensities were then corrected for Lorentz and polarization effects, Weissenberg geometry, and a relatively scaled set of $|F_o|$ and $|F_o|^2$ calculated.¹⁰ 1599 independent intensities were found to be statistically significant using the dual criteria:

$$I > 0 \quad \text{and} \quad \frac{\Delta(I)}{I} \leq 0.40$$

where $I = T - \tau B$

$$\Delta(I) = (T + \tau^2 B)$$

and $T = \text{Peak count}$

$B = \text{Total background count}$

$\tau = \text{ratio of peak counting time to the total}$

background counting time i.e. $\tau_T / (\tau_1 + \tau_2)$.

Only these statistically significant reflections were used during the subsequent refinement. Standard deviations in $|F_o|$ were derived, according to Doedens and Ibers,¹¹ from the standard deviations of the experimental intensities using an uncertainty factor, p , of 0.06. The weighting scheme used throughout the refinement was $\omega = \frac{1}{\sigma^2} \cdot (|F_o|)$. Absorption corrections ($\mu_{Cu} = 132.81 \text{ cm.}^{-1}$) were applied to the data⁹ after accurately measuring the crystal dimensions and a relatively scaled set of $|F_o|$ and $\sigma(F)$ were obtained. The calculated transmission factors were in the range 0.277 to 0.414.

SOLUTION AND REFINEMENT OF THE STRUCTURE

The successful structural solution of a three dimensional Patterson map calculated with the PAILED data, was accomplished by assuming that the six sulphur atoms were octahedrally coordinated to the chromium atom. This assumption implies that for a chromium atom with coordinates (x, y, z) , the six sulphur atoms will have coordinates $(x, y, z) \pm (\Delta x_n, \Delta y_n, \Delta z_n)$, $(n=1-3)$. The general Harker vectors, arising from the vectors between atoms related by the symmetry operations of the space group are listed in Table 15. The chromium-sulphur 'image vectors' located around each Harker plane, arise from the vectors between a chromium atom at one symmetry position and the sulphur atoms attached to a chromium atom at a symmetry related position. These vectors are listed in Tables 16-18. The sulphur-sulphur vectors between sulphur atoms attached to symmetry related chromium atoms are also listed in these three Tables.

Inspection of the Patterson map around the origin showed three distinct (i.e. not related by symmetry) chromium-sulphur vectors. These vectors are the intramolecular chromium-sulphur vectors and as the Patterson map had mmm symmetry at the origin, the sign combinations for these vectors were as follows:

$$0 \left\{ \begin{array}{c} + \\ + \\ + \\ + \\ - \\ - \\ - \\ - \end{array} \right\} \Delta x_n, \quad 0 \left\{ \begin{array}{c} + \\ + \\ - \\ - \\ + \\ + \\ - \\ - \end{array} \right\} \Delta y_n, \quad 0 \left\{ \begin{array}{c} + \\ - \\ + \\ - \\ + \\ - \\ + \\ - \end{array} \right\} \Delta z_n$$

The chromium-sulphur vectors provided the information:

	<u>n=1</u>	<u>n=2</u>	<u>n=3</u>
$ \Delta x_n $	0.193	0.067	0.157
$ \Delta y_n $	0.040	0.066	0.076
$ \Delta z_n $	0.150	0.169	0.078

and the problem was to find a consistent solution for the signs.

Analysis of the Patterson map using the general Harker vectors, might, at first sight, have been complicated by (i) the comparable atomic numbers of chromium, sulphur and phosphorus and (ii) the possibility of sulphur-sulphur, sulphur-phosphorus, and phosphorus-phosphorus vectors being superimposed, thus 'building' a peak to the height expected for a chromium-chromium vector only. However, a detailed analysis of the vector tables showed that this should only occur if any of the Δ 's (x_n , y_n or z_n) are zero. The search about the origin

showed this not to be the case and the chromium-chromium vectors, with a multiplicity of two, were readily identified. A solution for the coordinates of the chromium atom ($x = 0.042$, $y = 0.123$, $z = 0.209$) was then simply obtained from the largest vectors in the Harker planes.

Any possible solution of the Patterson map must be self consistent, therefore only the chromium-sulphur image vectors that have the same orientation with respect to the Harker planes and the origin may be used; this process of elucidating these orientations is an application of Buerger's Minimum Function.⁹⁰ Table 19 lists all of the possible sign combinations for the three Minimum Functions $M_2(x)$, $M_2(y)$ and $M_2(z)$ for the all positive region of vector space. The signs of the self consistent vector combinations are listed in Table 20.

Table 20

<u>Minimum Functions</u>		<u>Δx_n</u>	<u>Δy_n</u>	<u>Δz_n</u>
$M_2(x), M_2(y)$	share	\pm	\pm	\mp
$M_2(x), M_2(z)$	share	\pm	\mp	\pm
$M_2(y), M_2(z)$	share	\mp	\pm	\pm

It should be noted that each pair of combinations are related by an inversion centre. Table 20 implies that only image vectors that show a relationship $(+\Delta x_n, +\Delta y_n, -\Delta z_n)$ and $(-\Delta x_n, -\Delta y_n, +\Delta z_n)$ with respect to both Harker planes, $x = \frac{1}{2}$ and $y = \frac{1}{2}$, may be considered as possible solutions.

The solution now involved analysis of all peaks around each Harker plane that were at the same distance from the planes as were the three chromium-sulphur vectors from the origin. As mentioned before the Patterson map had mmm symmetry, therefore, initially any orientation (i.e. any combination of signs with respect to the Harker plane) was allowable because the correct orientation of the origin vectors was unknown. In this particular case the analysis needed to be carried out around the Harker planes, $x = \frac{1}{2}$ and $y = \frac{1}{2}$ only, i.e. determining $M_2(x) \cdot M_2(y)$, because of the assumption that placed a centre of symmetry at the chromium atom required both solutions, Δx_n positive and Δx_n negative. In the general case an examination of, for example, the peaks around the Harker planes, $x = \frac{1}{2}$ and $z = \frac{1}{2}$, would remove the remaining ambiguity.

The three origin vectors were used to search the vector space around the Harker planes, $x = \frac{1}{2}$ and $y = \frac{1}{2}$, and the following sign combinations were found and are listed in Table 21.

Table 21

	<u>$M_2(x)$</u>	<u>$M_2(y)$</u>	<u>Magnitude</u>
Δx_1	+ -	+ -	0.193
Δy_1	+ -	+ -	0.040
Δz_1	- +	- +	0.150
Δx_2	+ -	+ -	0.067
Δy_2	+ -	+ -	0.066
Δz_2	+ -	+ -	0.169
Δx_3	+ -	+ -	0.157
Δy_3	- +	- +	0.076
Δz_3	+ -	+ -	0.078

Δx_1 was chosen as positive and the final signs of Δx_1 , Δy_1 , etc. were fixed by combining the signs in Table 21 with those for $M_2(x) \cdot M_2(y)$ in Table 20:

	<u>Signs from Table 21</u>	<u>Signs of $M_2(x) \cdot M_2(y)$ from Table 20</u>	<u>Final Signs of $\Delta x_1, \Delta y_1, \text{ etc.}$</u>
Δx_1	+ -	+ -	+ -
Δy_1	+ -	+ -	+ -
Δz_1	- +	- +	+ -
Δx_2	+ -	+ -	+ -
Δy_2	+ -	+ +	+ -
Δz_2	+ -	- +	- +
Δx_3	+ -	+ -	+ -
Δy_3	- +	+ +	- +
Δz_3	+ -	- +	- +

The Patterson solution then gave the following starting coordinates.

<u>Atom</u>	<u>x</u>	<u>y</u>	<u>z</u>
Cr	0.042	0.123	0.209
S1	0.198	0.047	0.131
S2	0.108	0.189	0.041
S3	0.235	0.166	0.359
S4	-0.152	0.083	0.059
S5	-0.025	0.057	0.375
S6	-0.115	0.199	0.288

These parameters for the seven atoms using isotropic thermal parameters and scale factor as indicated by a Wilson plot⁹¹ were subjected to one cycle of least squares refinement using the PAILRED data and gave discrepancy indices of $R_1 = 0.39$ and $R_2 = 0.44$ *

The positions of the three phosphorus atoms were located from an observed Fourier map and the refinement may be summarised as follows:

<u>Cycle(s)</u>	<u>Conditions</u>	<u>R_1</u>	<u>R_2</u>
1	Cr, 6S isotropic	0.39	0.44
4	Cr, 6S, 3P isotropic	0.26	0.32
4	Cr, 6S, 3P, 6C all isotropic	0.132	0.155
3	Absorption, decomposition, Cr, 6S, and 3P anisotropic, 6C's isotropic	0.107	0.109
2	All atoms anisotropic	0.104	0.115

The above refinement did not include any corrections for anomalous dispersion and a new program¹⁴ which took account of this effect, became available at this stage. Refinement again terminated with $R_1 = 0.095$ and $R_2 = 0.106$ after a further four cycles.

* See page 10 for definition of R_1 , R_2 , etc.

Comparison of the observed and calculated structure factors at this point cast considerable doubt, because of very bad agreement, as to the quality of the PAILRED data. Hence a new data set was collected on the Picker diffractometer and all further discussion will be in reference to this data set. Using the atomic coordinates from the initial data set, refinement again converged after five cycles to $R_1 = 0.070$ and $R_2 = 0.092$.

Cruickshank and McDonald^{9,2} have discussed quantitatively the effects of anomalous dispersion for non-centrosymmetric crystals. Neglect of $\Delta f''$ (the imaginary component of the anomalous scattering) can lead to serious coordinate errors in polar space groups. An even more serious error may occur when $\Delta f''$ is allowed for and the structure model is the inverse of the true structure; for polar space groups the relative coordinate error will be twice as large as the error when $\Delta f''$ is neglected and for nonpolar space groups, e.g. $P2_12_12_1$, an increase in the mean square thermal vibration amplitude occurs. This choice of the inverse model corresponds to the ambiguity of the Patterson solution where an initial sign was fixed arbitrarily, in this case it was Δx_1 positive.

To investigate this effect the inverse of the model was derived by reflecting the model through a mirror plane coincident with the x axis, i.e. $x \rightarrow -x$.

with the thermal parameters transformed as indicated by Levy.⁹³ Refinement was continued and convergence was achieved after four cycles with $R_1 = 0.037$ and $R_2 = 0.061$ (with four $(\sin\theta)/\lambda \leq 0.8$ reflections rejected as they were thought to be suffering from secondary extinction). Comparison of the two solutions using Hamilton's statistical test⁹⁴ showed that the second model was very strongly confirmed at the 0.005 significance level.

In the final cycle of refinement no parameter changed by more than one sixth of its estimated standard deviation. A final difference Fourier map⁹⁵ showed no peak higher than $0.40e^-/\text{\AA}^3$ and an attempt to find the methyl hydrogen atoms was unsuccessful. The correct choice of the weighting scheme was reflected by the lack of dependence of $w\Delta^2$ ($\Delta = |F_o| - |F_c|$) on $|F_o|$ and $(\sin\theta)/\lambda$ in accordance with Cruickshank's criterion.¹⁵ Scattering factors by Cromer and Waber¹⁶ were used throughout the refinement and the anomalous dispersion corrections for chromium ($\Delta f' = -0.10e^-$, $\Delta f'' = 2.60e^-$), phosphorus ($\Delta f' = 0.2e^-$, $\Delta f'' = 0.5e^-$) and sulphur ($\Delta f' = 0.30e^-$, $\Delta f'' = 0.60e^-$), applied to F_{calc} ; were taken from International Tables of X-ray Crystallography.¹⁷

x, y, z $x-x, -y, x+z$ $x+x, x-y, -z$ $-x, x+y, x-z$

x, y, z	$0, 0, 0$	$x+2x, +2y, x$	$x, x+2y, 2z$	$2x, x, x+2z$
$x-x, -y, x+z$	$x-2x, -2y, x$	$0, 0, 0$	$-2x, x, x+2z$	$x, x-2y, +2z$
$x+x, x-y, -z$	$x, x-2y, -2z$	$2x, x, x-2z$	$0, 0, 0$	$x+2x, -2y, x$
$-x, x+y, x-z$	$-2x, x, x-2z$	$x, x-2y, -2z$	$x-2x, +2y, x$	$0, 0, 0$

Table 15. General Harker Vectors for the space group $P2_12_12_1$.

$$\begin{matrix} x - \Delta x_n \\ y - \Delta y_n \\ z - \Delta z_n \end{matrix} \quad \underline{S}$$

$$\begin{matrix} x + \Delta x_n \\ y + \Delta y_n \\ z + \Delta z_n \end{matrix} \quad \underline{S}$$

$$x, \quad y, \quad z$$

$$\underline{Cr}$$

	\underline{Cr}		\underline{S}	\underline{S}
$\frac{1}{2} + x, \frac{1}{2} - y, -z$	$\frac{1}{2}, \frac{1}{2} - 2y, -2z$	$-2z$	$\frac{1}{2} \begin{matrix} -\Delta x_n \\ -2y \\ -2z \end{matrix}$	$\frac{1}{2} \begin{matrix} +\Delta x_n \\ -2y \\ -2z \end{matrix}$
$\frac{1}{2} \begin{matrix} +x \\ -y \\ -z \end{matrix}$	$\frac{1}{2} \begin{matrix} +\Delta x_n \\ -2y \\ -2z \end{matrix}$	$\frac{1}{2} \begin{matrix} +\Delta x_n \\ -\Delta y_n \\ -\Delta z_n \end{matrix}$	$\frac{1}{2} \begin{matrix} -\Delta x_n \\ -2y \\ -2z \end{matrix}$	$\frac{1}{2} \begin{matrix} +2\Delta x_n \\ -2y \\ -2z \end{matrix}$
$\frac{1}{2} \begin{matrix} +x \\ -y \\ -z \end{matrix}$	$\frac{1}{2} \begin{matrix} -\Delta x_n \\ -2y \\ -2z \end{matrix}$	$\frac{1}{2} \begin{matrix} -\Delta x_n \\ +\Delta y_n \\ +\Delta z_n \end{matrix}$	$\frac{1}{2} \begin{matrix} -2\Delta x_n \\ -2y \\ -2z \end{matrix}$	$\frac{1}{2} \begin{matrix} -2\Delta x_n \\ -2y \\ -2z \end{matrix}$

Table 16. Derivation of the of Cr - S Image Vectors for the Harker Plane $x = \frac{1}{2}$.

$$\begin{matrix} x - \Delta x_n \\ y - \Delta y_n \\ z - \Delta z_n \end{matrix}$$

$$\begin{matrix} x + \Delta x_n \\ y + \Delta y_n \\ z + \Delta z_n \end{matrix}$$

$$\begin{matrix} x, & y, & z \end{matrix}$$

S

S

Cr

$-x$	$-2x$	$-2x$	$-2x$	$-2x$
$+y$	$\frac{1}{2}$	$\frac{1}{2}$	$\frac{1}{2}$	$\frac{1}{2}$
$-z$	$\frac{1}{2}$	$\frac{1}{2}$	$\frac{1}{2}$	$\frac{1}{2}$
$\frac{Cr}{S}$				
$-x$	$-2x$	$-2x$	$-2x$	$-2x$
$+y$	$\frac{1}{2}$	$\frac{1}{2}$	$\frac{1}{2}$	$\frac{1}{2}$
$-z$	$\frac{1}{2}$	$\frac{1}{2}$	$\frac{1}{2}$	$\frac{1}{2}$
$\frac{S}{S}$				
$-x$	$-2x$	$-2x$	$-2x$	$-2x$
$+y$	$\frac{1}{2}$	$\frac{1}{2}$	$\frac{1}{2}$	$\frac{1}{2}$
$-z$	$\frac{1}{2}$	$\frac{1}{2}$	$\frac{1}{2}$	$\frac{1}{2}$
$\frac{S}{S}$				

Table 17. Derivation of the Cr - S Image Vectors for the Harker Plane $y = \frac{1}{2}$.

$$\begin{matrix} x - \Delta x_n \\ y - \Delta y_n \\ z - \Delta z_n \end{matrix}$$

$$\begin{matrix} x + \Delta x_n \\ y + \Delta y_n \\ z + \Delta z_n \end{matrix}$$

$$\begin{matrix} x \\ y \\ z \end{matrix}$$

S

S

Cr

	<u>Cr</u>	<u>S</u>	<u>S</u>	
$\begin{matrix} -x \\ -y \\ +z \end{matrix}$	$\begin{matrix} -2x \\ -2y \end{matrix}$	$\begin{matrix} -2x - \Delta x_n \\ -2y - \Delta y_n \\ -2z - \Delta z_n \end{matrix}$	$\begin{matrix} -2x + \Delta x_n \\ -2y + \Delta y_n \\ -2z + \Delta z_n \end{matrix}$	
$\begin{matrix} -x \\ -y \\ +z \end{matrix}$	$\begin{matrix} -2x \\ -2y \\ +2z \end{matrix}$	$\begin{matrix} -2x - 2\Delta x_n \\ -2y - 2\Delta y_n \\ -2z \end{matrix}$	$\begin{matrix} -2x \\ -2y \\ +2\Delta z_n \end{matrix}$	
$\begin{matrix} -x \\ -y \\ +z \end{matrix}$	$\begin{matrix} -2x \\ -2y \\ -\Delta z_n \end{matrix}$	$\begin{matrix} -2x \\ -2y \\ -\Delta z_n \end{matrix}$	$\begin{matrix} -2x \\ -2y \\ -2\Delta z_n \end{matrix}$	

Table 18. Derivation of the Cr - S Image Vectors for the Harker Plane $z = \frac{1}{2}$.

$M_2(x)$	$\frac{1}{2} \begin{Bmatrix} + \\ - \\ - \\ + \end{Bmatrix} \Delta x_n, \frac{1}{2}-2y \begin{Bmatrix} - \\ + \\ - \\ + \end{Bmatrix} \Delta y_n, +2z \begin{Bmatrix} + \\ - \\ + \\ - \end{Bmatrix} \Delta z_n$
$M_2(y)$	$+2x \begin{Bmatrix} + \\ - \\ + \\ - \end{Bmatrix} \Delta x_n, \frac{1}{2} \begin{Bmatrix} - \\ + \\ + \\ - \end{Bmatrix} \Delta y_n, \frac{1}{2}-2z \begin{Bmatrix} - \\ + \\ - \\ + \end{Bmatrix} \Delta z_n$
$M_2(z)$	$\frac{1}{2}-2x \begin{Bmatrix} - \\ + \\ - \\ + \end{Bmatrix} \Delta x_n, 2y \begin{Bmatrix} + \\ - \\ + \\ - \end{Bmatrix} \Delta y_n, \frac{1}{2} \begin{Bmatrix} - \\ + \\ + \\ - \end{Bmatrix} \Delta z_n$

Table 19. Possible Sign Combinations for the Three Minimum Functions $M_2(x)$, $M_2(y)$, and $M_2(z)$.

RESULTS

Figure 5 is a perspective view of the $\text{Cr}(\text{S}_2\text{PMe}_2)_3$ molecule indicating the numbering scheme used, while Figure 6 and 7 show the molecular packing in the ab and bc planes respectively. Table 22 lists the final atomic coordinates and equivalent isotropic temperature factors for the asymmetric unit. Anisotropic temperature factors are listed in Table 23. Tables 24-27 contain data on molecular bond lengths, angles, intermolecular non-bonded contacts, and least squares planes. Table 28 reports the final calculated and observed structure amplitudes.

Figure 5

A perspective view of the $\text{Cr}(\text{S}_2\text{PMe}_2)_3$ molecule
with 50% probability ellipsoids.

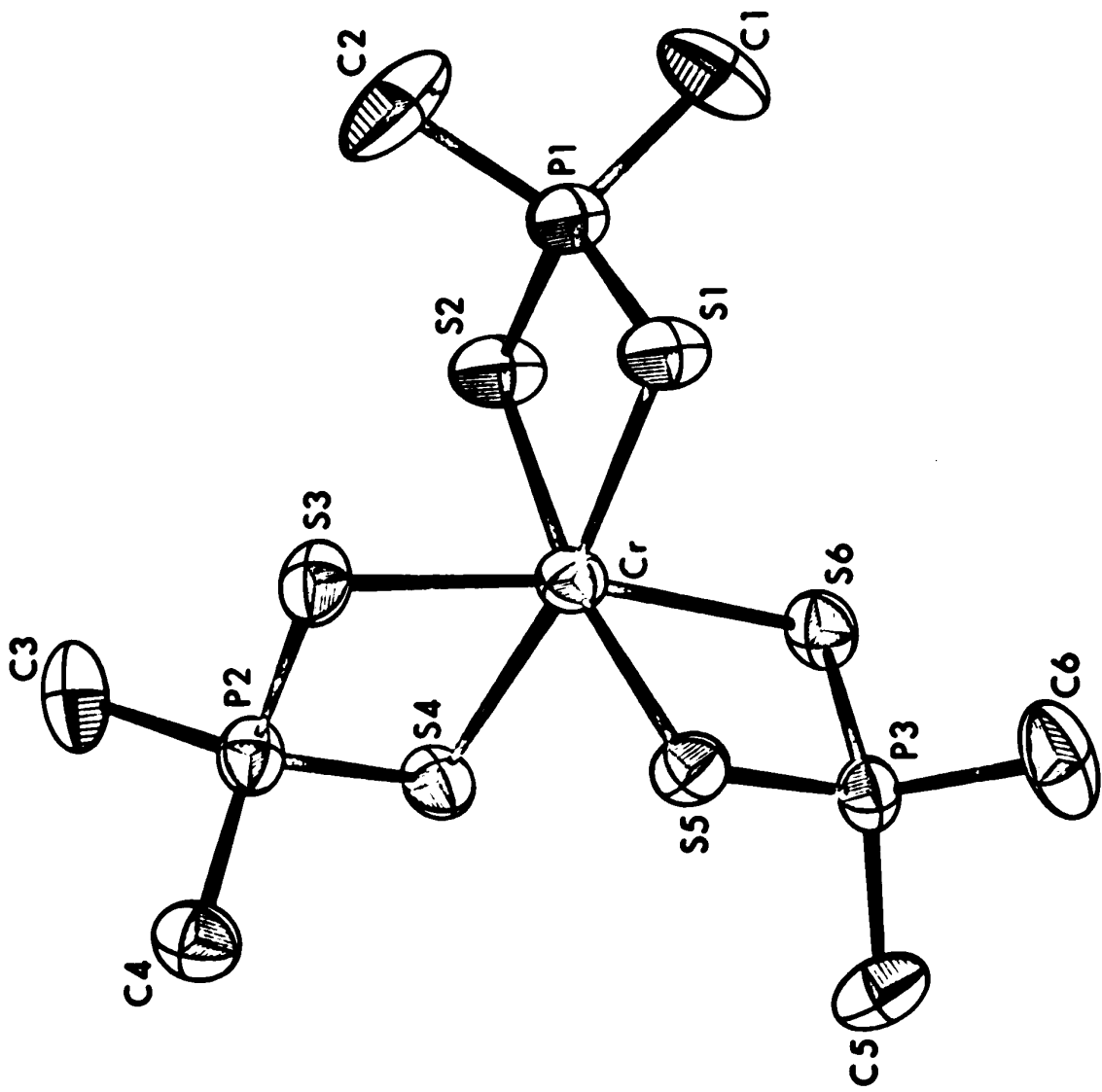


Figure 6

The molecular packing of $\text{Cr}(\text{S}_2\text{PMe}_2)_3$,
projected onto the ab plane.

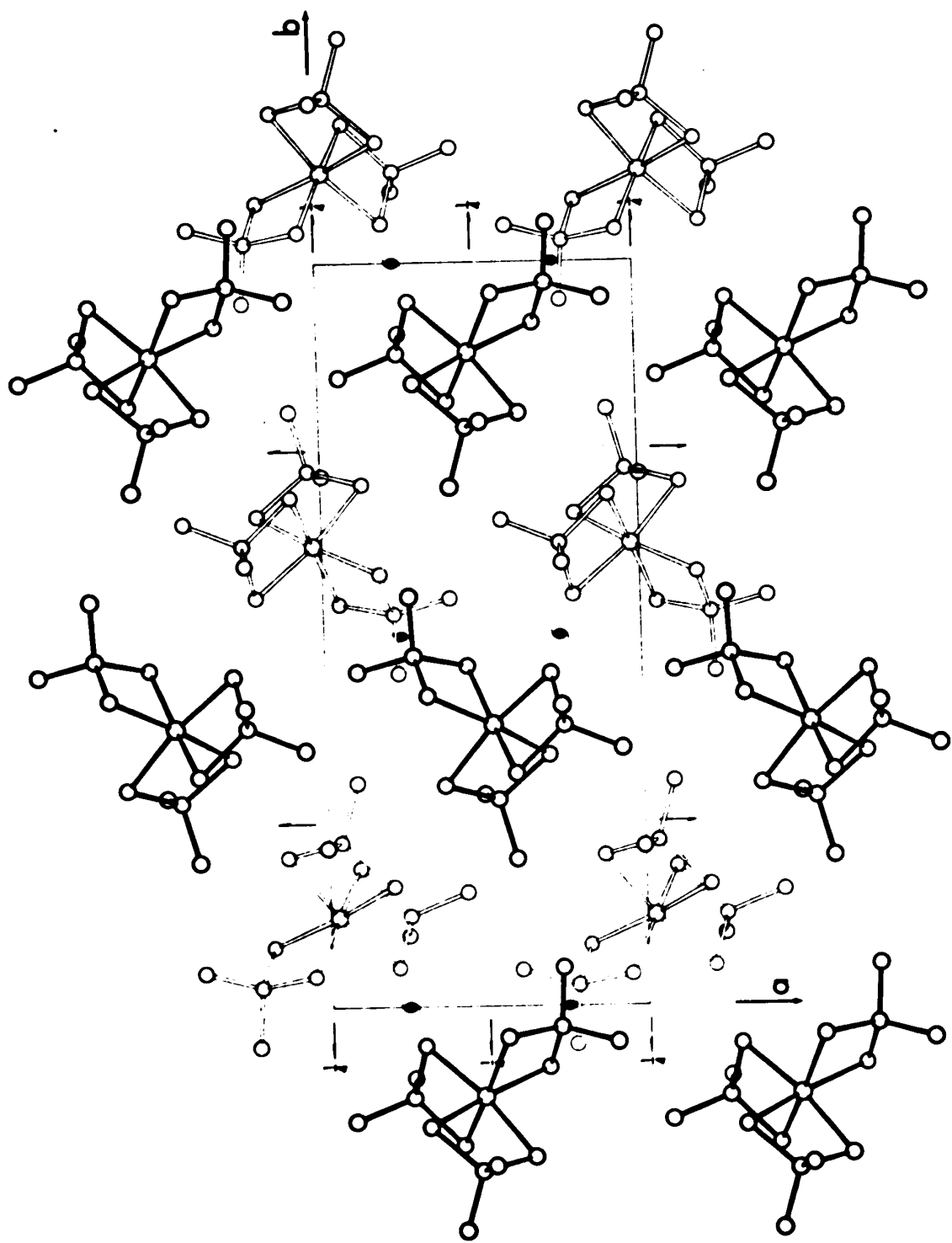


Figure 7

**The molecular packing of $\text{Cr}(\text{S}_2\text{PMe}_2)_3$,
projected onto the bc plane.**

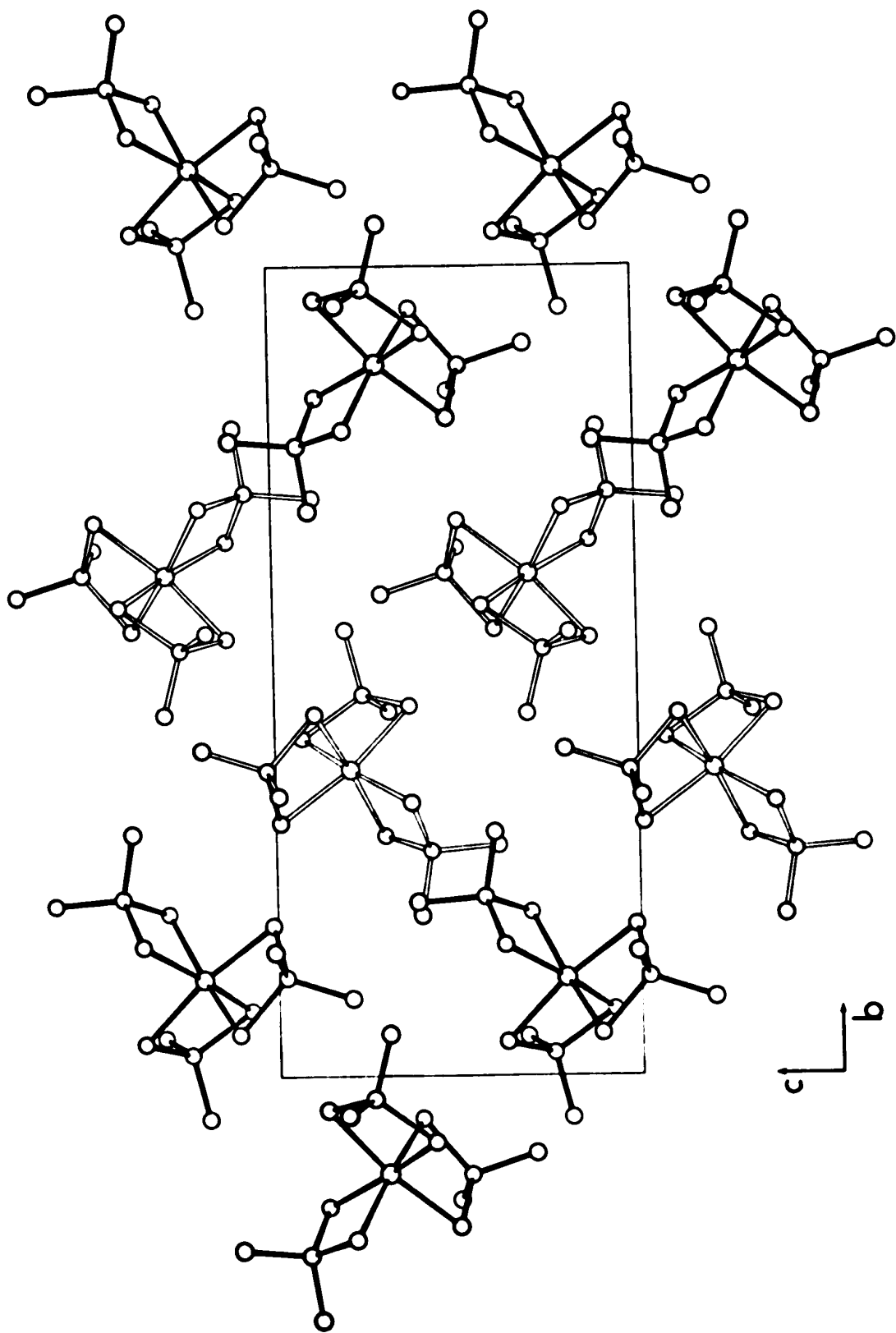


Table 22

Final Atomic Coordinates and Equivalent Isotropic

Temperature Factors for $\text{Cr}(\text{S}_2\text{PMe}_2)_3$

<u>Atom</u>	<u>x</u>	<u>y</u>	<u>z</u>	<u>$B, \text{\AA}^2$</u>
Cr	0.02655(13) ^a	0.12100(5)	0.20617(12)	3.56
S1	0.21198(23)	0.05250(8)	0.11005(22)	4.80
S2	0.09704(26)	0.18653(9)	0.01176(24)	5.23
S3	0.20239(21)	0.16202(8)	0.37515(24)	4.82
S4	-0.12927(19)	0.20273(9)	0.30011(21)	4.16
S5	-0.05116(21)	0.04192(9)	0.37187(18)	4.16
S6	-0.18003(23)	0.08179(9)	0.07513(18)	4.19
P1	0.25131(22)	0.12221(8)	-0.02241(20)	4.08
P2	0.04036(22)	0.22148(8)	0.42678(20)	3.86
P3	-0.22084(22)	0.02841(8)	0.24205(18)	3.68
C1	0.2491(12)	0.0955(4)	-0.2013(9)	6.62
C2	0.4342(10)	0.1545(4)	0.0032(13)	7.51
C3	0.0943(10)	0.3013(3)	0.4022(10)	5.49
C4	-0.0037(10)	0.2138(4)	0.6097(8)	5.46
C5	-0.3953(9)	0.0500(5)	0.3160(9)	5.69
C6	-0.2323(13)	-0.0527(4)	0.1965(9)	6.95

^aNumbers in parentheses are estimated standard deviations occurring in the last digits listed.

Table 23. Anisotropic Temperature Parameters^b ($\times 10^5$) for Cr(S₂PMe₂)₃.

Atom	β_{11}	β_{22}	β_{33}	β_{12}	β_{13}	β_{23}
Cr	1070(16) ^a	171(2)	1063(14)	25(6)	144(12)	-8(5)
S1	1571(31)	172(4)	1611(28)	142(9)	502(26)	114(9)
S2	1772(33)	192(4)	1673(29)	187(10)	596(28)	143(10)
S3	939(26)	235(5)	1877(31)	38(9)	-137(25)	-135(10)
S4	937(24)	248(5)	1278(24)	94(8)	-81(21)	-143(9)
S5	1250(27)	271(5)	884(19)	-66(9)	-73(21)	56(8)
S6	1605(30)	221(4)	845(19)	-34(9)	-136(22)	17(8)
P1	1281(26)	165(4)	1315(26)	66(9)	321(22)	61(8)
P2	1064(25)	183(4)	1250(23)	23(9)	-144(22)	-42(8)
P3	1331(29)	185(4)	853(20)	-61(9)	-144(20)	-1(7)
C1	2791(190)	355(26)	1070(95)	191(61)	333(135)	33(43)
C2	1476(144)	359(28)	2949(201)	-122(52)	95(153)	226(66)
C3	1793(141)	186(17)	1896(136)	-61(43)	-581(122)	37(42)
C4	1672(143)	357(24)	1121(98)	115(51)	-1(103)	26(41)
C5	1158(119)	416(27)	1477(110)	-41(48)	-16(101)	154(50)
C6	3825(246)	161(16)	1375(105)	-107(58)	-160(158)	-5(37)

^aNumbers in parentheses are estimated standard deviations occurring in the last digits listed.

^bAnisotropic thermal parameters defined by

$$\exp[-(\beta_{11}h^2 + \beta_{22}k^2 + \beta_{33}l^2 + 2\beta_{12}hk + 2\beta_{13}hl + 2\beta_{23}kl)]$$

Table 24Intramolecular Distances (\AA) for the $\text{Cr}(\text{S}_2\text{PMe}_2)_3$ Molecule.

<u>Atoms</u>	<u>Distance</u>
Cr - S1	2.429(2)
Cr - S2	2.433(2)
Cr - S3	2.451(2)
Cr - S4	2.438(2)
Cr - S5	2.441(2)
Cr - S6	2.421(2)
S1 - P1	2.004(3)
S2 - P1	2.003(3)
S3 - P2	2.019(3)
S4 - P2	2.012(3)
S5 - P3	2.012(3)
S6 - P3	2.012(3)
P1 - C1	1.818(9)
P1 - C2	1.825(10)
P2 - C3	1.806(8)
P2 - C4	1.816(8)
P3 - C5	1.805(9)
P3 - C6	1.806(8)

^aNumbers in parentheses are estimated standard deviations in the last digits listed.

Table 25

Intramolecular Angles (degrees) for the $\text{Cr}(\text{S}_2\text{PMe}_2)_3$ Molecule.

<u>Atoms</u>	<u>Angle</u>
S1 - $\hat{\text{C}}\text{r}$ - S2	82.82(7) ^a
S3 - $\hat{\text{C}}\text{r}$ - S4	82.78(7)
S5 - $\hat{\text{C}}\text{r}$ - S6	82.61(7)
S1 - $\hat{\text{C}}\text{r}$ - S4	170.73(9)
S2 - $\hat{\text{C}}\text{r}$ - S5	170.40(9)
S3 - $\hat{\text{C}}\text{r}$ - S6	169.13(9)
S1 - $\hat{\text{C}}\text{r}$ - S3	90.96(8)
S1 - $\hat{\text{C}}\text{r}$ - S5	91.57(7)
S1 - $\hat{\text{C}}\text{r}$ - S6	97.54(8)
S2 - $\hat{\text{C}}\text{r}$ - S3	97.43(9)
S2 - $\hat{\text{C}}\text{r}$ - S4	91.19(8)
S2 - $\hat{\text{C}}\text{r}$ - S6	90.38(9)
S3 - $\hat{\text{C}}\text{r}$ - S5	90.42(8)
S4 - $\hat{\text{C}}\text{r}$ - S5	95.29(8)
S4 - $\hat{\text{C}}\text{r}$ - S6	89.53(7)
Cr - $\hat{\text{S}}1$ - P1	84.95(9)
Cr - $\hat{\text{S}}2$ - P1	84.87(9)
Cr - $\hat{\text{S}}3$ - P2	85.03(9)
Cr - $\hat{\text{S}}4$ - P2	85.52(9)
Cr - $\hat{\text{S}}5$ - P3	85.28(8)
Cr - $\hat{\text{S}}6$ - P3	85.79(9)

Table 25 (continued)

Intramolecular Angles (degrees) for the $\text{Cr}(\text{S}_2\text{PMe}_2)_3$
Molecule.

<u>Atoms</u>	<u>Angle</u>
S1 - $\hat{\text{P}}1$ - S2	106.76(12)
S3 - $\hat{\text{P}}2$ - S4	106.64(11)
S5 - $\hat{\text{P}}3$ - S6	105.78(11)
S1 - $\hat{\text{P}}1$ - C1	111.4(3)
S1 - $\hat{\text{P}}1$ - C2	111.3(4)
S2 - $\hat{\text{P}}1$ - C1	111.6(3)
S2 - $\hat{\text{P}}1$ - C2	110.9(3)
S3 - $\hat{\text{P}}2$ - C3	111.9(3)
S3 - $\hat{\text{P}}2$ - C4	110.1(3)
S4 - $\hat{\text{P}}2$ - C3	108.7(3)
S4 - $\hat{\text{P}}2$ - C4	113.6(3)
S5 - $\hat{\text{P}}3$ - C5	113.3(3)
S5 - $\hat{\text{P}}3$ - C6	109.6(4)
S6 - $\hat{\text{P}}3$ - C5	109.3(3)
S6 - $\hat{\text{P}}3$ - C6	111.7(3)
C1 - $\hat{\text{P}}1$ - C2	105.0(6)
C3 - $\hat{\text{P}}2$ - C4	105.9(4)
C5 - $\hat{\text{P}}3$ - C6	107.1(5)

^aNumbers in parentheses are estimated standard deviations
in the last digits listed.

Table 26Intermolecular Non-Bonded Contacts ($\leq 4.0\text{\AA}$) of $\text{Cr}(\text{S}_2\text{PMe}_2)_3$.

<u>Atoms</u>	<u>Distance, \AA</u>	<u>Symmetry Position of Second Molecule</u>
S1 - C1	3.69	$\frac{1}{2}-x, -y, -\frac{1}{2}+z$
S2 - C2	3.74	$\frac{1}{2}+x, \frac{1}{2}-y, -z$
S3 - C4	3.79	$\frac{1}{2}+x, \frac{1}{2}-y, 1-z$
S4 - C3	3.82	$\frac{1}{2}+x, \frac{1}{2}-y, 1-z$
S4 - C4	3.96	$-\frac{1}{2}+x, \frac{1}{2}-y, 1-z$
S5 - C6	3.71	$-\frac{1}{2}-x, -y, \frac{1}{2}+z$
S6 - C5	3.84	$-\frac{1}{2}-x, -y, -\frac{1}{2}-z$
S6 - C6	3.79	$-\frac{1}{2}-x, -y, -\frac{1}{2}-z$
S6 - C2	3.91	$1+x, y, z$
C1 - C4	3.89	$x, y, 1+z$
C3 - C4	3.68	$\frac{1}{2}+x, -y, 1-z$
C3 - C6	3.52	$-x, \frac{1}{2}+y, \frac{1}{2}-z$
C5 - C6	3.85	$-\frac{1}{2}-x, -y, \frac{1}{2}+z$

Table 27. Weighted Mean Molecular Planes for Cr(S₂PMe₂)^a

<u>Atoms contained in the Plane</u>	<u>No.</u>	<u>Equation</u>
Cr, P1, P2, P3, M1, M2, M3 [*]	1	0.6027X - 0.5771Y + 0.5511Z = +0.2675
Cr, S1, S2	2	0.6950X + 0.4391Y + 0.5694Z = -2.4446
S1, S2, P1	3	0.5891X + 0.4369Y + 0.6798Z = -2.3545
Cr, S3, S4	4	-0.3488X - 0.6356Y + 0.6887Z = +0.3735
S3, S4, P2	5	-0.3503X - 0.6616Y + 0.6630Z = +0.5600
Cr, S5, S6	6	-0.5976X + 0.6664Y + 0.4459Z = -2.4788
S5, S6, P3	7	-0.4897X + 0.7589Y + 0.4293Z = -2.4526
Cr, M1, P1, C1, C2	8	+0.3293X - 0.8967Y + 0.2958Z = +1.6707
Cr, M2, P2, C3, C4	9	+0.9498X - 0.2459Y + 0.1934Z = +0.0261
Cr, M3, P3, C5, C6	10	+0.3467X - 0.2369Y + 0.9076Z = -1.2687

^{*}M1, M2, and M3 are the mid-points between atoms S1 and S2, S3 and S4, and S5 and S6 respectively.

Table 27 (continued) Distances of Atoms from Planes (Å)^{a,b}

Plane 1: Cr, 0.004; P1, 0.010; P2, 0.001; P3, -0.015; M1, -0.046; M2, -0.007;
M3, 0.050.

Plane 8: Cr, 0.000; M1, -0.001; P1, 0.001; C1, 0.000; C2, -0.001

Plane 9: Cr, -0.001; M2, 0.006; P2, -0.002; C3, -0.004; C4, -0.003

Plane 10: Cr, 0.001; M3, 0.005; P3, 0.005; C5, -0.011; C6, -0.016

Planes Dihedral Angle

2-3 171.2°

4-5 -177.9°

6-7 171.8°

^a The orthogonal coordinate system (X,Y,Z) corresponds to the crystal a,b,c* axes.

^b Average estimated standard deviations in atom positions derived from uncertainties in fractional coordinates are as follows, (Å): Cr, 0.001; P, 0.002; S, 0.002; C, 0.009; M, 0.003

Table 28

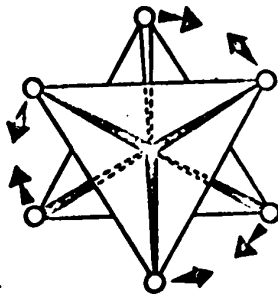
**Observed and calculated structure amplitudes ($\times 10$)
in electrons for $\text{Cr}(\text{S}_2\text{PMe}_2)_3$.**

DISCUSSION

The crystal consists of discrete molecules of $\text{Cr}(\text{S}_2\text{PMe}_2)_3$ which have no crystallographic symmetry; the approximate D_3 symmetry of the molecule is destroyed by the bending of each ligand along a line joining the two sulphur atoms of each ligand (see Figure 5). The six sulphur atoms are virtually equi-distant from the chromium atom with an average bond length of 2.436\AA , which compares with 2.451\AA for $\text{V}[\text{S}_2\text{P}(\text{OEt})_2]_3$,⁹⁶ and 2.418\AA for $\text{Fe}[\text{S}_2\text{CN}(\text{n-But})_2]_3$.⁹⁷ The trend of the variation in these M-S distances is that expected on the basis of covalent radii, viz. $\text{V}(\text{III}) > \text{Cr}(\text{III}) > \text{Fe}(\text{III})$. More detailed discussion of these distances is reserved until the final chapter.

The coordination polyhedra of the sulphur atoms is that of a slightly distorted octahedron where the mean of the sulphur-metal-sulphur angles, involving pairs of donor atoms furthest apart is 170.04° . The corresponding angle for the known trigonal prismatic structures⁶⁴⁻⁶⁷ is $136 \pm 1^\circ$ and for perfect octahedral symmetry 180° . Taking into account the constraint imposed on the geometry of the molecule by the rigid nature of the dithiophosphinato ligands and by the size of the 'bite' angles at the metal atom (for this compound the mean value is 82.73°), the mean trans sulphur-metal-sulphur angles should be ca. 173° .⁹⁸

Analysis of angles at the chromium atom suggests that the distortion of the complex is a combination of compression and rotation of the coordination octahedron as illustrated below:



Therefore the value found for this angle for $\text{Cr}(\text{S}_2\text{PMe}_2)_3$ is closer to that for a chelated octahedral structure, rather than a trigonal prismatic one.

$\text{Cr}(\text{S}_2\text{PMe}_2)_3$ is compared in Table 29, with the *tris* substituted dithiolene complexes which have trigonal prismatic coordination. The sulphur-metal-sulphur angles are equal to within a degree but for the trigonal and pseudo trigonal prismatic structures the metal-sulphur bond lengths lie within a narrow range of values, which is $0.08 - 0.10\text{\AA}$ less than for $\text{Cr}(\text{S}_2\text{PMe}_2)_3$, even though the metal atoms belong to different transition metal rows and have different atomic radii. This shortening of the metal-sulphur bond length is probably due to the greater delocalisation of electrons over the entire metal-sulphur system, and hence greater 'multiple bond' character, that is obtainable with the dithiolene ligands rather than the dithiophosphate ligands.

Table 29. Structural Data for tris-Substituted Dithio Complexes

Complex	Ref.	M-S(Å)	S-M-S(Deg)	S-S(Å) ^a	S-S(Å) ^b
Cr(S ₂ PMe ₂) ₂	—	2.436(2) ^c	82.73(7) ^c	3.219(3) ^c	3.512(3) ^{c,g} [3.409-3.670]
V(S ₂ P(OEt) ₂) ₂	96	2.451(6) ^c	81.8(2) ^c	3.205(6)	3.456(8) ^c
{Fe[S ₂ C ₂ (CN) ₂] ₂ } ²⁻	99	2.261(2) ^c	88.0(1)	3.147(2)	3.19 ^g
{V[S ₂ C ₂ (CN) ₂] ₂ } ^{2-f}	67	2.36(1) ^c	—	3.18(1) ^d 3.12(1) ^e	3.20 ^g
V(S ₂ C ₂ Ph ₂) ₂	66	2.338(4) ^c	81.7(1) ^c	3.058	2.927 3.088 3.178
Mo(S ₂ C ₂ H ₂) ₂	64	2.33(2) ^c	82.5 ^c	3.10	3.11
Re(S ₂ C ₂ Ph ₂) ₂	65	2.325(4) ^c	81.4 ^c	3.032(1)	3.050(8)

^aDistance within each ligand (intra).^bDistance between S atoms of different ligands (inter).^cAverage value.^dOn twofold axis.

Table 29. (continued)

• Other two ligands
of Me₂N⁺ salt

• The interligand S-S distances exhibit significant differences in the structure.

The distances between sulphur atoms within the ligands (intra) and between sulphur atoms of different ligands (inter) have been used as an indication of inter-donor atom bonding forces which help stabilise the trigonal prismatic coordination of the *tris* substituted dithiolene complexes.⁶⁸ These distances, as well as the metal-sulphur distance and sulphur-metal-sulphur angles, are compared in Table 29.

The intra sulphur-sulphur distances are different with the 'octahedral coordination' values for $\text{Cr}(\text{S}_2\text{PMe}_2)_3$, 0.18\AA greater than those observed for the 'most perfect' trigonal prismatic compound, $\text{Re}(\text{S}_2\text{C}_2\text{Ph}_2)_3$,⁶⁸ and 0.03\AA for the pseudo trigonal prismatic compound $\{\text{V}[\text{S}_2\text{C}_2(\text{CN}_2)]_3\}^{2-}$.⁶⁷ The inter sulphur-sulphur distances are approximately 0.5\AA longer for $\text{Cr}(\text{S}_2\text{PMe}_2)_3$, than the trigonal prismatic complexes but only 0.3\AA longer when compared to $\{\text{V}[\text{S}_2\text{C}_2(\text{CN}_2)]_3\}^{2-}$. Thus, the closer to octahedral coordination the longer the intra sulphur-sulphur distance becomes accompanied by increased inter sulphur-sulphur distances and metal-sulphur bond lengths.

The mechanism of interdonor atom bonding has been discussed in several treatments of the *tris* complexes^{68,99} and apparently two types of interaction may be involved; (i) direct sulphur $p_\pi-p_\pi$ bonding interactions between appropriate π_v molecular orbitals of the ligand systems

and (ii) strong involvement of the in-plane sulphur π_h orbitals with the metal d_{z^2} and p_z orbitals along the threefold axis of the prism leading to a more stable bonding orbital which is occupied in all of the trigonal prismatic complexes. In an octahedral configuration neither of the proposed bonding interactions would be as substantial as they are in the trigonal prismatic configuration. These trends do suggest, however, that the two modes of metal coordination are energetically closely related and that only small forces dictate which mode is preferred, e.g. chromium, as the $\text{Cr}(\text{S}_2\text{C}_2\text{Ph}_2)_3$ complex, is known to possess trigonal prismatic coordination on the basis of isomorphism and spectroscopic studies.^{64,65} An indication of the nature of these forces may be found in the ease of crystallization and the inter ligand forces of the complexes. Steifel *et al*⁶⁸ found that M (toluene-3,4,-dithiolate) ($\text{M} = \text{Mo}, \text{W}, \text{Re}$) did not readily form crystals, similar to what was found for $\text{Cr}(\text{S}_2\text{PMe}_2)_3$, and suggested this was due to (i) two possible orientations of the three methyl groups in either trigonal prismatic or octahedral coordination and (ii) the unsymmetrical nature of the tdt ligand.

Octahedral complexes with D_3 symmetry should be optically active but attempts at resolving the $\{\text{Co}[\text{S}_2\text{C}_2(\text{CN})_2]_3\}^{2-}$ complex into its optical enantiomers

have not met with success.¹⁰⁰ Similar experiments by Cavel *et al*¹⁰¹ have shown that a crystal of purified $\text{Cr}(\text{S}_2\text{PMe}_2)_3$ either racemises rapidly in various solvent or the resolution procedure failed. However, if racemisation were to occur without 'unhooking' of ligands then the complex must pass through the trigonal prismatic configuration, thus implying that the energy difference between trigonal prismatic and octahedral coordination is small. This argument has gained support from the structural studies on the *tris*-1,2-dithiolene complexes which have been found to possess both trigonal prismatic and trigonal antiprismatic (octahedral) coordination geometries.¹⁰² All other distances and angles (where applicable) are similar to other published values, as well as $\text{Co}(\text{S}_2\text{PMe}_2)_2$ and $\text{VO}(\text{S}_2\text{PMe}_2)_2$. These similarities will be discussed in the final chapter.

The geometry of the ligands is similar to that of $\text{VO}(\text{S}_2\text{PMe}_2)_2$ in that the ligands bend along a line joining the sulphur atoms contained within each ligand (see Figure 13). All other examples of the dithiophosphinato ligand have been planar (quite often because of symmetry requirements) except for (a) this thesis and (b) in dimeric molecules where the ligand is a bridging group linking two monomeric molecules together to form a dimer. (In these dimers^{78,79} the ligands that are bound wholly to one metal atom are planar, within experimental error). Table 27 lists the dihedral angles within each ligand; however,

analysis of the structure shows that the (S3, P2, S4) ligand is bent in the opposite sense to the other two ligands thus destroying the 'propellor' configuration of the molecule.

This flexing may be attributed to molecular packing and the resultant Van der Waals forces. For atoms C1, C2, C5, and C6 the intermolecular approach distances with the sulphur and carbon atoms of adjacent molecules are in the range 3.68 - 3.89Å (see Table 26) while the sums of the Van der Waals radii⁵ for a methyl group (2.0Å), or a carbon atom (1.7Å), and a sulphur atom (1.85Å) are 3.85Å and 3.55Å. However for C3 and C4 similar approach distances range from 3.52 - 3.96Å and represent the position of least interaction of this ligand with neighbouring molecules. If this ligand (S3, P2, S4) was bent in the same sense as the other two the intermolecular distances could be shortened by as much as ~0.2Å which would be energetically unfavourable. Hence it is evident that the configuration of the ligands is determined by molecular packing considerations.

CHAPTER IV
THE CRYSTAL STRUCTURE OF
***BIS*(DIMETHYLDITHIOPHOSPHINATO)COBALT(II)**

EXPERIMENTAL

The crystals of $\text{Co}^{\text{II}}(\text{S}_2\text{PMe}_2)_2$ were kindly supplied by D. Day as bright green prisms and were suitable for X-ray analysis as supplied. Preliminary Weissenberg photographs ($hk0 - hk2$) using Cu K α radiation ($\lambda = 1.5418\text{\AA}$) exhibited the following systematic absences:

$$hk0: h+k = 2n+1; 0k\ell; \ell = 2n+1; h0\ell: \ell = 2n+1$$

These absences are consistent with the orthorhombic space group $\text{Pccn}(D_{2h}^{10}, \text{No. } 56)$. Unit cell dimensions were obtained, at 21°C , on a manual Picker 4 circle diffractometer using Cu K α radiation ($\lambda = 1.5405\text{\AA}$), by accurately centering fourteen high 2θ reflections ($2\theta \geq 83.0^\circ$). The 2θ values obtained were refined by least squares⁶ and the axial lengths calculated were:

$$\begin{array}{ll} a = 15.446 \pm 0.001\text{\AA} & \alpha = 90.0^\circ \\ b = 8.093 \pm 0.001\text{\AA} & \beta = 90.0^\circ \\ c = 9.430 \pm 0.001\text{\AA} & \gamma = 90.0^\circ \end{array}$$

The experimental density, measured by flotation in a mixture of bromobenzene and dibromomethane, was $1.720 \pm 0.006 \text{ g./cm.}^3$. The value calculated for a formula weight of 303.16 a.m.u., a unit cell volume of 1178.8\AA^3 and $Z=4$ was 1.714 g./cm.^3

Intensity data were collected on a manual Picker 4 circle diffractometer with Mo K α radiation ($\lambda = 0.7107\text{\AA}$)

monochromatised by the (002) reflection of a graphite crystal and using a tube take-off angle of 2.0° . The prism used for data collection, which had major dimensions of $0.164 \text{ mm.} \times 0.32 \text{ mm.} \times 0.107 \text{ mm.}$, was mounted on a glass fibre, such that the c/c^* axis was coincident with the ϕ axis of the diffractometer. The crystal was twenty cm. from both the source and the counter windows. Source and counter collimators were both 1.0 mm. in diameter. Intensities were measured using a scintillation counter with the pulse height analyser set to accept approximately 96% of the transmitted peak when the window was centered on the $K\alpha$ peak. A coupled ω - 2θ moving crystal, moving counter technique was used with a scan rate of $2.0^\circ/\text{minute}$, to scan a range of 2.0° in 2θ , centered on the calculated position of the $K\alpha$ peak.⁶⁷ Stationary background counts were measured for thirty seconds immediately before and after each scan. A total of 1348 independent reflections were scanned with $2\theta \leq 55.0^\circ$. A periodic check (approximately every five hours) of five well distributed reflections showed no systematic variation in intensity indicative of crystal decomposition and none showed any deviation greater than 3% from its mean value. Ten very intense reflections, whose count ratios exceeded the linear response range of the counting system were remeasured at a lower power, obtained by lowering the milliamperage and voltage on the X-ray tube. To scale

these reflections to a level common with the rest of the data, five intense reflections, at full power, were also measured at the same reduced power and the resulting intensity ratios were then used as a scaling factor.

Experimental data were corrected for background assuming a linear variation over the scan range and the integrated intensities obtained were then corrected for Lorentz and polarization effects. A relatively scaled set of $|F_o|$ and $|F_o|^2$ was then calculated⁸⁶ and 815 independent intensities were found to be statistically significant using the dual criteria as stated before.*

Only these statistically significant reflections were used during the subsequent refinement. Standard deviations in $|F_o|$ were derived from the standard deviation of the experimental intensities according to Doedens and Ibers,¹¹ using an uncertainty factor, p^2 , of 0.002. The weighting scheme used throughout the refinement was $\omega = \frac{1}{\sigma^2} \cdot (|F_o|)$. In the final stages of refinement absorption corrections were applied to these data.⁸⁹ The crystal faces were identified as {221} {110} and {100}, but were idealised to (100), ($\bar{1}00$), (010), (0 $\bar{1}0$) and {201} and the dimensions were measured very carefully. Equations for the plane faces were calculated allowing slight variations (up to 10%) in the parameters

* See page 44.

for these equations, such that optimum agreement between the calculated and observed curves for the $00l$ reflections, obtained by rotation of the crystal about the ϕ axis at $\chi = 90.0^\circ$, was obtained. Absorption corrections ($\mu_{\text{Mo}} = 24.02 \text{ cm}^{-1}$) to I and $\sigma(F)$ gave a relatively scaled set of $|F_o|$ and $\sigma(F)$ and the calculated transmission factors were in the range 0.734 to 0.791.

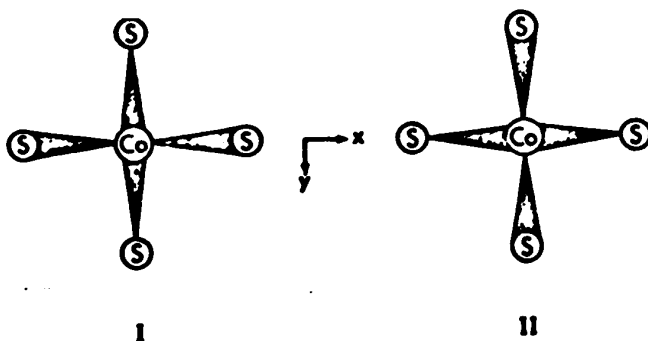
SOLUTION AND REFINEMENT OF THE STRUCTURE

Space group Pccn has eight general positions and density calculations had indicated four molecules of $\text{Co}(\text{S}_2\text{PMe}_2)_2$ per cell. This restriction required the cobalt atom to be located on a special position, either a centre of symmetry or a twofold axis. Spectroscopic studies (i.r., vis., u.v.) on similar compounds⁸² had indicated a tetrahedrally coordinated cobalt atom, so the cobalt atom was assigned a position on a twofold axis, viz. $(\frac{1}{2}, \frac{1}{2}, z)$ which was confirmed by the Patterson solution and successful refinement.

Using a three dimensional Patterson map, which had mmm symmetry, the z coordinate of the cobalt atom was, initially, calculated as 0.17 from the Harker line $(\frac{1}{2}, \frac{1}{2}, w)$. Only two peaks were at the correct distance from the origin to be considered as possible cobalt-sulphur vectors and they were:

	$ \Delta x $	$ \Delta y $	$ \Delta z $	<u>Distance, Å</u>
Vector 1.	0.12	0.00	0.12	2.17
Vector 2.	0.00	0.22	0.12	2.11

As the coordination around the cobalt atom was assumed to be tetrahedral there were two possible models using the above two vectors and knowing that the Patterson map had mmm symmetry. They were:



Assuming that the molecule was a discrete molecular species these two models would have been expected to produce:

(i) A cobalt-phosphorus vector at approximately 3.5\AA from the origin either along the z axis or in the xy plane at 45° to the cobalt-sulphur vectors. This peak was not located.

(ii) Sulphur-sulphur vectors between sulphur atoms attached to symmetry related cobalt atoms. These peaks were not located.

Hence no distinction between models (I) and (II) could be made so both models, with the phosphorus atoms

inserted by inspection, were subjected to a cycle of least squares refinement.¹⁴ Both models had $R_1 \approx 0.40$ and $R_2 \approx 0.60$ as did the models with the phosphorus atoms bridging between different pairs of sulphur atoms. The observed Fourier map calculated for each model showed no recognizable features.

The possibility that the compound may be a polymeric species was raised in trying to explain the largest peak in the Patterson map at (0.12, 0.24, 0.25). The distance between adjacent cobalt atoms was 4.6\AA , (i.e. $\frac{1}{2}c$) and a phosphorus atom, lying exactly half way between neighbouring cobalt atoms, would be able to bridge between sulphur atoms attached to adjacent cobalt atoms. This arrangement of atoms explained all major features of the Patterson map. The ambiguity as to the true structure brought about by the mmm symmetry could not be resolved except by trying each model. The first model tried gave an overall discrepancy factor, R , of 0.41 but for hkl ($l=2n$) $R \approx 0.20$ and for hkl ($l=2n+1$) $R = 0.45$. All four models exhibited the same discrepancy factors until the other possible solution for the cobalt atoms z coordinate was tried (corresponding to $\frac{1}{2}-2z$). This effectively altered the z coordinate of all atoms and these new coordinates, along with those of the two carbon atoms obtained from inspection of a model, were refined. The coordinates used were:

<u>Atom</u>	<u>x</u>	<u>y</u>	<u>z</u>	<u>B</u>
Co	0.25	0.75	0.08	2.0
S1	0.25	1.00	0.20	2.0
S2	0.125	0.76	0.96	2.0
P	0.13	0.99	0.83	2.0
C1	0.04	0.99	-0.26	3.0
C2	0.12	1.18	-0.05	3.0

The refinement may be conveniently listed:

<u>Comments</u>	<u>No. of Cycles</u>	<u>R₁[*]</u>	<u>R₂[*]</u>
All atoms isotropic.	6	0.064	0.095
Co, P, S anisotropic.	2	0.045	0.080
All anisotropic.	2	0.043	0.077
After absorption, all atoms anisotropic.	4	0.040	0.062
Same as above with 2 secondary extinction affected planes removed.	2	0.038	0.058

$$^*R_1 = \frac{\sum ||F_o| - |F_c||}{\sum |F_o|} \quad \text{and} \quad R_2 = \left[\frac{\sum w(|F_o| - |F_c|)^2}{\sum w|F_o|^2} \right]^{1/2}$$

where $w(|F_o| - |F_c|)^2$ was minimised.

A final difference Fourier map showed no peak higher than $0.39e^{-}/\text{\AA}$ and an attempt to find the methyl hydrogen atoms was unsuccessful. Analysis of the weighting scheme exhibited lack of dependence of $w\Delta^2$ ($\Delta = |F_o| - |F_c|$) when divided into ranges according to $|F_o|$ and $(\sin\theta)/\lambda$ values in accordance with Cruickshank's criterion.¹⁵ Scattering factors used were those due to Cromer and Waber¹⁶ and the anomalous dispersion corrections for cobalt ($\Delta f' = 0.40e^{-}$, $\Delta f'' = 1.10e^{-}$), sulphur ($\Delta f' = 0.10e^{-}$, $\Delta f'' = 0.20e^{-}$), and phosphorus ($\Delta f' = 0.10e^{-}$, $\Delta f'' = 0.20e^{-}$) applied to F_{calc} were taken from International Tables of X-ray Crystallography.¹⁷

RESULTS

Figure 8 is a perspective view of the $\text{Co}(\text{S}_2\text{PMe}_2)_2$ polymeric chain (with the c axis vertical) indicating the numbering scheme used. Figure 9 illustrates the molecular packing seen from approximately down the b axis. Table 30 lists the final atomic coordinates, along with the equivalent isotropic thermal parameters, for the asymmetric unit, while the anisotropic thermal parameters are given in Table 31. Tables 32, 33, and 34 list intramolecular bond lengths, bond angles, and the final calculated and observed structure amplitudes.

Figure 8

A perspective view of the $\text{Co}(\text{S}_2\text{PMe}_2)_2$ entity
with 60% probability ellipsoids.

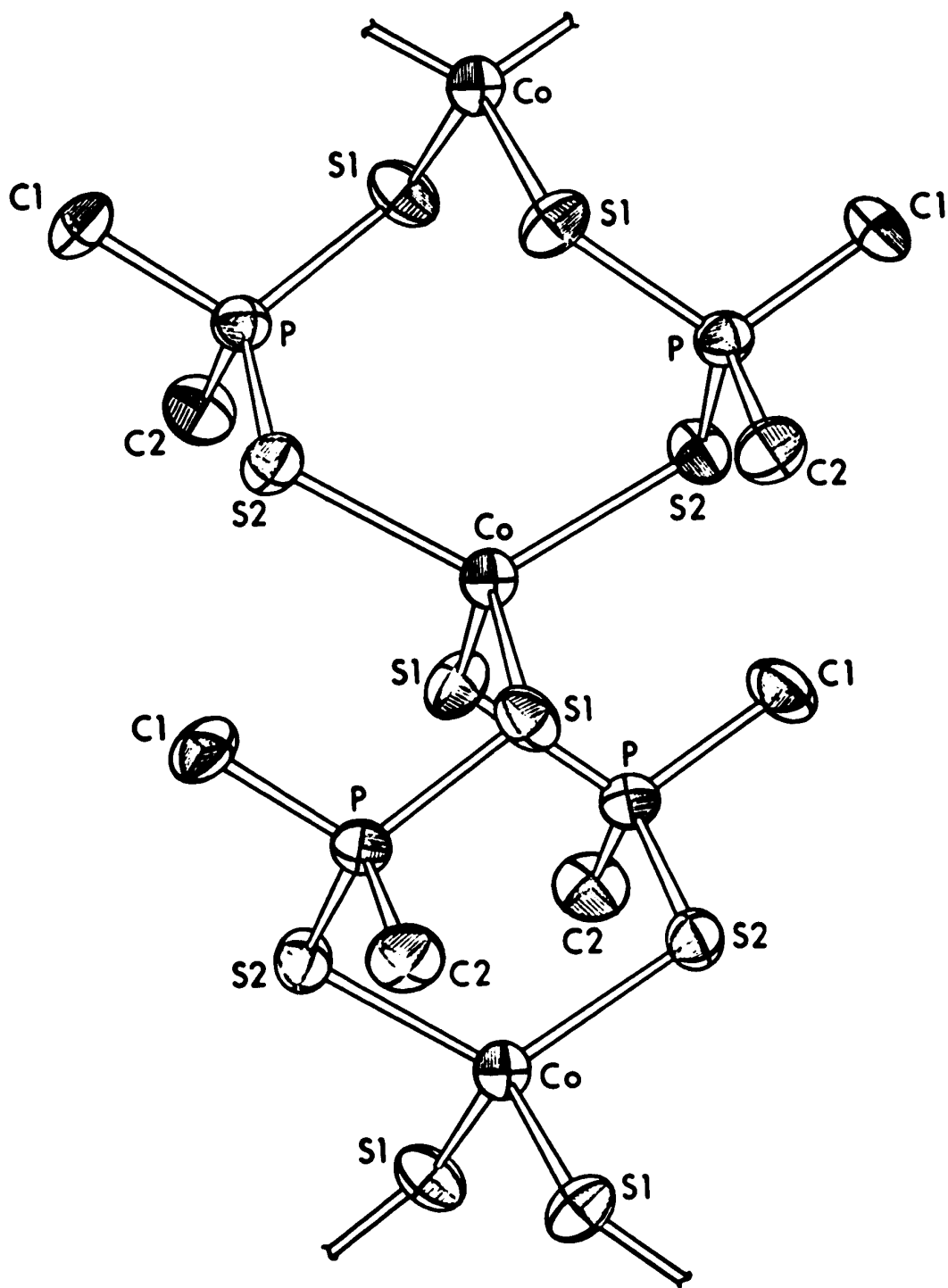


Figure 9

The molecular packing of $\text{Co}(\text{S}_2\text{PMe}_2)_2$ viewed approximately down the b axis.

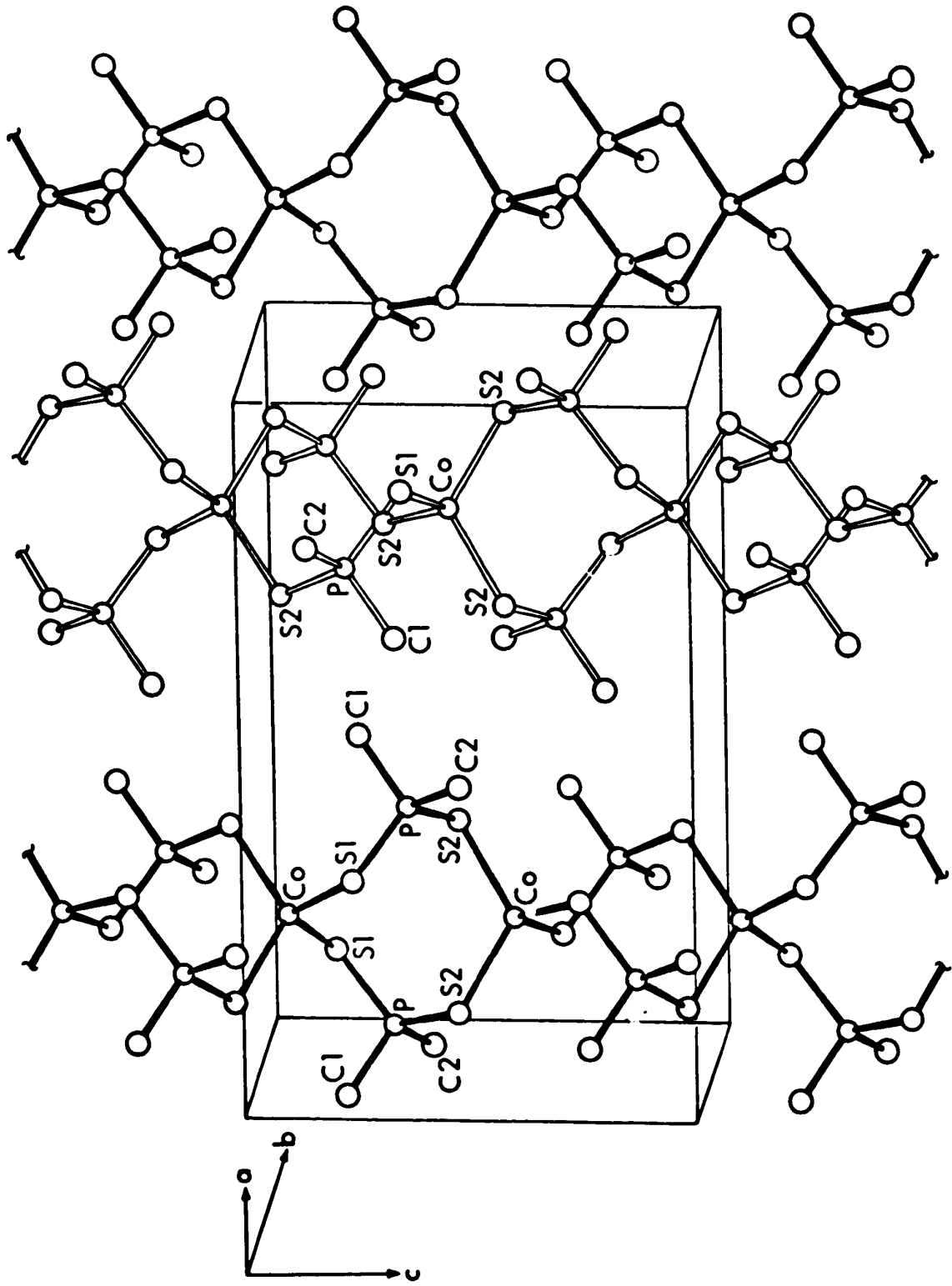


Table 30

Final Atomic Coordinates and Equivalent Isotropic
Temperature Parameters for $\text{Co}(\text{S}_2\text{PMe}_2)_2$

<u>Atom</u>	<u>x</u>	<u>y</u>	<u>z</u>	<u>B, Å²</u>
Co	0.25000(0)*	0.75000(0)*	0.08468(8) ^a	1.82
S1	0.26270(7)	0.99567(12)	0.20918(12)	2.36
S2	0.12040(7)	0.78855(12)	-0.03834(12)	2.19
P	0.13115(7)	0.98761(12)	-0.16659(11)	1.82
C1	0.0327(3)	0.9923(6)	-0.2721(5)	2.76
C2	0.1304(3)	1.1782(5)	-0.0662(5)	2.69

^a Numbers in parentheses are estimated standard deviations occurring in the last digits listed.

* These parameters were not refined because of restraints due to site symmetry.

Table 31 Anisotropic Temperature Parameters ($\times 10^5$) for $\text{Co}(\text{S}_2\text{PMe}_2)_2$.

Atom	β_{11}^b	β_{22}	β_{33}	β_{12}	β_{13}	β_{23}
Co	195(8) ^a	651(10)	559(9)	2(5)	0*	0*
S1	271(5)	738(14)	723(13)	79(7)	-144(6)	91(11)
S2	208(4)	873(15)	652(13)	66(6)	39(6)	210(11)
P	211(4)	663(14)	486(11)	23(6)	9(5)	1(10)
C1	250(16)	1324(80)	681(49)	71(32)	-166(26)	31(54)
C2	329(19)	861(58)	754(56)	73(30)	13(27)	-285(50)

* These parameters were not refined because of restraints due to site symmetry.

^a Numbers in parentheses are estimated standard deviations occurring in the last digits listed.

^b Anisotropic thermal parameters defined by

$$\exp[-\beta_{11}h^2 + \beta_{22}k^2 + \beta_{33}l^2 + 2\beta_{12}hk + 2\beta_{13}hl + 2\beta_{23}kl]$$

Table 32
Intramolecular Distances (Å) for $\text{Co}(\text{S}_2\text{PMe}_2)_2$.

<u>Atoms</u>	<u>Distance</u>
Co - S1	2.316(2) ^a
Co - S2	2.331(1)
S1 - P	2.014(1)
S2 - P	2.019(2)
P - C1	1.817(2)
P - C2	1.809(4)

^aNumbers in parentheses are estimated standard deviations in the last digits listed.

Table 33Intramolecular Angles (Degrees) for $\text{Co}(\text{S}_2\text{PMe}_2)_2$.^a

<u>Atoms</u>	<u>Angle</u>
S1 - $\hat{\text{C}}\text{o}$ - S2	102.04(5) ^b
S1 - $\hat{\text{C}}\text{o}$ - S1'	119.26(9)
S1' - $\hat{\text{C}}\text{o}$ - S2	107.03(4)
S2 - $\hat{\text{C}}\text{o}$ - S2	120.55(7)
Co - $\hat{\text{S}}1$ - P ^{''}	109.53(6)
Co - $\hat{\text{S}}2$ - P	109.40(5)
S1 - $\hat{\text{P}}$ - S2'	107.03(4)
S1'' - $\hat{\text{P}}$ - C1	111.4(2)
S1'' - $\hat{\text{P}}$ - C2	106.3(2)
S2 - $\hat{\text{P}}$ - C1	105.9(2)
S2 - $\hat{\text{P}}$ - C2	111.6(2)
C1 - $\hat{\text{P}}$ - C2	105.2(2)

^aSymmetry transformations are as follows:prime: $\frac{1}{2}-x, \frac{1}{2}-y, z$ double prime: $\frac{1}{2}-x, y, \frac{1}{2}+z$ ^bNumbers in parentheses are estimated standard deviations occurring in the last digits listed.

Table 34

Observed and calculated structure amplitudes ($\times 10$)
in electrons for $\text{Co}(\text{S}_2\text{PMe}_2)_2$.

DISCUSSION

The crystal structure of $\text{Co}(\text{S}_2\text{PMe}_2)_2$ consists of polymeric chains (in the [001] direction) built up by double dithiophosphate bridges between cobalt atoms which have distorted tetrahedral coordination (see Figure 8). The identity period of the chain is equal to one half of the c axis (4.701\AA) of the unit cell and the symmetry of the structure is determined by the crystallographic twofold screw axes with the cobalt atoms situated on special positions of twofold symmetry. The $\text{S}-\hat{\text{C}}\text{o}-\text{S}$ angles that range from 102.04° to 120.55° show considerable deviation from the tetrahedral angle of 109.47° . However, this distortion is probably less than would be found in a monomeric *bis* complex with tetrahedral coordination where for example the $\text{S}-\hat{\text{C}}\text{o}-\text{S}$ angles within the chelate ring would probably be less than 90° .

The cobalt sulphur bond lengths of 2.316\AA and 2.331\AA are intermediate between the values reported for *bis*-dithiolato complexes which have cobalt-sulphur bond lengths in the range $2.16 - 2.18\text{\AA}$, e.g. $[\text{n-C}_4\text{H}_9)_4\text{N}]_2^+[\text{Co}(\text{S}_2\text{C}_4\text{N}_2)_2]^{2-}$,⁵⁰ of 2.161\AA and the average value of 2.463\AA reported for $[\text{Zn}(\text{S}_2\text{PEt}_2)_2]_2$;⁷⁸ this latter complex being isostructural with its cobalt analogue, and contains both four and eight membered rings (see Figure 11), the value quoted being for the four membered rings.

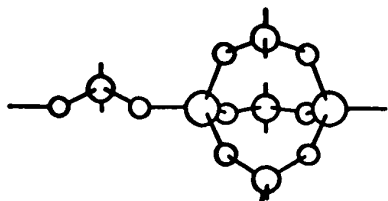


Figure 10

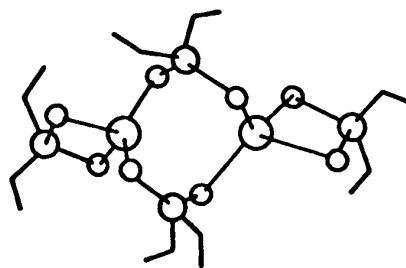


Figure 11

These values agree well with the cobalt-sulphur bond length found in compounds that exist as dimers or polymers. In $[\text{Zn}(\text{S}_2\text{PEt}_2)_2]_2$ ⁷⁸ the values within the eight membered are 2.302 - 2.382Å and in the $\text{Co}(\text{SOPPh}_2)_2$ polymer.¹⁰³ The cobalt-sulphur distances are 2.318 - 2.356Å (see Figure 10 for a schematic view of the molecule). In the dimeric compound $\{[(\text{CF}_3)_2\text{C}_2\text{S}_2]_2\text{Co}_2\}$ ⁵² linkage occurs between each half of the dimer by two cobalt-sulphur bonds of length 2.38Å while Alderman *et al*¹⁰⁴ report a pyramidal coordinated cobalt atom with four sulphur atoms at the corners of the base where two cobalt sulphur bonds have an average length of 2.39Å and the other two, an average of 2.22Å. The phosphorus-carbon bond lengths are in excellent agreement (see Table 44) with those of $\text{Cr}(\text{S}_2\text{PMe}_2)_3$, and $\text{VO}(\text{S}_2\text{PMe}_2)_2$ and compare favourably with similar compounds. The coordination of the phosphorus atom will be discussed in the final chapter. The bond angles found, except for the $\text{C1}-\hat{\text{P}}-\text{C2}$ angle which agrees well with similar angles (see Table 35), are representative of those found in dimeric

and polymeric thiophosphinic compounds and are summarized below:

Table 35

<u>Compound</u>	<u>S-M-S</u>	<u>M-S-P</u>	<u>S-P-S</u>	<u>S-P(A)^o</u> ^a	<u>Ref.</u>
$[\text{Co}(\text{S}_2\text{PMe}_2)_2]_n$	102.04°, 119.26°	109.53, 109.40°	107.03°	2.016	—
$[\text{Co}(\text{OSPPH}_2)_2]_n$	104.5- 115.4°	88.7- 106.2°	—	2.01	103
$[\text{Zn}(\text{S}_2\text{PEt}_2)_2]_2^b$	119.3- 122.4°	99.2- 106.6°	115.3- 116.7°	2.017	78

^aThe values quoted are averages.

^bIsomorphous with $[\text{Co}(\text{S}_2\text{PEt}_2)_2]_2$.

The $\text{Co}(\text{S}_2\text{PMe}_2)_2$ complex is the first example of a polymeric structure with phosphinate ligands in which both oxygen atoms have been replaced with sulphur atoms. As early as 1962 Coates *et al*¹⁰⁵ predicted a polymeric structure for $\text{Co}(\text{O}_2\text{PR}_2)$ ($\text{R} = \text{Me}, \text{Ph}$) on the basis of solubility in various solvents. The structure proposed was one with a backbone of two phosphinic bridges between distorted tetrahedrally coordinated cobalt atoms (as in Figure 8). F. Giordano and co-workers found, however, that the backbone structure for the $\{\text{Zn}[(n\text{-C}_4\text{H}_9)(\text{C}_6\text{H}_5)\text{PO}_2]_2\}$ ¹⁰⁶ polymer was alternate singly and triply bridging phosphinate groups between tetrahedral zinc atoms, (see Figure 10), in common with the zinc(II) and cobalt(II)

di-n-alkylphosphinate polymers.^{107,108} A similar structure (Figure 10) was found for the $\text{Co}(\text{OSPPH}_2)_2$, the backbone structure being different from the double bridge structure (see Figure 8) proposed by Kuchen *et al*¹⁰⁹

All previous structures of dithiophosphinate complexes that have been solved have either been monomeric or dimeric. The dimeric ones, $\{\text{Zn}[\text{S}_2\text{P}(\text{i-C}_3\text{H}_7\text{O})]_2\}_2$,⁷⁹ $\{\text{Cd}[\text{S}_2\text{P}(\text{i-C}_3\text{H}_7)]_2\}_2$,⁷⁷ $[\text{Co}(\text{S}_2\text{PEt}_2)_2]_2$,⁷⁸ and $[\text{Zn}(\text{S}_2\text{PEt}_2)_2]_2$ ⁷⁸ all feature a molecule formed by tetrahedral metal atoms bridged by two R_2PS_2^- groups, the coordination polyhedron of the metal atom being completed by R_2PS_2^- groups behaving as chelate ligands to form four membered rings (see Figure 11).

The structure of $\text{Co}(\text{S}_2\text{PMe}_2)_2$ may be viewed as a combination of both the dimeric and polymeric structures. It consists of severely distorted tetrahedral cobalt atoms linked by two three atom (-S-P-S-) groups (see Figure 8). This structure does not support the suggestions of M. Calligaris *et al*¹⁰³ based on the behaviour of diphenyl and di-n-alkyl phosphinothionates in solution, that (i) the presence of at least one sulphur atom in the ligands facilitates the formation of stable four membered rings and (ii) the stability of the bridges between metal atoms is decreased when the ligand species changes from the phosphinates to the phosphinothionates and then to the phosphinodithionates.

$\text{Co}(\text{S}_2\text{PMe}_2)_2$ is the only example of a phosphinato polymer without the single and triple bridging backbone structure (as in Figure 10), notwithstanding the fact that the bridging ligand contains two sulphur atoms thus violating the trend noted by Calligaris *et al.*¹⁰³ The probable reason for this polymerisation is the desire of the complex to relieve the steric strain that is present on chelate ring formation with the S_2PR_2^- ligand. (This steric strain will be discussed in the final chapter).

CHAPTER V
THE CRYSTAL STRUCTURE OF
***BIS*(DIMETHYLDITHIOPHOSHINATO)OXOVANADIUM(IV)**

EXPERIMENTALCollection and Reduction of Data

Bright blue needle crystals of $\text{VO}(\text{S}_2\text{PMe}_2)_2$ were kindly supplied by D. Day and were suitable for X-ray analysis as supplied. Preliminary Weissenberg photographs ($hk0 - hk3$) with the needle axis as the rotation axis, taken with Cu K α radiation ($\lambda = 1.5418\text{\AA}$) exhibited the following systematic absences:

$$hkl: h+l = 2n+1; h0l: l = 2n+1; 0k0: k = 2n+1$$

These absences are consistent with the nonstandard monoclinic space group $B2_1/c$. Precession photographs ($h0l - h2l, 0kl - 2kl$) taken with Mo K α radiation ($\lambda = 0.7107\text{\AA}$) showed that standard space group $P2_1/c$ (C_{2h}^5 , No. 14) would be a preferable choice. As it was possible to align the crystal to take advantage of this standard space group, $P2_1/c$ was used throughout the structural analysis. The axial lengths of the $B2_1/c$ cell were measured from the $0kl$ and $h0l$ precession photographs taken with Mo K α radiation ($\lambda = 0.7107\text{\AA}$). The axial lengths of the $P2_1/c$ cell were obtained, at 21°C , on a manual Picker 4 circle diffractometer, using Cu K α radiation ($\lambda = 1.5405\text{\AA}$) by accurately centering twelve high 2θ reflections ($2\theta \geq 81.0^\circ$). The 2θ values obtained were refined by least squares.¹⁶

The axial lengths obtained for the two cells were:

	<u>P2₁/c</u>	<u>B2₁/c</u>
a	10.889 ± 0.002Å	15.175Å
b	12.072 ± 0.002Å	12.065Å
c	10.208 ± 0.001Å	14.662Å
α	90.0°	90.0°
β	91.96 ± 0.01°	93.7°
γ	90.0	90.0°
v	1341.1Å ³	2684.4Å ³

The experimental density, measured, with difficulty, in a mixture of chlorobenzene and dibromethane was 1.57 ± 0.01 g./cm.³ The value calculated for a formula weight of 317.29 a.m.u., a unit cell volume of 1341.1Å³ and Z=4 was 1.571 g./cm.³

Intensity data were collected on a manual Picker 4 circle diffractometer with Cu Kα radiation ($\lambda = 1.5418\text{Å}$), monochromatised by the (002) reflection of a graphite crystal and using a tube take-off angle of 2.0°. Copper radiation was chosen for use in the data collection; usually it would be desirable to use Mo Kα radiation in order to minimise absorption effects ($\mu_{\text{Cu}} = 140.01 \text{ cm}^{-1}$; $\mu_{\text{Mo}} = 15.79 \text{ cm}^{-1}$). However because of the small size of the crystals available the lower background and increased intensities obtainable with Cu Kα radiation made it

preferable. The crystal used had dimensions of 0.098 mm. \times 0.098 mm. \times 0.301 mm. and was mounted, on a glass fibre, such that the a^* of the $P2_1/c$ cell was coincident with the ϕ axis of the diffractometer. The crystal was twenty cm. from both the source and the counter windows. Source and counter collimators were both 1.0 mm. in diameter. Intensities were measured with a scintillation counter with the pulse height analyser set to accept approximately 96% of the transmitted peak when the window was centered on the $K\alpha$ peak. A coupled ω - 2θ moving crystal, moving counter technique was used with a scan rate of 2.0/minute, to scan a range of 2.0° in 2θ , centered on the calculated position of the $K\alpha$ peak.⁸⁷ Stationary background counts were measured for thirty seconds immediately before and after each scan. A total of 1682 independent reflections were scanned with $2\theta \leq 110.0^\circ$. A periodic check (approximately every ten hours) of seven well distributed reflections showed no systematic variation in intensity that is indicative of crystal decomposition and none showed any deviation greater than 3σ from its mean. Twenty very intense reflections, whose count ratios exceeded the linear response range of the counting system, were remeasured at a lower power, obtained by lowering the nulliamperage and voltage on the X-ray tube. To scale these reflections to a level common with the rest of the

data, seven intense reflections, at full power, were also measured at the same reduced power and the resulting intensity ratios were then used as a scaling factor.

Experimental data were corrected for background assuming a linear variation over the scan range. The integrated intensities obtained were then corrected for Lorentz and polarization effects and a relatively scaled set of $|F_o|$ and $|F_o|^2$ calculated.⁸⁸ A total of 1198 independent intensities were found to be statistically significant using the dual criteria stated previously.*

Only these statistically significant reflections were used during the subsequent refinement. Standard deviations in $|F_o|$ were observed from the standard deviation of the experimental intensities according to Doedens and Ibers,¹¹ using an uncertainty factor, p^2 , of 0.002. The weighting scheme used throughout the refinement was $\omega = \frac{1}{\sigma^2} \cdot (|F_o|)$. In the final stages of refinement absorption corrections were applied to these data.⁸⁹ The crystal faces were identified as {100} and {111} and the crystal dimensions were measured very carefully. Equation for the plane faces were calculated allowing slight variation (up to 10%) on the parameters

* See page 44.

for these equations such that optimum agreement between the calculated and observed curves for the h00 reflections, obtained by rotation of the crystal about the ϕ axis at $\chi = 90.0^\circ$, was obtained. Absorption corrections ($\mu_{\text{Cu}} = 142.01 \text{ cm}^{-1}$) gave a relatively scaled set of $|F_o|$ and $\sigma(F)$. The calculated transmission factors were in the range 0.147 - 0.395 and the variation in I_{h00} of 27% before absorption was reduced to approximately 10% after absorption.

SOLUTION AND REFINEMENT OF THE STRUCTURE

An attempt was made to solve the structure of $\text{VO}(\text{S}_2\text{PMe}_2)_2$ using a three dimensional Patterson map. This was unsuccessful because of (a) the comparable atomic numbers of vanadium, phosphorus, and sulphur and the consequent comparable heights of the vector peaks. (b) the superposition of vector peaks due to the similar sulphur-sulphur, phosphorus-phosphorus and vanadium-vanadium distances between like atoms of symmetry related molecules.

The next attempt was made using the Σ_2 relationship of Karle and Hauptman,^{110,111} the 'direct methods' approach utilising the programs MAGIC and FAME.¹¹² These programs allow automatic application of the Σ_2 relationship to intensity data for any centrosymmetric space group of orthorhombic or lower symmetry.

These two programs utilise the normalised structure factor E_{hkl} , but the unitary structure factor, U_{hkl} , must be defined first:

$$U_{hkl} = \frac{F_{hkl}}{\sum_{i=1}^N f_i}$$

where F_{hkl} = the structure factor for the reflection with indices (hkl) .

N = number of different atoms in the unit cell

and f_i = the scattering factor for the i th atom.
 $= f_0 \cdot e^{-B(\sin^2\theta)/\lambda^2}$

where B = the temperature factor

and λ = wavelength of the radiation used.

As U_{hkl} is a structure factor it may be calculated in an exactly analogous manner to F_{hkl} , i.e. for the centrosymmetric case

$$U_{hkl} = \frac{1}{2} \sum_{i=1}^N n_i \cdot \cos 2\pi(hx_i + ky_i + lz_i)$$

where $n_i = \frac{f_i}{\sum_{i=1}^N f_i}$ i.e. the fraction of the scattering power represented by the i th atom.

The average mean square value of the unitary structure factor is given by*

$$\overline{U^2} = \sum_{i=1}^N n_i^2$$

*This is exactly analogous to $\overline{F^2}$. See reference 91.

The normalised structure factor, E_{hkl} , as defined by Karle and Hauptman¹¹³ is given by

$$E_{hkl}^2 = \frac{U_{hkl}}{U^2}$$

E_{hkl} 's have a particular advantage in that they allow the normalisation of all reflections to a common basis, thus avoiding the error of comparing special sets of reflections. Consequently a significant factor in the calculation of E_{hkl} is that a given U_{hkl} must be related to the true U^2 for the class of reflections to which it belongs, i.e. account must be taken of the multiplicity of the class of reflections. Therefore, in general

$$E_{hkl}^2 = \frac{U_{hkl}^2}{\sum_{i=1}^N \epsilon n_i^2}$$

where ϵ is a multiplicity factor.¹¹⁴ An equivalent form of this expression, which is used by FAME, is

$$E_{hkl}^2 = \frac{|F_{hkl}|^2}{\sum_{i=1}^N \epsilon f_i^2} \quad (1)$$

The distribution of $|E|$ values is in principle, and often in practice, independent of the size and content of the unit cell. It does depend, however, on the presence or absence of a centre of symmetry in the space group and therefore the values of the $|E_{hkl}|^2$ afford a statistical test for acentric or centric distributions of intensities.¹¹⁵ The results obtained in this case were:

<u>Quantity</u>	<u>Observed</u> [*]	<u>Calculated</u>	
		<u>Centric</u>	<u>Acentric</u>
Average $ E $	0.853	0.798	0.886
Average $ E ^2$	1.0	1.0	1.0
Average $ E^2-1 $	0.853	0.968	0.736
$ E > 1.0\%$	31.80	32.00	36.80
$ E > 2.0\%$	3.51	5.00	1.80
$ E > 3.0\%$	0.25	0.30	0.01

^{*}Scaled such that average $|E|^2 = 1.0$

The indication in this case was that the space group of $\text{VO}(\text{S}_2\text{PMe}_2)_2$ was centrosymmetric.

The Σ_2 relationship says that the sign of a structure factor may be calculated in terms of a pair of reflections whose signs are known when the following

condition is satisfied: the algebraic sum of the Miller indices of the known reflections must be equal to the indices of the unknown. For example, if a pair of knowns have indices 210 and $3\bar{1}\bar{3}$ then the unknown would be $50\bar{3}$, i.e. the known pair is said to have a Σ_2 interaction with the unknown. If an unknown has one or more interactions with pairs of knowns then the probability of the unknown having the same signs of the known pair, i.e. the probability, P , of a reflection with indices hkl having the phase given by the product of the phases of other reflections having indices $[(h-h'), (k-k'), (l-l')]$ and $h'k'l'$ is given by

$$P(E_{hkl}) = 0.5 + 0.5 \cdot \tanh[\sigma \cdot |E_{hkl}| \cdot \sum E_{h'k'l'} \cdot E_{h-h', k-k', l-l'}] \dots(2)$$

where E = the normalised structure factor

Σ = the sum over all pairs of knowns which have a Σ_2 interaction with the particular known under consideration.

and σ = probability factor

$$= \frac{\sum_{i=1}^N n_i^3}{\left[\sum_{i=1}^N n_i^2 \right]^{3/2}}$$

The value of sigma, σ , for $\text{VO}(\text{S}_2\text{PMe}_2)_2$ was 0.176.

Values of $P < 0.5$ indicate that the sign of E_{hkl} is negative with a probability P_- given by

$$P_- = 1 - P(E_{hkl})$$

In practice there are no reflections whose signs are known absolutely at the start (except for origin signs that may be chosen as positive or negative) so a small group of reflections is assigned a set of symbols (e.g. A, B, etc.) and these are used in lieu of genuine knowns. Treatment of the unknowns is then just as before, using products of the symbols of the pairs instead of the sign products; as this procedure progresses, with more reflections joining the list of the knowns as they are determined, the symbols exhibit systematic relationships with each other, which indicate the signs the symbols represent. Finally the equivalences may be evaluated and + or - signs assigned to each symbol, thus making a 'most consistent' set. This procedure is known as 'Symbolic Addition'.

FAME converted the structure factors, F_{hkl} to normalised structure factors, E_{hkl} , using the formula

$$|E_{hkl}|^2 = \left\{ \frac{1}{S^2} \cdot F_{obs}^2 \cdot \exp[B(\sin\theta)^2/\lambda^2] \right\} / (\epsilon \Sigma f_i^2)$$

where λ = wavelength of radiation used

S = scale factor obtained from a Wilson plot

B = overall temperature factor obtained from a

Wilson plot^{112,91} and then substituting $|F_{hkl}|^2$

in Equation (1) for use in the Σ_2 relationship. The

values of S and B for $\text{VO}(\text{S}_2\text{PMe}_2)_2$ were 1.985 and 4.359 respectively.

The assignment of a fixed number of starting symbols was done using the following criteria:

- (i) symbols are assigned to as many different parity groups as possible.
- (ii) higher E's are favoured.
- (iii) reflections that have more Σ^2 interactions with other large E's are favoured.

The symbols assigned were:

<u>h</u>	<u>k</u>	<u>l</u>	Parity	<u>E</u>	<u>Symbol</u>
1	6	4	oee	2.537	A
4	$\bar{3}$	$\bar{2}$	eeo	2.847	B
6	4	3	eeo	3.049	C
4	$\bar{1}$	$\bar{5}$	ooo	3.722	D
5	$\bar{2}$	$\bar{1}$	oeo	2.298	E
1	$\bar{3}$	$\bar{4}$	eeo	2.722	F
5	1	7	ooo	2.864	G
0	6	8	eee	2.717	H
5	0	$\bar{6}$	oee	2.698	J

The specification of the origin was made by assigning phases arbitrarily to a properly chosen set of $|E_{hkl}|$ using the largest suitable $|E_{hkl}|$'s.¹¹⁶ For $\text{VO}(\text{S}_2\text{PMe}_2)_2$ the following choice was made: A+, B+, and C+.

MAGIC is a high speed program for the completely automatic generation of phases using the Karle-Hauptman Σ_2 relationship, which in practise, starting with a small group of knowns, either known to be plus (origin signs) or assigned symbolic signs and using an iterative procedure, may be used to phase enough E's to give a meaningful E map. Four parameters are used to decide whether a sign indication is strong enough to allow addition of the unknown E to the list of knowns and they are:

- (i) The minimum acceptable probability as defined by (2). This is usually ≥ 0.95 .
- (ii) The minimum number of contributors - normally one.
- (iii) The maximum number of inconsistencies, i.e. contributors with opposite sign - usually zero.
- (iv) The minimum ratio of contributors to inconsistencies - usually 1.0.

In this case, symbols A-E were inputted into the symbolic addition procedure along with all of the unknown E_{hkl} 's and 156 signs were determined with the following assignments.

<u>Symbol</u>	<u>Sign</u>	<u>Probability</u>	<u>No. of Determinations</u>
BCD	-	0.880 - 0.998	13
BCD	+	0.880 - 0.998	19
A C E	-	0.880 - 0.985	9
A C E	+	0.860 - 1.000	138
AB DE	-	0.860 - 0.985	12
AB DE	+	0.860 - 0.992	17

The best choice of signs for the symbols was then A+, B+, C+, D+ or D-, E+. Due to inexperience MAGIC was initially run with all E_{hkl} 's but use of E_{hkl} 's ≥ 1.5 is more likely to give a correct solution. Hence the five initial symbols plus six more that had been determined in the first run of MAGIC were used as input to MAGIC with all $E_{hkl} \geq 1.5$ as unknowns. The assignment of signs was confirmed and a total of 106 $E_{hkl} \geq 1.5$ had their signs determined.

A Fourier map (i.e. E map) using these 106 known E's (i.e. signs known) was computed for both cases, D+ve or D-ve. The solution extracted from the D+ map gave, after one cycle of refinement, $R_1 = 0.48$ and $R_2 = 0.56$

where

$$R_1 = \frac{\sum ||F_o| - |F_c||}{\sum |F_o|} \quad \text{and} \quad R_2 = \left[\frac{\sum w(|F_o| - |F_c|)^2}{\sum w|F_o|^2} \right]^{1/2}$$

and the function $\sum w(|F_{\text{obs}}| - |F_{\text{calc}}|)^2$ was minimised and where $w = 1/\sigma^2 \cdot (F)$. The D-map solution gave $R_1 = 0.49$ and $R_2 = 0.60$. The observed Fourier maps calculated after these cycles showed no solution was obtainable. It was therefore decided to introduce two more symbols, F and G from FAME, into the symbolic addition procedure in the hope of determining more signs of E_{hkl} 's because of the increased number of variables. This was done and all $E_{hkl} \geq 1.5$ (251) had their signs determined with the following assignments:

<u>Symbol</u>	<u>Sign</u>	<u>Probability</u>	<u>No. of Determinations</u>
C FG	-	0.860 - 1.000	76
CDE G	+	0.960	1
B E G	-	0.880 - 1.000	14
B E G	+	0.900	1
A EFG	-	0.860 - 1.000	47
BC EF	-	0.940	1
BC EF	+	0.880 - 0.985	9
A C E	+	0.860 - 1.000	54
AB F	-	0.940	1
AB F	+	0.860 - 0.992	12
ABC G	-	0.860 - 0.996	10
ABC G	+	0.930 - 0.930	2

The choice of signs for the symbols when only five symbols used was confirmed along with F+ and G-, i.e.

the signs were:

A+, B+, C+, D+ or D-, E+, F+, G+.

These E_{hkl} 's were then used to compute two E maps one with D-ve and one with D+ve. The D+ve solution enabled the coordinates of all atoms, except the carbon and oxygen atoms to be found (N.B. with the smaller number of E's the D-ve solution seemed more hopeful). These coordinates were subjected to two cycles of isotropic refinement and gave $R_1 = 0.276$ and $R_2 = 0.409$. An F_{obs} Fourier synthesis was calculated and revealed the remaining five atoms. A further three cycles of isotropic refinement resulted in $R_1 = 0.116$ and $R_2 = 0.158$. Refinement with all atoms anisotropic converged with $R_1 = 0.100$ and $R_2 = 0.141$. Absorption corrections were performed at this juncture and refinement again converged after five cycles with all of the atoms anisotropic with $R_1 = 0.062$ and $R_2 = 0.102$.

Comparison of the observed and calculated structure factors, especially at low $\sin\theta$, indicated that secondary extinction effects may be affecting the refinement. Thus, secondary extinction corrections were undertaken using the method of Zachariasen.¹¹⁷ Zachariasen defines

$$F_{corr} = KF_{obs} [1 + \beta(2\theta) \cdot C \cdot J_{obs}]$$

where F_{corr} = the observed structure factor corrected for secondary extinction.

F_{obs} = the observed structure factor

J_{obs} = the observed integrated intensity on an arbitrary scale

K, C = scale factors, refined in the program SFLS5.

$\beta(2\theta)$ = angular variation of the extinction correction. It is assumed to be normalised to unity at $2\theta = 0.0^\circ$

$\beta(2\theta)$ may be expressed as

$$\beta(2\theta) = \text{Polarization Term} \cdot \frac{A^{*\prime}(2\theta)}{A^{*\prime}(0)}$$

where $A^{*\prime}(2\theta) = \frac{dA^*}{d\mu}$ at $2\theta^\circ$

and $A^{*\prime}(0) = \frac{dA^*}{d\mu}$ at $2\theta = 0.0^\circ$

and $A^* = 1/(\text{transmission factor}, A)$

The polarization term for Picker diffractometer geometry is:

$$\frac{(1 + \cos^2 2\theta_m)(\cos^2 2\theta_m + \cos^4 2\theta)}{(\cos^2 2\theta_m + \cos^2 2\theta)^2}$$

where $2\theta_m$ = 2θ angle of the monochromator crystal.

and 2θ = 2θ angle of the reflection under consideration.

The ratio $A^{*'}(2\theta)/A^{*'}(0)$ was evaluated, numerically, as follows:

$$\begin{aligned} \frac{dA}{d\mu} &\approx \frac{\Delta A}{\Delta \mu} \\ \therefore \frac{A^{*'}(2\theta)}{A^{*'}(0)} &= \frac{\frac{\Delta A^{*'}(2\theta)}{\Delta \mu}}{\frac{\Delta A^{*'}(0)}{\Delta \mu}} \\ &= \frac{\Delta A^{*'}(2\theta)}{\Delta A^{*'}(0)} \\ &= \frac{\Delta A(0)}{\Delta A(2\theta)} \end{aligned}$$

where ΔA was computed by taking the difference of two transmission factors calculated with the absorption coefficient, μ , having the values of μ and $(\mu + 0.1\mu)$. Three cycles of refinement were undertaken refining the secondary extinction coefficient, C , as well as all the other usual parameters and resulted in $R_1 = 0.060$ and $R_2 = 0.097$.

The values of the extinction coefficient and its estimated standard deviation along with no improvement in the agreement between F_{obs} at low $\sin\theta$ indicated that the expected secondary extinction effects were not significant in this structure. Two more cycles of refinement without secondary extinction corrections converged to $R_1 = 0.059$ and $R_2 = 0.088$.

An electron density difference map based on the final parameters contained no residual peaks greater than $0.46e^{-}/\text{\AA}^3$. An attempt was made to find the methyl hydrogen atoms, but was unsuccessful. The experimental weighting scheme satisfied, within acceptable limits, Cruickshank's criterion¹⁵ and in the final cycle of refinement no parameter changed by more than one quarter of its standard deviation. The structure factors used were these due to Cromer and Waber¹⁶ and the anomalous dispersion corrections for vanadium ($\Delta f' = 0.1e^{-}$, $\Delta f'' = 2.3e^{-}$), phosphorus ($\Delta f' = 0.2e^{-}$, $\Delta f'' = 0.5e^{-}$), and sulphur ($\Delta f' = 0.30e^{-}$, $\Delta f'' = 0.60e^{-}$) applied to f_{calc} , were taken from International Tables for X-ray Crystallography.¹⁷

RESULTS

Figure 12 is a perspective view of the $\text{VO}(\text{S}_2\text{PMe}_2)_2$ molecule, indicating the numbering scheme used. Figure 13 is a side view of the molecule showing the bending of the ligands, and where M1 and M2 are the mid-points between the atoms S1-S2 and S3-S4 respectively. Figure 14 shows the molecular packing of the molecules projected onto the ac plane. Table 42 lists the final calculated and observed structure amplitudes. Table 36 reports the fractional coordinates and the equivalent isotropic temperature factors, while Table 37 lists the anisotropic thermal parameters. Tables 38 to 41 contain data on intramolecular distances, intramolecular angles, intermolecular non-bonded contacts, and least squares planes respectively.

Figure 12

A perspective view of the $\text{VO}(\text{S}_2\text{PMe}_2)_2$ molecule
with 50% probability ellipsoids.

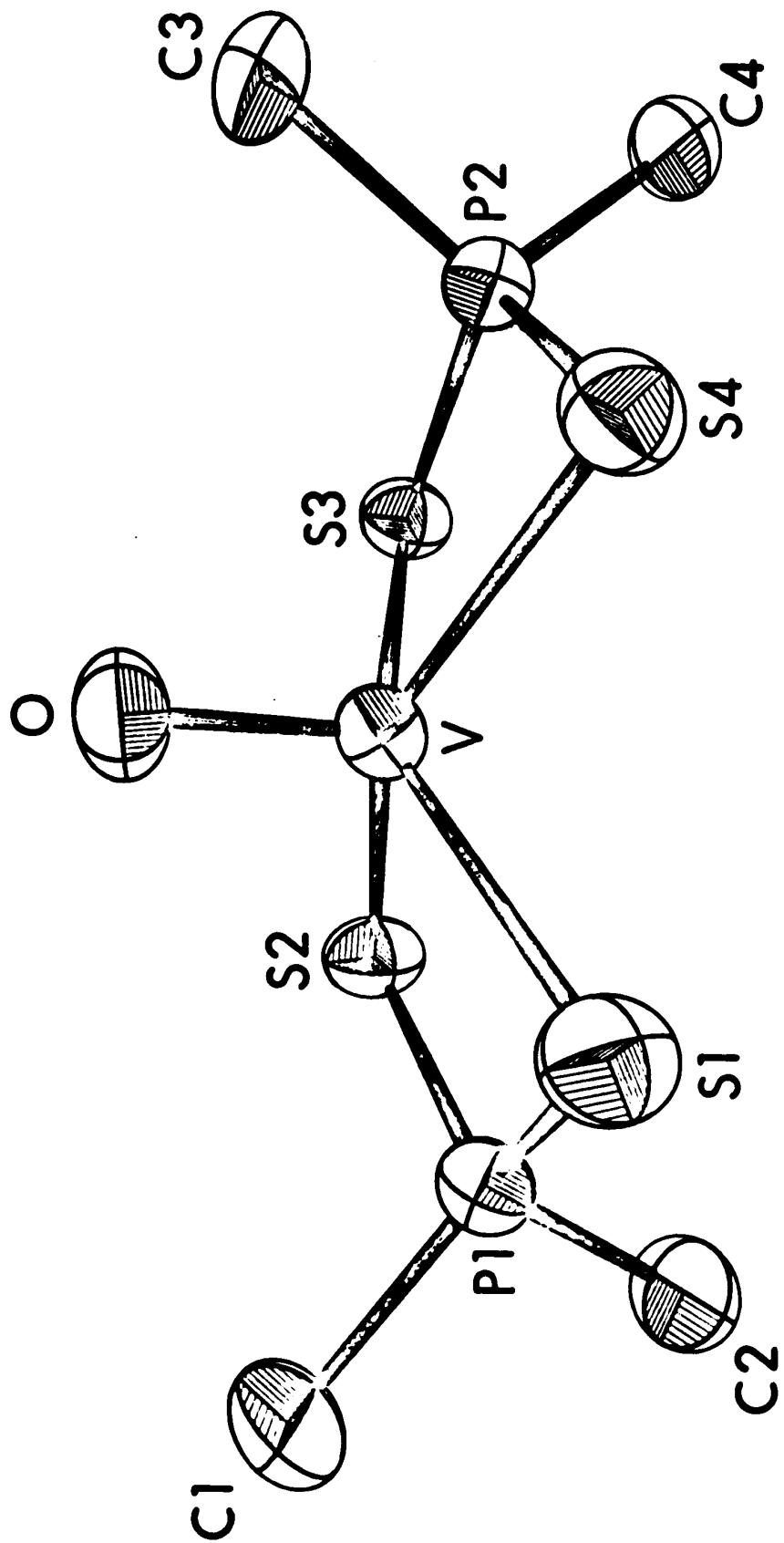


Figure 13

A side on view of the $\text{VO}(\text{S}_2\text{PMe}_2)_2$ molecule where M1 and M2 are the mid points between the atoms S1-S2 and S3-S4 respectively. The atoms are scaled in the ratio of their isotropic temperature factors. M1 and M2 have a pseudo temperature factor, B, of 4.95\AA^2 , the mean of the sulphur atoms' temperature factors.

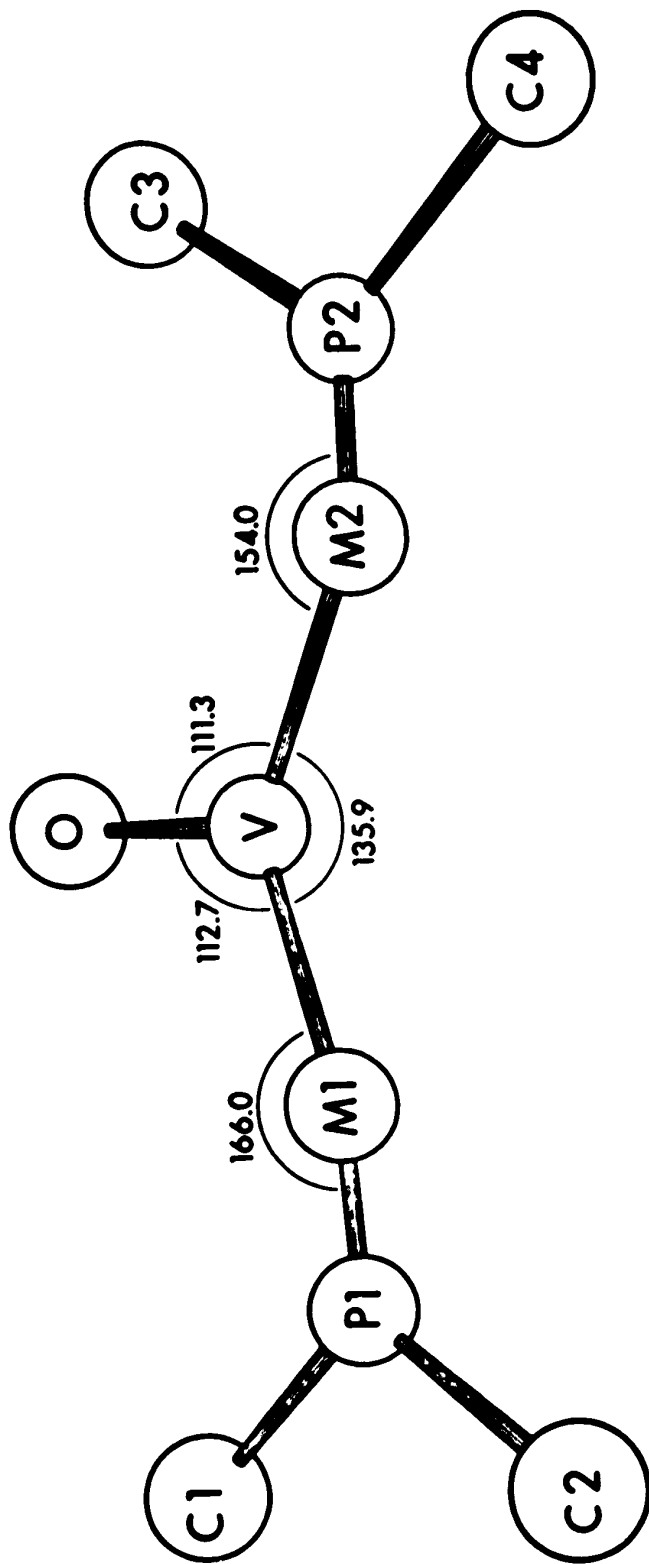


Figure 14

The molecular packing of $\text{VO}(\text{S}_2\text{PMe}_2)_2$ onto
the ac plane.

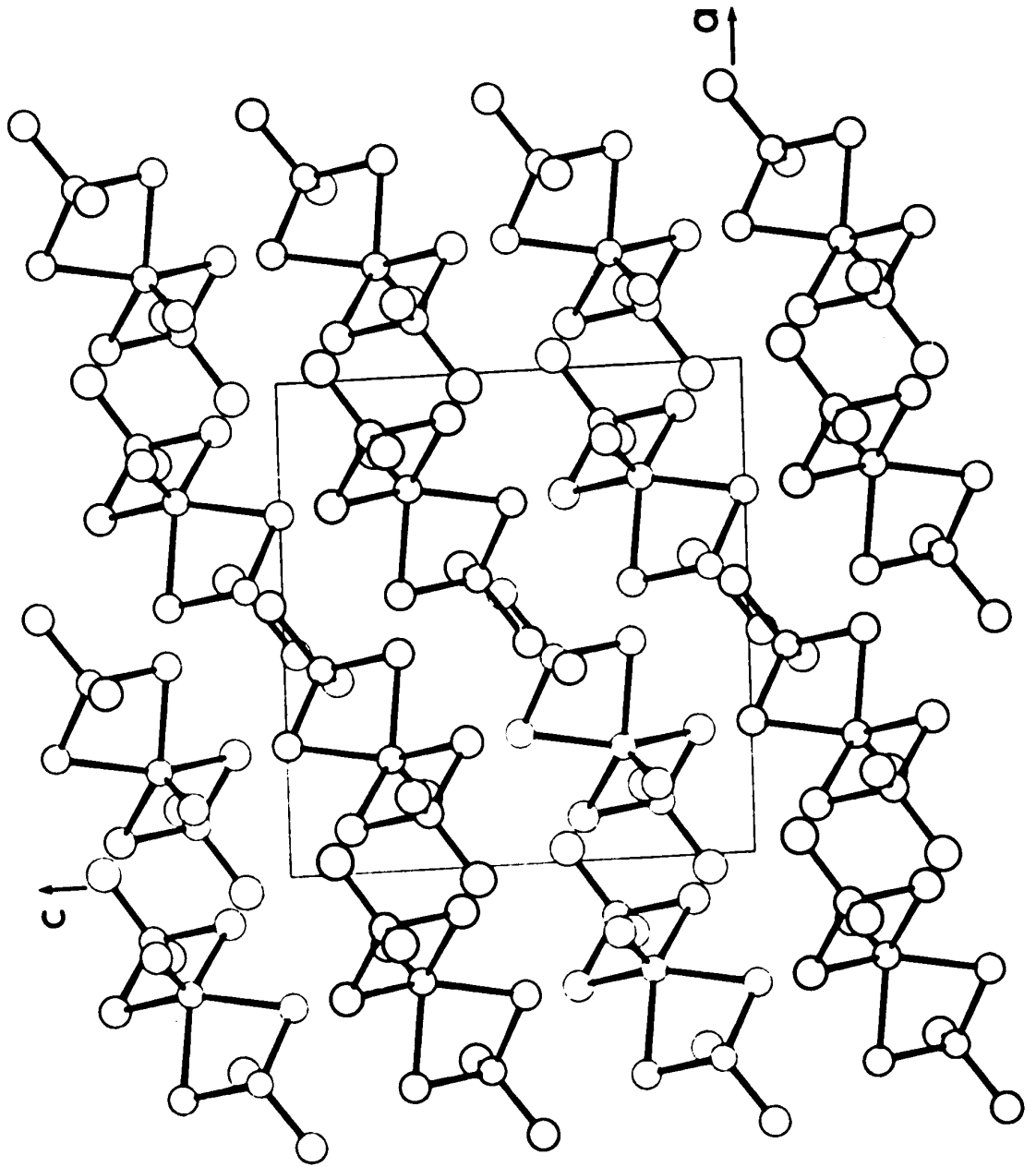


Table 36

Final Atomic Coordinates and Equivalent Isotropic

<u>Atom</u>	Temperature Parameters for VO(S ₂ PMe ₂) ₂			
	<u>x</u>	<u>y</u>	<u>z</u>	<u>B, Å²</u>
V	0.22739(11) ^a	0.45025(10)	0.27629(11)	4.20
S1	0.0890(2)	0.5846(2)	0.3659(2)	5.57
S2	0.2539(2)	0.5918(2)	0.1121(2)	5.50
S3	0.4406(2)	0.4000(2)	0.2532(2)	4.93
S4	0.2656(2)	0.3827(2)	0.4977(2)	4.82
P1	0.1139(2)	0.6690(2)	0.1993(2)	4.65
P2	0.4158(2)	0.3145(1)	0.4202(2)	4.16
C1	-0.0262(7)	0.6679(7)	0.0971(8)	6.63
C2	0.1488(8)	0.8127(6)	0.2320(9)	6.58
C3	0.3927(8)	0.1681(6)	0.3870(8)	5.96
C4	0.5506(7)	0.3245(6)	0.5271(7)	5.28
O	0.1485(5)	0.3567(4)	0.2045(4)	5.75

^a Numbers in parentheses are estimated standard deviations occurring in the last digits listed.

Table 37. Anisotropic Temperature Parameters ($\times 10^5$) for $\text{VO}(\text{S}_2\text{PMe}_2)_2^{\text{a}}$

Atom	β_{11}	β_{22}	β_{33}	β_{12}	β_{13}	β_{23}
V	971(12) ^b	705(9)	902(13)	7(9)	137(9)	-19(9)
S1	1275(22)	1019(17)	1127(22)	180(16)	166(18)	161(15)
S2	1245(21)	944(17)	1215(22)	258(15)	129(17)	199(15)
S3	1115(19)	884(16)	1037(21)	113(14)	101(16)	141(14)
S4	1098(20)	896(16)	950(19)	100(14)	28(15)	39(14)
P1	1025(20)	800(15)	1034(21)	138(14)	-134(16)	18(14)
P2	988(20)	628(14)	963(20)	42(13)	-151(16)	25(13)
C1	1290(93)	1236(84)	1516(106)	244(74)	-610(81)	-120(74)
C2	1478(101)	761(65)	1964(120)	-19(67)	-252(90)	-117(70)
C3	1667(101)	606(57)	1508(99)	-59(63)	-263(83)	-214(61)
C4	1235(87)	880(66)	1112(87)	31(60)	-442(70)	-50(60)
O	1480(62)	876(43)	1181(59)	-294(43)	-315(48)	-100(40)

^aAnisotropic thermal parameters defined by

$$\exp[-(\beta_{11}h^2 + \beta_{22}k^2 + \beta_{33}l^2 + 2\beta_{12}hk + 2\beta_{13}hl + 2\beta_{23}kl)]$$

^bNumbers in parentheses are estimated standard deviations occurring in the last digits listed.

Table 38

Intramolecular Distances ($\overset{\circ}{\text{A}}$) for the $\text{VO}(\text{S}_2\text{PMe}_2)_2$
Molecule.

<u>Atoms</u>	<u>Distance</u>
V - S1	2.415(2) ^a
V - S2	2.418(2)
V - S3	2.419(2)
V - S4	2.425(2)
V - O	1.583(5)
S1 - P1	2.009(3)
S2 - P1	2.019(3)
S3 - P2	2.019(2)
S4 - P2	2.017(2)
P1 - C1	1.819(8)
P1 - C2	1.804(8)
P2 - C3	1.815(7)
P2 - C4	1.803(7)

^a Numbers in parentheses are estimated standard deviations
in the last digits listed.

Table 39

Intramolecular Angles (degrees) for the VO(S₂PMe₂)₂ Molecule.

<u>Atoms</u>	<u>Angle</u>
O - \hat{V} - S1	108.6(2) ^a
O - \hat{V} - S2	105.0(2)
O - \hat{V} - S3	106.5(2)
O - \hat{V} - S4	105.3(2)
S1 - \hat{V} - S2	82.03(7)
S3 - \hat{V} - S4	82.65(7)
S1 - \hat{V} - S4	87.81(7)
S2 - \hat{V} - S3	88.40(7)
S1 - \hat{V} - S3	144.95(8)
S2 - \hat{V} - S4	149.63(8)
V - $\hat{S}1$ - P1	85.16(9)
V - $\hat{S}2$ - P1	84.88(9)
V - $\hat{S}3$ - P2	83.65(8)
V - $\hat{S}4$ - P2	83.53(8)
S1 - $\hat{P}1$ - S2	105.39(11)
S3 - $\hat{P}2$ - S4	104.83(10)
S1 - $\hat{P}1$ - C1	110.3(3)
S1 - $\hat{P}1$ - C2	111.4(3)
S2 - $\hat{P}1$ - C1	112.0(3)
S2 - $\hat{P}1$ - C2	111.6(3)
S3 - $\hat{P}2$ - C3	111.2(3)
S3 - $\hat{P}2$ - C4	110.3(3)
S4 - $\hat{P}2$ - C3	111.2(3)
S4 - $\hat{P}2$ - C4	112.9(3)
C1 - $\hat{P}1$ - C2	106.3(4)
C3 - $\hat{P}2$ - C4	106.5(4)

^aNumbers in parentheses are estimated standard deviations occurring in the last digits listed.

Table 40Intermolecular Non-Bonded Contacts ($\leq 4.0\text{\AA}$) of $\text{VO}(\text{S}_2\text{PMe}_2)_2$.

<u>Atoms</u>	<u>Distance</u>	<u>Symmetry Position of Second Molecule</u>
S1 - S1	3.97	-x, 1-y, 1-z
S1 - C2	3.97	x, $\frac{1}{2}$ -y, $\frac{1}{2}$ +z
S2 - C2	3.96	1-x, $\frac{1}{2}$ +y, $\frac{1}{2}$ -z
S2 - C4	3.83	1-x, $\frac{1}{2}$ +y, $\frac{1}{2}$ -z
S3 - C3	3.85	x, $\frac{1}{2}$ -y, $\frac{1}{2}$ +z
S3 - C3	4.00	1-x, $\frac{1}{2}$ +y, $\frac{1}{2}$ -z
S3 - C4	3.78	x, $\frac{1}{2}$ -y, $\frac{1}{2}$ +z
S4 - C1	3.78	-x, $\frac{1}{2}$ +y, $\frac{1}{2}$ -z
S4 - O	3.82	x, $\frac{1}{2}$ -y, $\frac{1}{2}$ +z
P1 - O	3.80	-x, $\frac{1}{2}$ +y, $\frac{1}{2}$ -z
C1 - O	3.36	-x, -y, -z
C1 - O	3.33	-x, 1-y, -z
C2 - O	3.37	-x, $\frac{1}{2}$ +y, $\frac{1}{2}$ -z

Table 41. Weighted Mean Molecular Planes for VO(S₂PMe₂)₂^a

<u>Atoms contained in the Plane</u>	<u>No.</u>	<u>Equation</u>
S1, S2, S3, S4	1	0.5406X + 0.7065Y + 0.4567Z = -7.0950
V, O, P1, P2	2	-0.6174X - 0.0496Y + 0.7851Z = -0.4729
V, O, P1, P2, C1, C2, C3, C4	3	-0.6126X - 0.0455Y + 0.7891Z = -0.5191
S1, S3, V, O	4	-0.0490X - 0.5238Y + 0.8504Z = -0.5638
S2, S4, V, O	5	-0.8460X + 0.4494Y + 0.2868Z = -1.2341
S1, S2, P1	6	0.6367X + 0.6006Y + 0.4836Z = -6.5798
V, S1, S2	7	0.7383X + 0.3899Y + 0.5504Z = -5.4274
V, S3, S4	8	0.2684X + 0.9183Y + 0.2911Z = -6.4506
S3, S4, P2	9	0.5639X + 0.6536Y + 0.5049Z = -7.1159

Table 41 (continued). Distances of Atoms from Planes (Å)^{a,b}

Plane 1:	S1, 0.0051; S2, -0.051; S3, 0.043; S4, -0.042; V, -0.681; O, -2.264
Plane 2:	V, 0.001; O, -0.003; P1, -0.0002; P2, -0.0002; S1, 1.588; S2, -1.612; S3, -1.592; S4, 1.606; C1, 0.102; C2, -0.052; C3, -0.031; C4, -0.033.
Plane 3:	V, -0.0002; O, -0.016; P1, 0.003; P2, 0.007; C1, 0.091; C2, -0.041; C3, -0.033; C4, -0.014; S1, 1.590; S2, -1.611; S3, -1.586; S4, 1.612.
Plane 4:	S1, 0.001; S3, 0.001; V, -0.003; O, 0.007.
Plane 5:	S2, -0.001; S4, -0.001; V, 0.004; O, -0.008.

Planes Dihedral Angles

6-7	154.0°
7-8	135.9°
8-9	166.0°

^aThe orthogonal coordinate system (X,Y,Z) corresponds to the crystal a,b,c* axes.

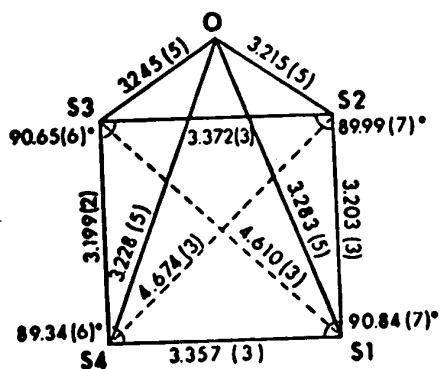
^bAverage estimated standard deviations in atom positions derived from uncertainties in fractional coordinates are as follows (Å): V, 0.0008; S, 0.002; P, 0.002; O, 0.005; C, 0.008.

Table 42

Observed and calculated structure amplitudes ($\times 10$)
in electrons for $\text{VO}(\text{S}_2\text{PMe}_2)_2$.

DISCUSSION

The crystal consists of discrete molecules of $\text{VO}(\text{S}_2\text{PMe}_2)_2$ which have no crystallographic symmetry; the approximate C_{2v} symmetry of the molecule is maintained even though there is considerable bending of each ligand along the line joining the two sulphur atoms (see Figure 13). As shown below the coordination around the vanadium is square pyramidal with only slight deviations:



The average vanadium-sulphur distance of 2.419\AA lies within the range of published values; 2.338\AA for $\text{V}(\text{S}_2\text{C}_2\text{Ph}_2)_3$,⁶⁶ 2.36\AA for $(\text{Me}_4\text{N})_2[\text{V}(\text{mnt})_3]$,⁶⁷ and 2.451\AA for $\text{V}[\text{S}_2\text{P}(\text{OEt})_2]_3$.⁷⁴ The apical oxygen-vanadium atom bond length is $1.583(5)\text{\AA}$, which is within the range of $1.56\text{--}1.67\text{\AA}$ reported by other workers for vanadyl compounds.^{83,121} Sulphur-phosphorus, phosphorus-carbon bond lengths and ligand angles (where applicable) for this complex are in excellent agreement with those of the $\text{Cr}(\text{S}_2\text{PMe}_2)_3$ and $\text{Co}(\text{S}_2\text{PMe}_2)_2$ complexes, as well as with similar compounds. These features will be discussed, along with the coordination of the phosphorus atom, in the final chapter.

The molecule exhibits bending of each ligand about the sulphur-sulphur line similar to $\text{Cr}(\text{S}_2\text{PMe}_2)_3$, but to a much greater degree, the dihedral angles are 166.0° and 154.0° (Figure 13), while those for the chromium complex are 171.2° , 171.8° and 177.9° . For the (S3, S4, P2, C3, C4) ligand there are no intermolecular approaches less than 3.78\AA , while for the (S1, S2, P1, C1, C2) ligand there are two close approach distances, viz. 3.33\AA between C1 and O and 3.37\AA between C2 and O (Table 40). These latter values are in the range of the sum of Van der Waals radii for an oxygen atom (1.4\AA) and a carbon atom (1.7\AA) or a methyl group (2.0\AA).⁵ All other intermolecular approach distances are normal, greater than 3.83\AA , thus bending of the ligands seems to be the method by which the crystal achieves stability between attractive and repulsive intermolecular forces. All other S_2PR_2^- monomeric ligands (R = OEt,^{73-76,96} Ph,⁷⁷) reported (except for this thesis and $\text{Ni}(\text{S}_2\text{PMe}_2)_2$),⁸⁰ are planar because of restrictions due to crystallographic symmetry.

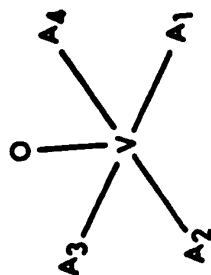
The molecule has a pseudo mirror plane passing through the P1, V, O, and P2 atoms (Table 41). The four carbon atoms are almost coplanar with this plane, the greatest deviation from the plane being 0.102\AA for C1 while the sulphur atoms are approximately equi-distant from the plane. The four sulphur atoms are themselves planar with a maximum deviation of 0.01\AA for S1. The vanadium atom is

0.681Å above the basal plane defined by the four sulphur atoms and the dihedral angle between the planes (S1, S2, V) and (S3, S4, V) is 135.9°, which may be compared to 132.3° for VO(acen),⁸⁵ 134.7° for VO(acac)₂,¹¹⁸ and 135.6° for VO(bzac)₂.¹¹⁹

The coordination 'pyramid' data for this and the three previously determined vanadyl complexes is summarised in Table 43 and as analysis will show the corresponding angles for each complex are equal within experimental error. The distances of the vanadium atom above the basal planes are 0.58Å for VO(acen), 0.55Å for VO(acac)₂, and 0.54Å for VO(bzac)₂ and are consistent with the value of 0.681Å for VO(S₂PMe₂)₂, the difference being due to the increase of the vanadium-ligand distance from an average length of 1.98Å for the three previously determined structures to 2.42Å for VO(S₂PMe₂)₂.

There is no indication, in the solid state, of even weak coordination to the vanadium atom in the vacant sixth coordinate position from below the basal plane; the closest approach is 4.12Å by a C4 atom. Similar results were found for the other complexes although Dichman *et al* recently reported the structure of the [VO(acac)₂]₂: 1,4-dioxan adduct¹²⁰ to have coordination in this sixth vacant position with a vanadyl-oxygen bond length of 2.51Å. A similar result was found by Ballhausen *et al*¹²¹ for

Table 43. Comparison of the Vanadium Coordination of $\text{VO}(\text{S}_2\text{PMe}_2)_2$ with other Reported Oxovanadium(IV) Complexes.



<u>Angle (Degrees)</u>	<u>$\text{VO}(\text{S}_2\text{PMe}_2)_2$^a</u>	<u>$\text{VO}(\text{acen})_2$^b</u>	<u>$\text{VO}(\text{acac})_2$^c</u>	<u>$\text{VO}(\text{bzac})_2$^d</u>
O-V-A ₁	108.6(2) ^e	110.4(3)	106.2(4)	106.6(4)
O-V-A ₂	105.3(2)	106.0(3)	105.6(4)	104.0(4)
O-V-A ₃	106.5(2)	[103.1(4)] ^f	108.4(4)	106.9(4)
O-V-A ₄	105.0(2)	[107.7(4)]	104.8(4)	106.0(4)
<u>Average</u>	<u>106.2</u>	<u>106.8</u>	<u>106.2</u>	<u>106.0</u>
A ₁ -V-A ₂	87.81(7)	86.2(3)	85.3(3)	85.8(3)
A ₂ -V-A ₃	82.65(7)	[87.3(3)]	87.8(3)	87.5(3)
A ₃ -V-A ₄	88.40(7)	[79.9(3)]	83.9(3)	82.2(3)
A ₄ -V-A ₁	82.03(7)	[87.7(3)]	86.9(3)	87.3(3)
<u>Average</u>	<u>85.22</u>	<u>85.3</u>	<u>85.5</u>	<u>85.7</u>

Table 43 (continued)

<u>Angle (Degrees)</u>	<u>VO(S₂PMe₂)₂^a</u>	<u>VO(acen)^b</u>	<u>VO(acac)₂^c</u>	<u>VO(bzac)₂^d</u>
A ₁ -V-A ₃	144.95(8)	[150.7(3)]	145.5(3)	146.5(3)
A ₂ -V-A ₄	149.63(8)	[141.6(3)]	149.6(3)	149.9(3)
	<u>Average 147.79</u>	<u>146.1</u>	<u>147.5</u>	<u>148.2</u>
<u>Distance (Å)</u>	<u>VO(S₂PMe₂)₂</u>	<u>VO(acen)</u>	<u>VO(acac)₂</u>	<u>VO(bzac)₂</u>
V-O	1.583(5)	1.585(7)	1.571(10)	1.612(10)

^aFor VO(S₂PMe₂) A₁, A₂, A₃, and A₄ corresponds to S1, S4, S3, and S2 respectively.

^bFor VO(acen) A₁, A₂, A₃, and A₄ corresponds to O₂, O₁, N₁, and N₂ respectively.

Reference number 85.

^cVanadyl(IV) bisacetylacetonate. Values are those obtained from the anisotropic refinement of data of Dodge *et al.* Reference no. 118.

^dVanadyl(IV) bisbenzoylacetonate. Reference no. 119.

^eStandard deviations of least significant figures in parentheses.

^fValues involving nitrogen atom are enclosed in brackets.

$\text{VO}_2 \cdot 5\text{H}_2\text{O}$ where the 'bond length' of the fifth water molecule was $2.223(5)\text{\AA}$. This adduct differs from the other vanadyl complexes in that the angles O-V-M1 and O-V-M2 (see Figure 13) is 107.2° , while for the penta coordinated complexes these angles had values of $112 \pm 1.5^\circ$. This difference is probably due to coordination by the sixth atom, thereby compressing the tetragonal pyramid coordination of the vanadium atom. Thus it is evident that when there is no modification of the vanadium coordination by a sixth atom the dominating feature of oxovanadium complexes is the unchanging coordination pyramid of the vanadium atom even when different ligands are present. However, intermolecular forces have a considerable effect on the geometry of the ligands.

CHAPTER VI

THE (S₂PR₂) LIGAND

Molecular dimensions for $\text{Cr}(\text{S}_2\text{PMe}_2)_3$, $\text{Co}(\text{S}_2\text{PMe}_2)_2$, and $\text{VO}(\text{S}_2\text{PMe}_2)_2$ are compared with other S_2PR_2 complexes in Table 44. The average value of the sulphur-phosphorus bond length for the complexes of this thesis is 0.017\AA longer than for the other dithiophosphinato complexes. Also when compared to the 1,2-dithiolene complexes the metal-sulphur bond length is 0.25\AA longer.

Estimates of the expected bond lengths may be made using the sums of covalent radii. For chromium(III) the covalent radii of 1.45\AA was derived from the difference of the $(\text{Cr}-\text{NH}_3)$ bond length in $[\text{Cr}(\text{SCN})_4(\text{NH}_3)_2]^{-122}$ and the radii of tetrahedral nitrogen (0.70\AA).⁵ This value when summed with the covalent radii of sulphur (1.04\AA)⁵ gives a bond length of 2.49\AA . The covalent radii of cobalt(II) was similarly estimated, using the $\text{Co}-\text{Cl}$ bond length from CoCl_4^{2-} ,¹²³ and gave a cobalt-sulphur bond length of 2.37\AA . Sulphur-phosphorus and phosphorus-carbon lengths were also estimated. The results are as follows:

<u>Distance</u>	<u>Estimated (\AA)</u>	<u>Found (\AA)</u>
Cr-S	2.49	2.436
Co-S	2.37	2.320
S-P	2.14	2.014
P-C	1.87	1.812

Table 44. Comparison of (S_2PR_2) ligand bond lengths and bond angles.

Complex	Ref.	$S-P(\text{\AA})^a$	$P-C(\text{\AA})$	$S-\hat{M}-S^\circ$	$M-\hat{S}-P^\circ$	$S-\hat{P}-S^\circ$	$C-\hat{P}-C^\circ$
$Cr(S_2PMe_2)_3$	-	2.011	1.813	82.74	85.24	106.20	106.0
$Co(S_2PMe_2)_2$	-	2.016	1.813	-	109.46 ^C	107.03	105.2
$VO(S_2PMe_2)_2$	-	2.014	1.810	85.22	84.51	105.11	106.4
<u>Average</u>		<u>2.014</u>	<u>1.812</u>	<u>83.98</u>	<u>84.86</u>	<u>106.11</u>	<u>105.9</u>
$Ni(S_2PPh_2)_2$	77	2.014	1.781	88.3	85.2	101.3	107.2
$Ni(S_2PMe_2)_2$	80	2.004	-	87.7	85.3	101.6	-
$Ni(S_2P(OEt)_2)_2$	76	1.970	-	88.0	84.5	103.0	-
$Ni[S_2F(OEt)_2]_2$	73	1.990	-	88.5	84.2	103.1	-
$Ni[S_2P(OEt)_2]_2 \cdot PY$	75	1.985	-	81.7	84.0	110.4	-
$V[S_2P(OEt)_2]_3$	73	1.98	-	81.1	85.0	108.0	-
$[Zn(S_2PET_2)_2]_2^b$	78	2.017	1.860	85.9	82.1	109.6	103.0
$[Zn(S_2P\{1-C_3H_7O\}_2)_2]_2$	79	1.970	-	85.5	82.6	109.7	-
$[Cd(S_2P\{1-C_3H_7O\}_2)_2]_2$	79	1.965	-	79.1	84.4	112.2	-
$Et_3P_2S_2$	124	-	1.83	-	-	-	-
$[(1-C_3H_7O)_2PS_2]_2$	125	2.072	-	-	-	-	-

Table 44. Comparison of (S₂PR₂) ligand bond lengths and bond angles.

Complex	Ref.	S-P(Å) ^a	P-C(Å)	S-M-S°	M-S-P°	S-P-S°	C-P-C°
Cr(S ₂ PMe ₂) ₂	-	2.011	1.813	82.74	85.24	106.20	106.0
Co(S ₂ PMe ₂) ₂	-	2.016	1.813	-	109.46 ^C	107.03	105.2
VO(S ₂ PMe ₂) ₂	-	2.014	1.810	85.22	84.51	105.11	106.4
<u>Average</u>		<u>2.014</u>	<u>1.812</u>	<u>83.98</u>	<u>84.86</u>	<u>106.11</u>	<u>105.9</u>
Ni(S ₂ PPh ₂) ₂	77	2.014	1.781	88.3	85.2	101.3	107.2
Ni(S ₂ PMe ₂) ₂	80	2.004	-	87.7	85.3	101.6	-
Ni(S ₂ P(OEt) ₂) ₂	76	1.970	-	88.0	84.5	103.0	-
Ni(S ₂ F(OEt) ₂) ₂	73	1.990	-	88.5	84.2	103.1	-
Ni(S ₂ P(OEt) ₂) ₂ ·PY	75	1.985	-	81.7	84.0	110.4	-
V(S ₂ P(OEt) ₂) ₂	73	1.98	-	81.1	85.0	108.0	-
[Zn(S ₂ PET ₂) ₂] ₂ ^b	78	2.017	1.860	85.9	82.1	109.6	103.0
[Zn(S ₂ P{(i-C ₃ H ₇ O) ₂ }) ₂] ₂	79	1.970	-	85.5	82.6	109.7	-
[Cd(S ₂ P{(i-C ₃ H ₇ O) ₂ }) ₂] ₂	79	1.965	-	79.1	84.4	112.2	-
Et ₂ P ₂ S ₂	124	-	1.83	-	-	-	-
[(i-C ₃ H ₇ O) ₂ PS ₂] ₂	125	2.072	-	-	-	-	-

Table 44 (continued).

<u>Complex</u>	<u>Ref.</u>	<u>S-P(Å)^a</u>	<u>P-C(Å)</u>	<u>S-M-S°</u>	<u>M-S-P°</u>	<u>S-P-S°</u>	<u>C-P-C°</u>
$[(\text{Ph}) \cdot (\text{Me}) \cdot \text{PS}]_2$	126	-	1.82	-	-	-	-
$(\text{Me} \cdot \text{PS})_2$	127	-	1.83	-	-	-	-
<u>Average</u>		<u>1.997</u>	<u>1.82</u>	<u>85.1</u>	<u>84.2</u>	<u>106.5</u>	<u>105.1</u>

^aAll values quoted are the average for a particular molecule.

^bThis is isostructural with $[\text{Co}(\text{S}_2\text{P}(\text{Et})_2)_2]_2$

^cNot included in average.

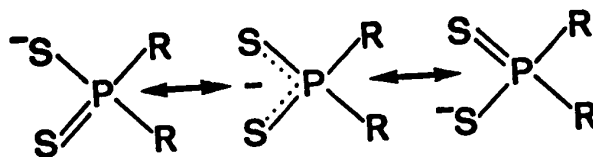
While the estimated chromium-sulphur bond length is longer than the experimental value the difference is probably not significant, as the error in the chromium radius may be as high as five per cent; similarly for the estimated cobalt-sulphur bond length.

As there is a lack of V(IV) data the acceptability of the bond length was estimated as follows:

$$\begin{aligned}
 \text{V-S in VO(S}_2\text{PMe}_2)_2 &= 2.419 \\
 \text{V-O in VO(acac)}_2^{85} &= \underline{1.968} \\
 \therefore \Delta_1 &= 0.451\overset{\circ}{\text{A}} \\
 \text{Tetrahedral radius of S} &= 1.04 \\
 \text{Tetrahedral radius of O} &= \underline{0.66} \\
 \therefore \Delta_2 &= 0.38\overset{\circ}{\text{A}} \\
 \therefore \Delta_1 - \Delta_2 &= \underline{\underline{0.07\overset{\circ}{\text{A}}}}
 \end{aligned}$$

The difference of $0.07\overset{\circ}{\text{A}}$ for the VO(acac)_2 complex when compared with $\text{VO(S}_2\text{PMe}_2)_2$ indicates that more delocalisation may occur in the acetylacetonato ligand than the dithiophosphinato ligand (although the difference of $0.07\overset{\circ}{\text{A}}$ is of the same order as for the chromium and cobalt-sulphur bond lengths, more significance may be attached to it, because of the similarity between the two compounds, $\text{VO(S}_2\text{PMe}_2)_2$ and VO(acac)_2 , being compared).

Several structures of the S_2PR_2^- ligand may be



drawn implying a certain amount of delocalisation in the chelate's electronic structure. Jorgensen⁵⁶ stated that the sulphur-phosphorus bond for the O,O'-dialkyldithio-phosphate systems has very little double bond character, but the average value of 2.014\AA for the complexes of this thesis and $1.96(1)\text{\AA}$ for the potassium salt of $[\text{S}_2\text{P}(\text{OCH}_3)_2]^{-128}$ are closer to the calculated double bond value of 1.94\AA than to the single bond sum of 2.4\AA ;⁵ Lawton¹²⁵ reports a value of 1.908 for a P=S bond in $[(i - \text{C}_3\text{H}_7\text{O})_2\text{PS}_2]_2$ and on this basis a sulphur-phosphorus bond in $\text{VO}(\text{S}_2\text{PMe}_2)_2$ has a bond order of ≈ 1.50 . Hence there is delocalisation of the odd electron in the π system over the three atoms which coordinate with the metal ion to form the four membered chelate ring. This, as well as the longer metal-sulphur bond lengths in the S_2PR_2^- complexes when compared to the 1,2-dithiolene complexes, does not necessarily imply the existence of metal-ligand π bonding. For this to occur the ligand molecular orbitals have to be of the correct symmetry and corresponding energy for extensive overlap and bonding with metal valence orbitals to occur.

These results indicate that the \bar{S}_2PR_2 complexes are more analagous to the \bar{S}_2C-R complexes than the 1,2-dithiolenes. Although all of these sulphur donor chelating agents possess π systems extending over the atoms which form the backbone of the metal-chelate ring, the difference between the bonding of the 1,1- and the 1,2-dithiolato ligand systems is the extent of the metal-ligand π bonding.

All other distances and angles of $Cr(S_2PMe_2)_3$, $VO(S_2PMe_2)_2$, and $Co(S_2PMe_2)_2$ compare well (where applicable) with small differences ($\sim 2^\circ$) in ligand bond angles the most variable parameter. (See Table 29). These differences are probably due to the strained S-P-S bond angle despite the 'normality' of the S-M-S bond angle. The coordination of the phosphorus atoms in all complexes is best described as tetrahedral with the average deviation from 109.5° listed below:

<u>Complex</u>	<u>Atom</u>	<u>Deviation from 109.5°</u>	
		<u>Range (Deg)</u>	<u>Average (Deg)</u>
$Cr(S_2PR_2)_3$	P1	1.8-4.5	2.41
	P2	0.6-4.2	3.03
	P3	0.1-3.8	2.07
$Co(S_2PR_2)_2$	P1	1.9-4.2	2.93
$VO(S_2PR_2)_2$	P1	0.8-4.11	2.44
	P2	0.8-4.63	2.54

For the complexes $\text{Cr}(\text{S}_2\text{PMe}_2)_3$ and $\text{VO}(\text{S}_2\text{PMe}_2)_2$ the major feature of the ligands is the bending about the line joining the sulphur atoms of each ligand. This flexing does not seem to be a function of the 'bite angle' of the ligand or of the metal-sulphur distance. The metal, sulphur, and phosphorus thermal parameters for other S_2PR_2 complexes, that were not restricted to a planar ligand because of symmetry, were of such values that disorder and therefore flexing of the ligand may have been disguised by thermal motion. The only exception to this is the $\text{Ni}(\text{S}_2\text{PMe}_2)_2$ complex⁸⁰ where the phosphorus atom deviates significantly, but not too much, from the NiS_4 plane.

Apparently for $\text{Co}(\text{S}_2\text{PMe}_2)_2$ the flexing of the ligand and/or the strain of ring formation was excessive and a polymeric species was formed. While the sulphur-phosphorus-sulphur bond angle is comparable to the other two complexes the ligand 'bite angle' is 102.0° - 120.6° for $\text{Co}(\text{S}_2\text{PMe}_2)_2$ as compared to 82.9° and 82.3° for $\text{Cr}(\text{S}_2\text{PMe}_2)_3$ and $\text{VO}(\text{S}_2\text{PMe}_2)_2$ respectively, (see Table 29), thus the strain within the 'chelate ring' is probably reduced, especially as the metal-sulphur-phosphorus bond angle increased to 109.46° from 84.86° . Both the $\text{Cr}(\text{S}_2\text{PMe}_2)_2$ and $\text{VO}(\text{S}_2\text{PMe}_2)_2$ complexes may also have a tendency to polymerise, but the coordination of the metal, octahedral and pyramidal respectively, does not lend itself to polymerisation as

well as the tetrahedral coordination of the cobalt(II) species does.

It appears then, that polymer formation cannot be attributed wholly to the strain placed upon the ligand by flexing and/or ring formation of the ligand, but is also influenced by the ability of the metal species to exist in the required coordination.

REFERENCES

1. International Tables for X-Ray Crystallography, Vol. I, II, and III, Kynoch Press, Birmingham, England (1962).
2. G.H. Stout and L.H. Jensen, X-Ray Structure Determination, MacMillan, New York (1968).
3. M. J. Buerger, Crystal Structure Analysis, John Wiley, New York (1960).
4. N.A. Matwiyoff, Inorg. Chem., 5, 788 (1966).
5. L. Pauling, The Nature of the Chemical Bond, 2nd ed., Cornell University Press, Ithaca, New York; A.F. Wells, Structural Inorganic Chemistry, 3rd ed., Oxford University Press, London (1962).
6. N.S. Angerman, private communication.
7. A.L. Patterson and W.E. Love, Amer. Minn., 45, 325 (1960).
8. W.C. Hamilton, J.S. Rollet and R.A. Sparks, Acta Cryst., 18, 129 (1968).
9. GNABS, D.P. Shoemaker, M.I.T. (1962).
10. DATAPREP, M. Elder, University of Alberta (1967).
11. R. J. Doedens, and J. A. Ibers, Inorg. Chem., 6, 204 (1967).
12. 'ORFLS', a Fortran Crystallographic Least Squares program, W.R. Busing, K.O. Martin, and H.A. Levy, Report ORNL-TM-305, Oak Ridge National Laboratory, Oak Ridge, Tenn. (1962); modified D. Hall, University of Alberta (1967).

13. NRC-8 Fourier Program, F.R. Ahmed, N.R.C., Ottawa (1966).
14. SFLS5, C.T. Prewitt, modified by B.M. Foxman and M.J. Bennett, M.I.T. (1967).
15. D.W.J. Cruickshank, Computing Methods in Crystallography, J.S. Rollet (Ed.), Pergamon Press, New York (1965), p. 113.
16. D.T. Cromer and J.T. Waber, *Acta Cryst.*, 18, 104 (1965).
17. International Tables for X-Ray Crystallography, Vol. III, Kynoch Press, Birmingham, England (1962), p. 213.
18. 'ORTEP', a Fortran Thermal Ellipsoid Plot Program for Crystal Structure Illustrations, C.K. Johnson, Report ORNL-3794, Oak Ridge National Laboratory Oak Ridge, Tenn. (1964).
19. E.C. Lingafelter and R.L. Braun, *J. Amer. Chem. Soc.*, 88, 2951 (1966).
20. M.J. Bennett, F.A. Cotton, and D.L. Weaver, *Acta Cryst.*, 23, 581 (1967).
21. L. Brun and C. Bränden, *Acta Cryst.*, 20, 749 (1966).
22. M. Calligaris, G. Nardin, R. Randaccio, and A. Ripamonti, *J. Chem. Soc. (A)*, 1069, 1970.
23. Y. Gobillon, P. Pinet, and M. Van Meerssche, *Bull. Soc. Chim. Fr.*, 551 (1962).

24. L.V. Vilkov, P.A. Akishin, and V.M. Presynkova,
Zh. Strukt, Khim, 3, 5 (1962).
25. J. Ladell and B. Post, Acta Cryst., 7, 559 (1956).
26. L. Cavalca, M. Nardelli, and G. Fava, Acta Cryst.,
13, 594 (1960).
27. M. Nardelli, L. Cavalca, and G. Fava, Gazz. Chim.
Ital., 87, 1232 (1957).
28. L. Cavalca, M. Nardelli, and L. Coghi, Nuovo Amento,
6, 278 (1967).
29. F.A. Cotton and G. Wilkinson, Advanced Inorganic
Chemistry, J. Wiley, New York (1966), p. 112.
30. D. Lide, Tetrahedron, 17, 125 (1962).
31. G. Archambault and R. Rivest, Can. J. Chem.,
38, 1331 (1960).
32. 'ORFEE', a Fortran Crystallographic Function and
Error Program, Report ORNL-TM-306, Oak Ridge
National Laboratory, Oak Ridge, Tenn. (1964).
33. H.C. Freeman and I.E. Maxwell, Inorg. Chem., 8, 1293
(1969).
34. L.P. Haugen and R. Eisenberg, *ibid*, 8, 1072 (1969).
35. C.L. Coulter, P.K. Gantzel, and J.D. McCullough,
Acta Cryst., 16, 676 (1963).
36. P.D. Cradwick, Hydrogen Atom Locator Program,
University of Alberta, 1969.
37. R.B. Jordan, private communications.

38. S.G. La Placa, *Inorg. Chem.*, 4, 778 (1965).
39. N.A. Baily, J.M. Jenkins, R. Mason, and B.R. Shaw,
Chem. Comm., 237, 1965.
40. P.G. Owston and J.M. Rowe, *J. Chem. Soc.*, 3411, 1963.
41. G.N. Schrauzer and V. Mayveg, *J. Amer. Chem. Soc.*,
84, 3221 (1962).
42. H.B. Gray, R. Williams, J. Bernal, and E. Billig,
ibid., 84, 3596 (1962).
43. H.B. Gray and E. Billig, *ibid.*, 85, 2019 (1963).
44. A. Davison, N. Edelstein, R.H. Holm, and A.H. Maki,
ibid., 85, 2029 (1963).
45. A. Davison, N. Edelstein, R.H. Holm, and A.H. Maki,
Inorg. Chem., 2, 1227 (1963).
46. E. Billig, R. Williams, J. Bernal, J.H. Waters, and
H.B. Gray, *ibid.*, 3, 663 (1964).
47. A. Davison, N. Edelstein, R.H. Holm, and A.H. Maki,
ibid., 3, 814 (1964).
48. C.J. Fritchie, Jr., *Acta Cryst.*, 20, 107 (1966).
49. D. Sartain and M.R. Truter, *J. Chem. Soc. (A)*, 1264,
1967.
50. J.D. Forrester, A. Zalkin, and D.H. Templeton, *Inorg.*
Chem., 3, 1500 (1964).
51. J.D. Forrester, A. Zalkin, and D.H. Templeton, *ibid.*,
3, 1507 (1964).

52. J.H. Enemark and W.N. Lipscomb, *ibid.*, 4 1729 (1965).
53. R. Eisenberg and J.A. Ibers, *ibid.*, 4, 605 (1965);
J. Amer. Chem. Soc., 86, 113 (1964).
54. J.A. McCleverty, Prog. Inorg. Chem., 10, 49 (1968).
55. S.E. Livingstone, Quart. Rev., 19, 386 (1965);
C.M. Harris and S.E. Livingstone, Bidentate Chelates
in Chelating Agents and Metal Chelates, F.P. Dwyer
and D.P. Mellors, Eds., Academic Press, New York
(1964), p. 95.
56. C.K. Jorgensen, Inorganic Complexes, Academic Press,
London, 1963.
57. H.B. Gray, Trans. Metal. Chem., 1, 240 (1965).
58. R.B. King, Inorg. Chem., 3, 641 (1963).
59. G.N. Schrauzer, H.W. Finik, and V. Mayneg, Angew,
Chem., 76, 715 (1964).
60. A. Davison, N. Edelstein, R.H. Holm, and A.H. Maki,
J. Amer. Chem. Soc., 86, 2799 (1964).
61. J.H. Walters, R. Williams, H.B. Gray, G.N. Schrauzer,
and H.W. Finik, *ibid.*, 86, 4198 (1964).
62. C.H. Langford, E. Billig, S.L. Shupack, and H.B. Gray,
ibid., 86, 2958 (1964).
63. A. Davison, N. Edelstein, R.H. Holm, and H.A. Maki,
Inorg. Chem., 4, 55 (1965).
64. A.E. Smith, G.N. Schrauzer, V.P. Mayneg, and W. Heinrick,
J. Amer. Chem. Soc., 87, 5798 (1965).
65. R. Eisenberg and J.A. Ibers, Inorg. Chem., 5 411 (1966).

66. R. Eisenberg and H.B. Gray, *ibid.*, 6, 1844 (1967).
67. E.I. Steifel, Z. Dori, and H.B. Gray, *J. Amer. Chem. Soc.*, 89, 3353 (1967).
68. E.I. Steifel, R. Eisenberg, R.C. Rosenberg, and H.B. Gray, *ibid.*, 88, 2956 (1966).
69. G.F. Gaspari, M. Nardelli, and A. Villa, *Acta Cryst.*, 23, 384 (1967).
70. M. Bonamico, G. Dessy, C. Mariani, A. Vaciago, and L. Zambonelli, *ibid.*, 19, 619 (1965).
71. J.S. McKechnie, S.L. Meisel, and I.C. Paul, *Chem. Comm.*, 152, 1967.
72. R. Beckett and B.F. Hoskins, *ibid.*, 909, 1967.
73. J.F. McConnell, V. Kastalsky, *Acta Cryst.*, 22, 853 (1967).
74. C. Furlani, P. Porta, A. Sgamellotti, and A.A.G. Tomlinson, *Chem. Comm.*, 1046, 1969.
75. S. Ooi and Q. Fernando, *Inorg. Chem.*, 6, 1558 (1967).
76. Q. Fernando and C.D. Green, *J. Inorg. Nucl. Chem.*, 29, 647 (1967).
77. P. Porta, A. Sgamellotti, and N. Vinciguerra, *Inorg. Chem.*, 7, 2625 (1968).
78. M. Calligaris, G. Nardin, and A. Ripamonti, *J. Chem. Soc. (A)*, 714, 1970.
79. S.L. Lawton and G.T. Kokotailo, *Inorg. Chem.*, 8, 2410 (1969).
80. P.E. Jones, G.B. Ansell, and L. Katz, *Chem. Comm.*, 78, 1968.

81. D. Day, W. Byers and R.G. Cavell, private communications.
82. C.K. Jorgensen, *J. Inorg. Nucl. Chem.*, 24, 1571 (1962).
83. J. Selbin, *Coord. Chem. Rev.*, 1, 293 (1966).
84. J. Selbin, *Chem. Rev.*, 65, 153 (1965).
85. D. Bruins and D.L. Weaver, *Inorg. Chem.*, 9, 130, 1970.
86. D-Refine, M. Elder, University of Alberta (1968).
87. MIXG2, D.P. Shoemaker, M.I.T. Goniometer package (1962).
88. PMMO, M.J. Bennett, M.I.T. (1965).
89. GONO9, W.C. Hamilton.
90. M.J. Buerger, Vector Space, J. Wiley, New York (1959), p. 239.
91. A.J.C. Wilson, *Nature*, 150, 151 (1942).
92. D.W.J. Cruickshank and W.S. McDonald, *Acta Cryst.*, 23, 9 (1967).
93. H.A. Levy, *ibid.*, 9, 679 (1956).
94. W.C. Hamilton, *ibid.*, 18, 502 (1965).
95. FORDAP, A. Zalkin, University of California, modified by B. Foxman (M.I.T.).
96. C. Furlani, P. Porta, A. Sgamellotti, and A.A.G. Tomlinson, *J. Chem. Soc. (A)*, 2929, 1970).
97. B.J. Hoskin and B.P. Kelly, *Chem. Comm.*, 1517, 1968.
98. J.N. van Nierkerk and F.R.L. Schoing, *Acta Cryst.*, 5, 499 (1952).

99. G.N. Schrauzer and V.P. Mayveg, *J. Amer. Chem. Soc.*, 88, 3235 (1966).
100. C.H. Langford and H.B. Gray, unpublished work, see R. Eisenberg, *Progr. Inorg. Chem.*, 12, 295 (1970).
101. R.G. Cavell, private communications.
102. E.L. Muetterties, *J. Amer. Chem. Soc.*, 90, 5097 (1968).
103. M. Calligaris, A. Ciana, S. Mercani, G. Nardin, L. Randaccio and A. Ripamonti, *J. Chem. Soc. (A)*, 3386, 1970.
104. P.R.H. Alderman, P.G. Owston, and J.M. Rowe, *J. Chem. Soc.*, 668, 1962.
105. G.E. Coates and D.S. Golightly, *J. Chem. Soc.*, 2523, 1962.
106. F. Giodano, L. Randaccio, and A. Ripamonti, *Acta Cryst.*, B25, 1057 (1969).
107. F. Giodano, L. Randaccio, and A. Ripamonti, *Chem. Comm.*, 19, 1967(a).
108. V. Giancotti, F. Giodano, L. Randaccio, and A. Ripamonti, *J. Chem. Soc. (A)*, 757, 1968.
109. W. Kuchen and H. Herdel, *Angew. Chem. Internat. Edit.*, 8, 89 (1969) and references therein.
110. J.L. Karle, *Adv. Chem. Phys.*, 16, 131 (1969).

111. J.L. Karle and H. Hauptman, *Acta Cryst.*, 21, 849 (1966).
112. MAGIC and FAME, B.K. Dewar and A.L. Stone, Chicago, 360 version, P.F. Stokely 6-231 M.I.T. X4359.
113. J.L. Karle and H. Hauptman, *Acta Cryst.*, 9, 635 (1956).
114. International Tables for X-Ray Crystallography, Vol.II, Kynoch Press, Birmingham, England (1962) p. 355.
115. J.L. Karle, K.S. Dragonetti, and S.A. Brenner, *Acta Cryst.*, 19, 713 (1965); G.H. Stout and L.H. Jensen, X-Ray Structure Determination. MacMillan, New York (1968), p. 320.
116. H. Hauptman and J.L. Karle, Solution of the Phase Problem I, The Centrosymmetric Crystal, A.C.A. monograph no. 3, Pittsburg, Polycrystal Book Service; J.L. Karle and H. Hauptman, *Acta Cryst.*, 12, 404 (1959).
117. W.H. Zachariasen, *Acta Cryst.*, 16, 1139 (1963).
118. R.P. Dodge, D.H. Templeton, and A. Zalkin, *J. Chem. Phys.*, 35, 55 (1961).
119. P.K. Hon, R. Linn Belford, and C.E. Pfluger, *J. Chem. Phys.*, 43, 1323 (1965).
120. K. Dichmann, G. Hamer, S.C. Nyberg, and W.F. Reynolds, *Chem. Comm.*, 1295, 1970.
121. C.J. Ballhauser, B.F. Djurinskij, and K.J. Watson, *J. Amer. Chem. Soc.*, 90, 3305 (1968).

122. Y. Saito, V. Takenchi, and R. Pepinsky, *Zr. Krist.*, 106, 476 (1955).
123. H.M. Powell and A.F. Wells, *J. Chem. Soc.*, 359, 1935.
124. S.N. Dutta and M.M. Woolfson, *Acta Cryst.*, 14, 178 (1961).
125. S.L. Lawton, *Inorg. Chem.*, 9, 2296 (1970).
126. P.J. Wheatley, *J. Chem. Soc.*, 523 (1960).
127. J.J. Daly, *J. Chem. Soc.*, 4056, 1964.
128. P.J. Coppens, C.H. MacGillavry, S.G. Hovenkamp, and H. Downes, *Acta Cryst.*, 19, 898 (1965).
129. R.G. Cavell, private communication.

APPENDIX A

CONVENTIONAL CRYSTALLOGRAPHIC SYMBOLS
AS DEFINED IN VOL. I, PAGE xi, OF THE
INTERNATIONAL TABLES FOR X-RAY CRYSTAL-
LOGRAPHY

APPENDIX A

h, k, l	indices of the reflection from a set of parallel planes; co-ordinates of a reciprocal lattice point
F_{hkl}	structure factor for the unit cell, corresponding to the Bragg reflection hkl
$a, b, c,$	lengths of unit cell edges
α, β, γ	interaxial angles
a^*, b^*, c^*	lengths of reciprocal lattice unit cell edges
$\alpha^*, \beta^*, \gamma^*$	interaxial angles in reciprocal space
x_i, y_i, z_i	fractional co-ordinates of an atom i (co-ordinates of atom i in units of a, b, c)
$\rho_{x, y, z}$	electron density at the point x, y, z
μ	linear absorption coefficient
\bar{u}^2	mean square amplitude of atomic vibration
B	Debye isotropic temperature parameter $B = 8\pi^2 \bar{u}^2$

APPENDIX A (continued)

$\beta_{11}, \beta_{22}, \beta_{33},$
 $\beta_{12}, \beta_{13}, \beta_{23}$

anisotropic temperature parameters
 used to describe ellipsoidal
 electron distribution of the
 anisotropically vibrating atom;
 the temperature factor expression
 is then: $\exp[-(\beta_{11}h^2 + \beta_{22}k^2$
 $+ \beta_{33}l^2 + 2\beta_{12}hk + 2\beta_{13}hl + 2\beta_{23}kl)]$

F_o observed structure factor
 F_c calculated structure factor

APPENDIX B

<u>Author</u>	<u>Title</u>	<u>Description</u>
D. P. Shoemaker	MIXG2	calculates Picker diffractometer settings
M. J. Bennett	PMMO	calculates intensities, makes Lp corrections for Picker data
M. Elder	Dataprep	as for PMMO, except for PAILRED data
K. Simpson and M. Elder	D-refine	refines axial lengths for all space groups
A. Zalkin	FORDAP	Fourier summation for Patterson, Fourier, and E maps
W. C. Hamilton	GONO9	absorption corrections - Picker data, modified by R. H. Sumner for rigorous extinction correction
D. P. Shoemaker	GNABS	absorption corrections - PAILRED data
C. T. Prewitt	SFLS5	structure factor calculation and least squares refinement of parameters, modified by B. M. Foxman and M. J. Bennett for a rigid body routine
G. J. Williams	CROMERS	calculates form factor curves using Cromer coefficients
J. S. Wood	MGEOM	calculates bond lengths, angles and best planes
P. D. Cradwick	H ATOM	locates hydrogen atoms by vector methods
W. Busing and H. A. Levy	ORFFE2	calculates bond lengths, angles and associated errors, modified by B. Penfold for IBM 360

APPENDIX B (continued)

<u>Author</u>	<u>Title</u>	<u>Description</u>
C. Johnson	ORTEP	writes plot command tape for Calcomp plotter
R. B. K. Dewar and A. L. Stone (360 version by P. F. Stokely)	FAME	Fortran program for Automatic Manufacturing of E's
R. B. K. Dewar and A. L. Stone (360 version by P. F. Stokely)	MAGIC	Multiphase Automatic Generation from Intensities in centric crystals